GRAN SASSO SCIENCE INSTITUTE

The high-energy Galactic gamma-ray emission:

the diffuse component and the role of unresolved pulsar wind nebulae

Presented by: Vittoria Vecchiotti

Supervisors: Dr. G. Pagliaroli, Prof. F. L. Villante

Galactic gamma rays:

- Increasing number of observations of the GeV-PeV gamma-ray sky (catalogs of sources, etc);
- High-energy gamma rays are produced by the interaction of CRs with the ambient medium via hadronic interaction and Inverse Compton.
- Observation of Galactic high-energy gamma rays implies the existence of powerful accelerators in our Galaxy.
- Gamma rays propagate along straight lines hence they keep the information on the location where the interaction took place;
- Gamma rays can be used to probe Galactic CRs.

Abdalla et al, A&A, 612, A1 (2018)

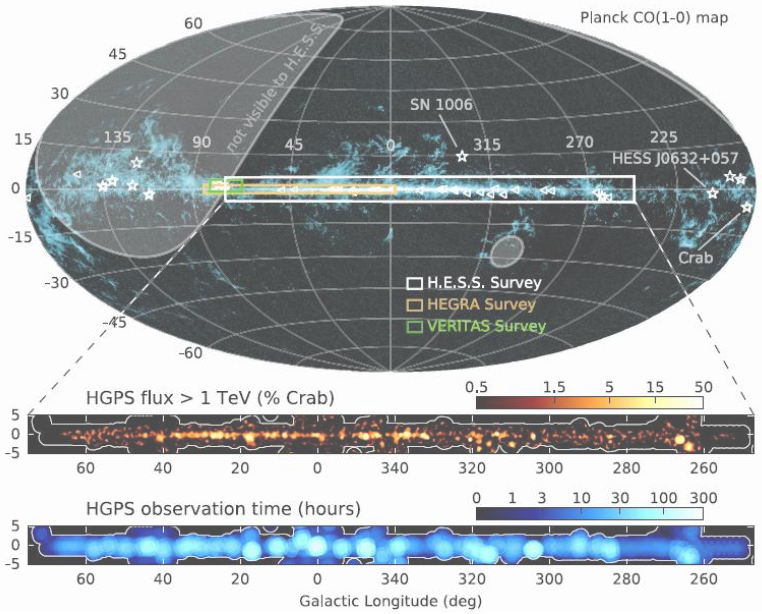

https://fermi.gsfc.nasa.gov/ssc/observations/types/allsky/

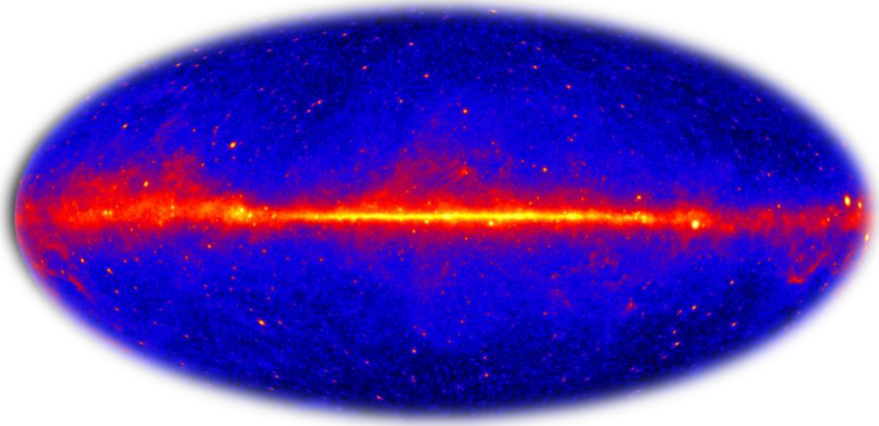

Total Galactic emission above GeV:

$$\phi_{\gamma,tot} = \phi_{\gamma,S} + \phi_{\gamma,\mathrm{diff}} + \phi_{\gamma,IC}$$

Source component is due to the interaction of accelerated particles (hadrons or leptons) with the ambient medium (ISM or CMB) within or close to an acceleration site;

Candidate sources:

- *PWNe* (dominant class in the H.E.S.S. catalog, CRAB Nebula first detected PeVatron, high energy sources observed by HAWC);
- *Pulsars;*
- *Supernova Remnants (SNRs)*;
- *Star clusters*;

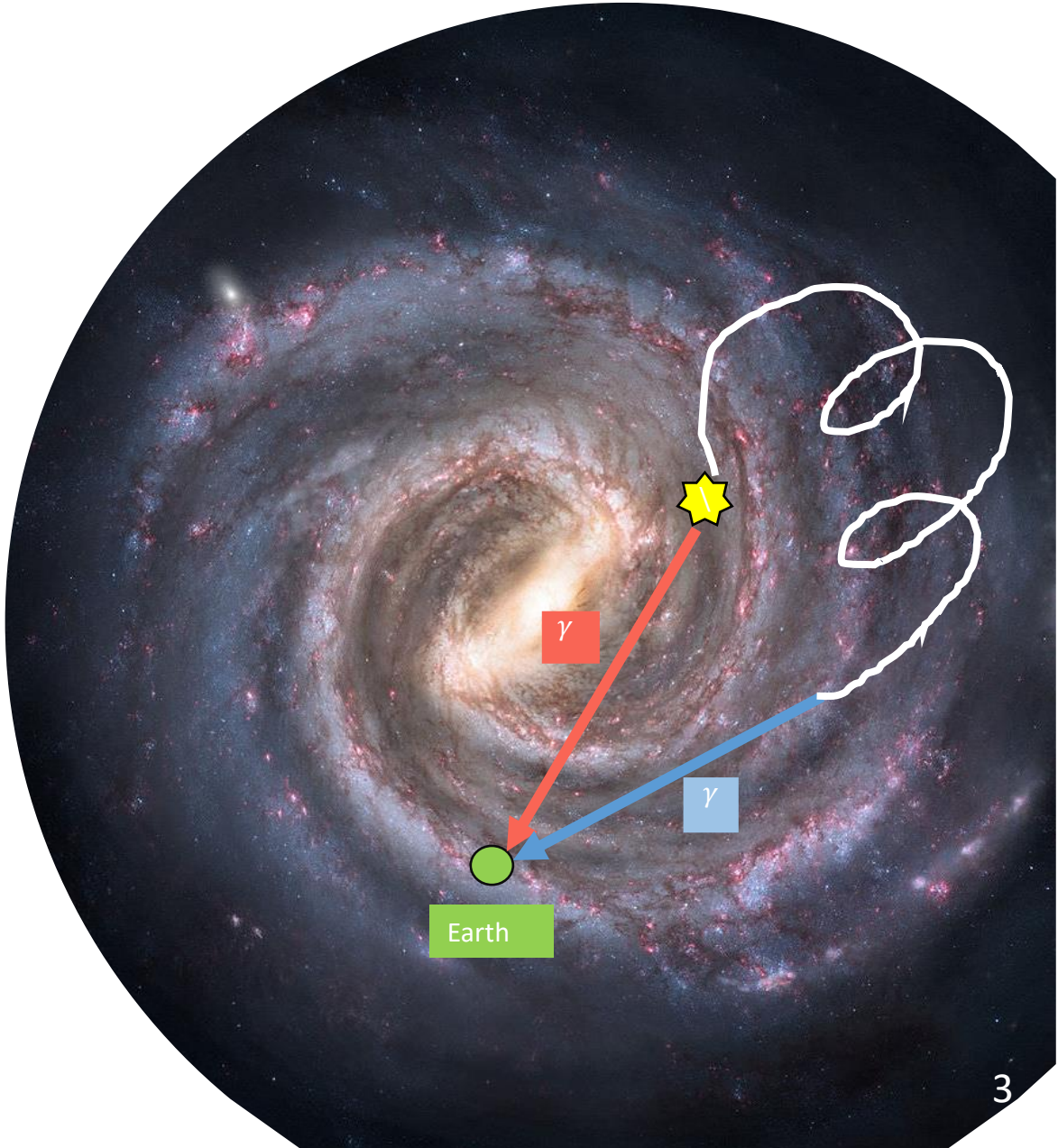

Total Galactic emission above GeV:

$$\phi_{\gamma,tot} = \phi_{\gamma,S} + \phi_{\gamma,\mathrm{diff}} + \phi_{\gamma,IC}$$

Source component is due to the interaction of accelerated particles (hadrons or leptons) with the ambient medium (ISM or CMB) within or close to an acceleration site (such as PWNe, SNRs).

Diffuse component is due to the interaction of accelerated hadrons with the interstellar medium;

Inverse Compton is due to the interaction of accelerated leptons with the radiation fields (CMB, etc);

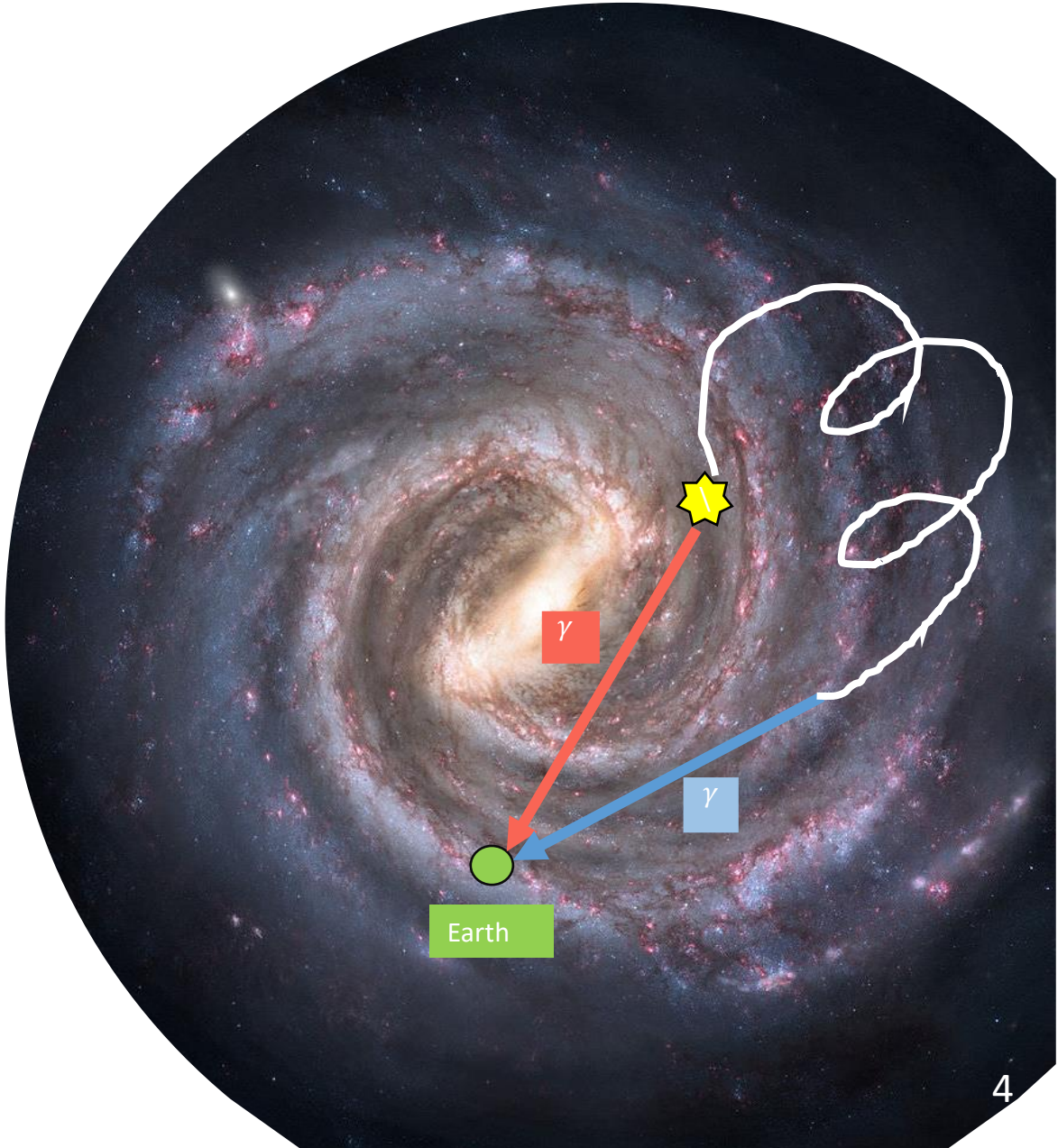

Total Galactic emission above GeV:

$$\phi_{\gamma,tot} = \phi_{\gamma,S} + \phi_{\gamma,\mathrm{diff}} + \cancel{\phi_{\gamma,IC}}$$

The relative importance of the above terms changes accordingly to the considered energy range:

- $\phi_{\gamma,\mathrm{IC}}$ negligible compared to $\phi_{\gamma,\mathrm{diff}}$
- GeV energy: $\phi_{\gamma,\mathrm{diff}} > \phi_{\gamma,S}$
- TeV energy: $\phi_{\gamma,\mathrm{diff}} \simeq \phi_{\gamma,S}$

This behavior is due to the fact that sources have harder spectrum than the diffuse emission.

Abdalla et al, A&A, 612, A1 (2018)

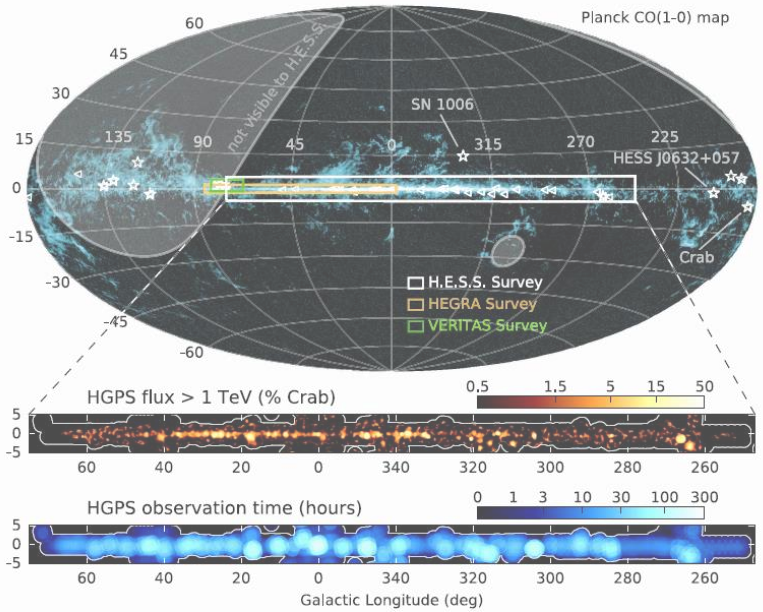

https://fermi.gsfc.nasa.gov/ssc/observations/types/allsky/

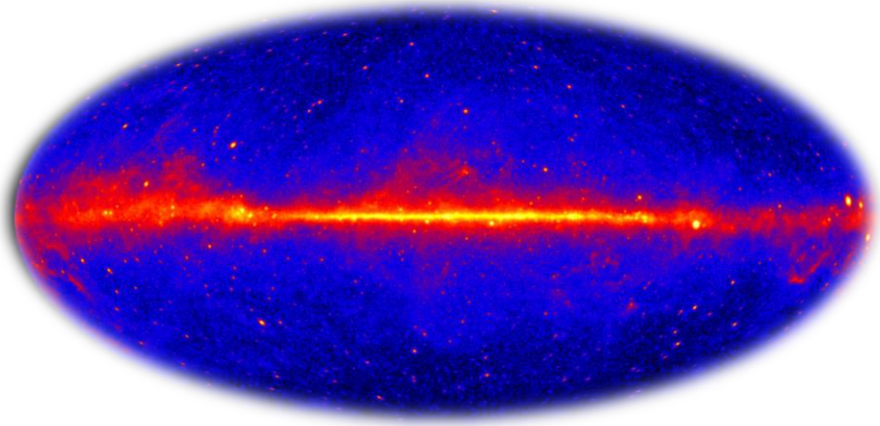

Diffuse Galactic gamma-ray emission:

$$\phi_{\gamma,tot} = \phi_{\gamma,S} + \phi_{\gamma,\mathrm{diff}} + \cancel{\phi_{\gamma,IC}}$$

The study of the diffuse emission is useful to constrain the CR transport properties in our Galaxy;

Standard picture: CRs diffuse in our Galaxy and the diffusion coefficient is homogeneous throughout the Galaxy→ CR properties are the same everywhere in the Galaxy

Recent results (GeV energy):
Study of the Fermi-LAT diffuse emission, the CR spectral index may depend on the Galactocentric radius *Acero et al. (2016), Yang et al. (2016), Pothast et al. (2018)*→ signature of non-standard CR propagation;
Molecular Clouds are the ideal environment to probe local CR properties: in the ring 4 kpc - 6 kpc the CR spectral index appears scattered but still harder than the local one *Peron et al., Astrophys. J (2018);*

New measurement at higher energy: H.E.S.S., Tibet ASγ, (preliminary results from HAWC and LHAASO);

Unresolved sources:

$$\phi_{\gamma,tot} = \phi_{\gamma,S} + \phi_{\gamma,\mathrm{diff}} + \cancel{\phi_{\gamma,IC}}$$

Measured

$$\phi^{r}_{\gamma,S} + \phi^{unr}_{\gamma,S}$$

Detectors can resolve only a fraction of Galactic sources due to their limited sensitivity threshold → unresolved sources;

The Galactic diffuse gamma-ray emission provided by experiments is obtained by masking the contribution of known sources → unresolved sources contribute to the measured diffuse emission

If not negligible →it changes the interpretation of data

Outline:

- Diffuse gamma-rays and neutrino emission (different hypotheses on the CR spatial and energy distribution);
- Test the models with TeV observations;
- Unresolved sources;

  Cataldo et al. Astrophys.J. (2020)

- Population study of the H.E.S.S. Galactic Plane Survey (HGPS) under the hypothesis that the signal is dominated by pulsar-powered sources;

  Cataldo et al. Astrophys.J. (2020)

  Vecchiotti et al, ICRC 2021, Journal of Physics: Conference Series.

- Prediction in the **GeV energy** range (Fermi-LAT)

  Vecchiotti et al, Communication Physics. (2022)

  Pagliaroli et al, ICRC 2021, Journal of Physics: Conference Series.

- Prediction in the **sub-PeV energy** range (Tibet ASγ)

  Vecchiotti et al, Astrophys. J. (2022)

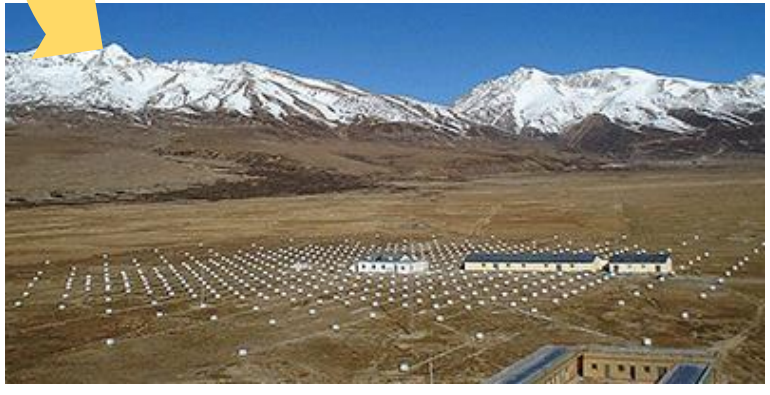

High-energy γ and ν Galactic diffuse emission

Cataldo et al. Astrophys.J. 904 (2020)

Diffuse Galactic γ and ν emission:

$$\varphi_i^{diff}(E_i, \hat{n}_i) = A_i \int_{E_i}^{\infty} dE \frac{d\sigma(E, E_i)}{dE_i} \int_0^{\infty} dl \, \varphi_{CR}(E, \bar{r}_{Sun} + l\hat{n}_i) n_H (\bar{r}_{Sun} + l\hat{n}_i)$$

Where: A_γ=1 and A_ν=1/3 (due to neutrino oscillation)

Differential inelastic cross section of pp interaction from the SYBILL code *[Kelner,Aharonian,Bugayov (2006)]*

Cosmic-ray energy and spatial distribution

Interstellar gas distribution in the Galaxy [*Galprop*]

4 models for the diffuse fluxes **for 4 assumptions of the CR distribution** in the Galaxy.

Cosmic ray distribution:

$$\varphi_{CR}(E,\vec{r}) = \varphi_{CR,\,Sun}(E)\, g\,(\vec{r},R)\; h(E,\vec{r})$$

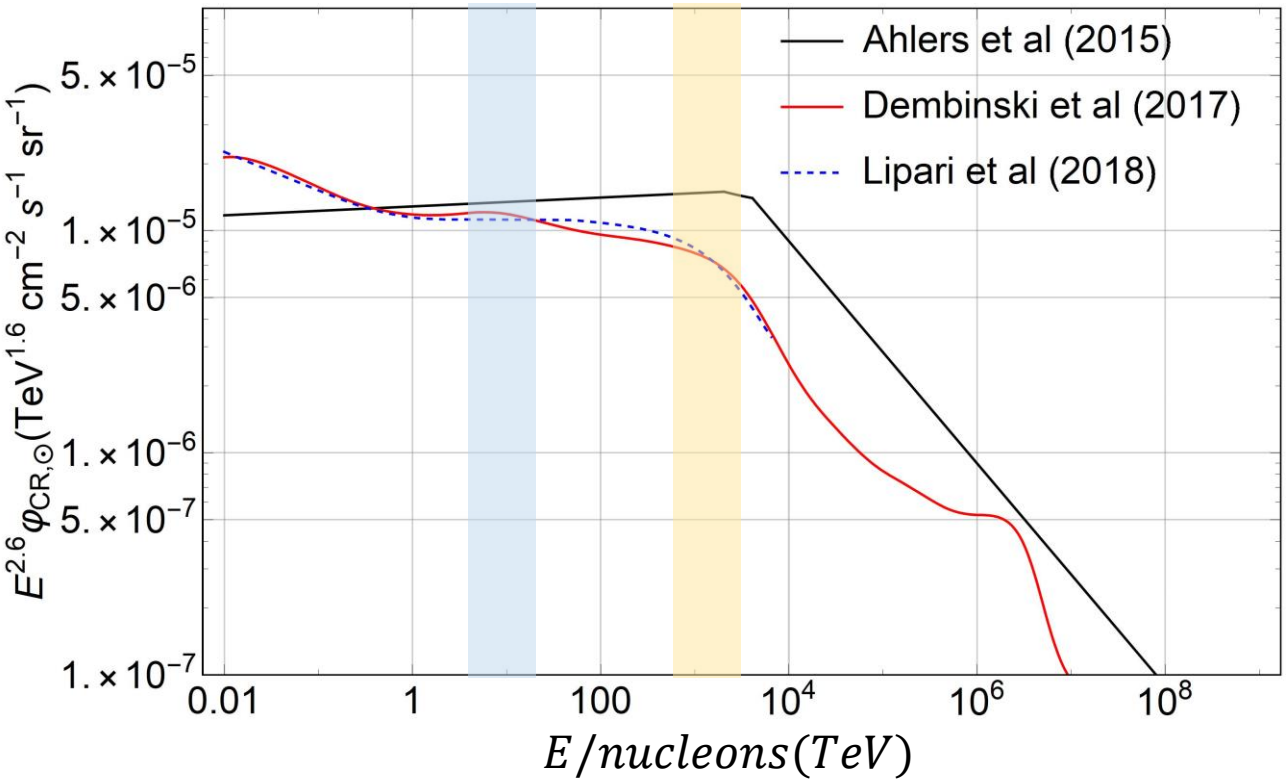

- Data driven local CR spectrum;
  Dembinski, Engel, Fedynitch et al. (2018)

The gamma-ray (neutrino) flux at $E_\gamma = 1\ TeV$ ($E_\nu = 100\ TeV$) is determined by CRs with $E_{CR} = 10\ TeV$ ($E_{CR} = 2\ PeV$);

Cosmic ray distribution:

$$\varphi_{CR}(E,\vec{r}) = \varphi_{CR,\,Sun}(E)\, g\,(\vec{r},R)\, h(E,\vec{r})$$

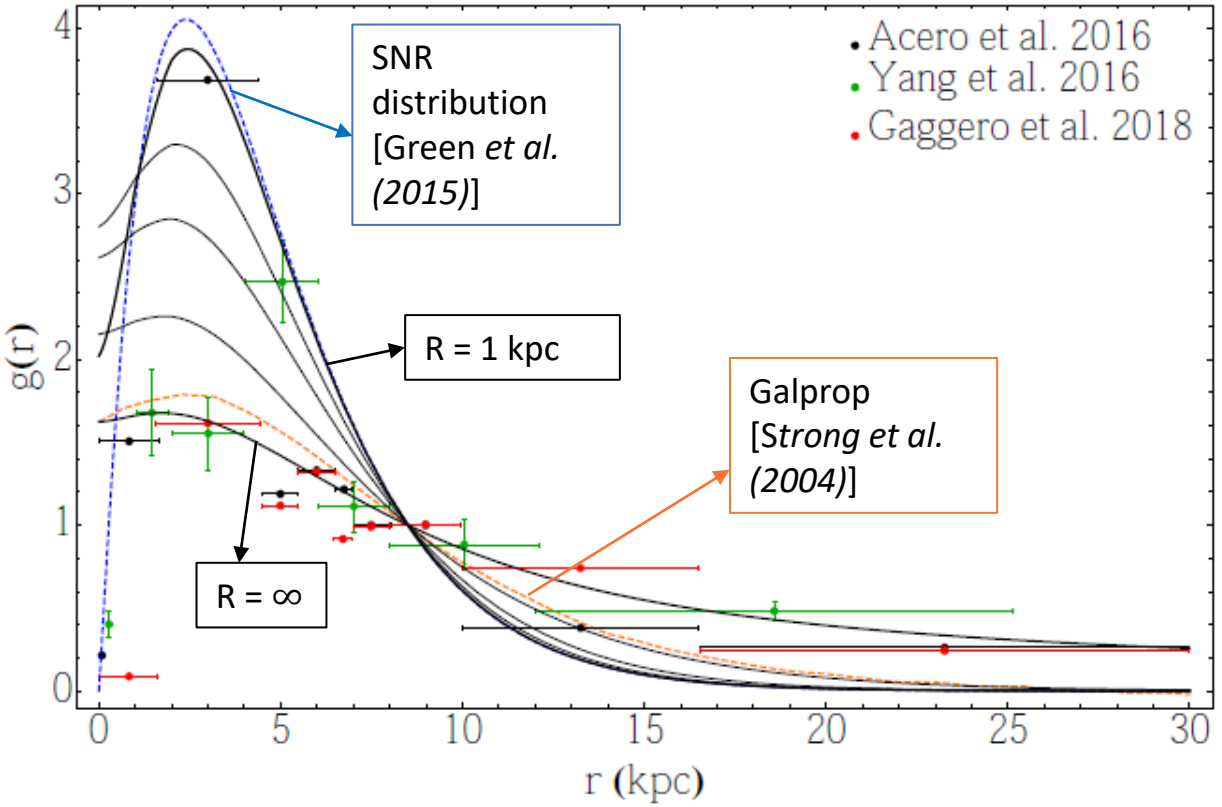

- Data driven local CR spectrum;
  Dembinski, Engel, Fedynitch et al. (2018)
- The function g(r) is determined by the distribution of the CR sources $f_s\,(\vec{r})$ and by the propagation of CR in the Galaxy;

$$g(\vec{r}) = \frac{1}{N}\int d^3x \frac{f_s(\vec{r}-\vec{x})F\left(\frac{|x|}{R}\right)}{|x|}$$

$$F(\nu) = \frac{1}{\sqrt{2\,\pi}}\int_{\nu}^{\infty} d\gamma\ \exp(-\gamma^2/2)|$$

Cosmic ray distribution:

$$\varphi_{CR}(E,\vec{r}) = \varphi_{CR,\,sun}(E)\, g\,(\vec{r},R)\, h(E,\vec{r})$$

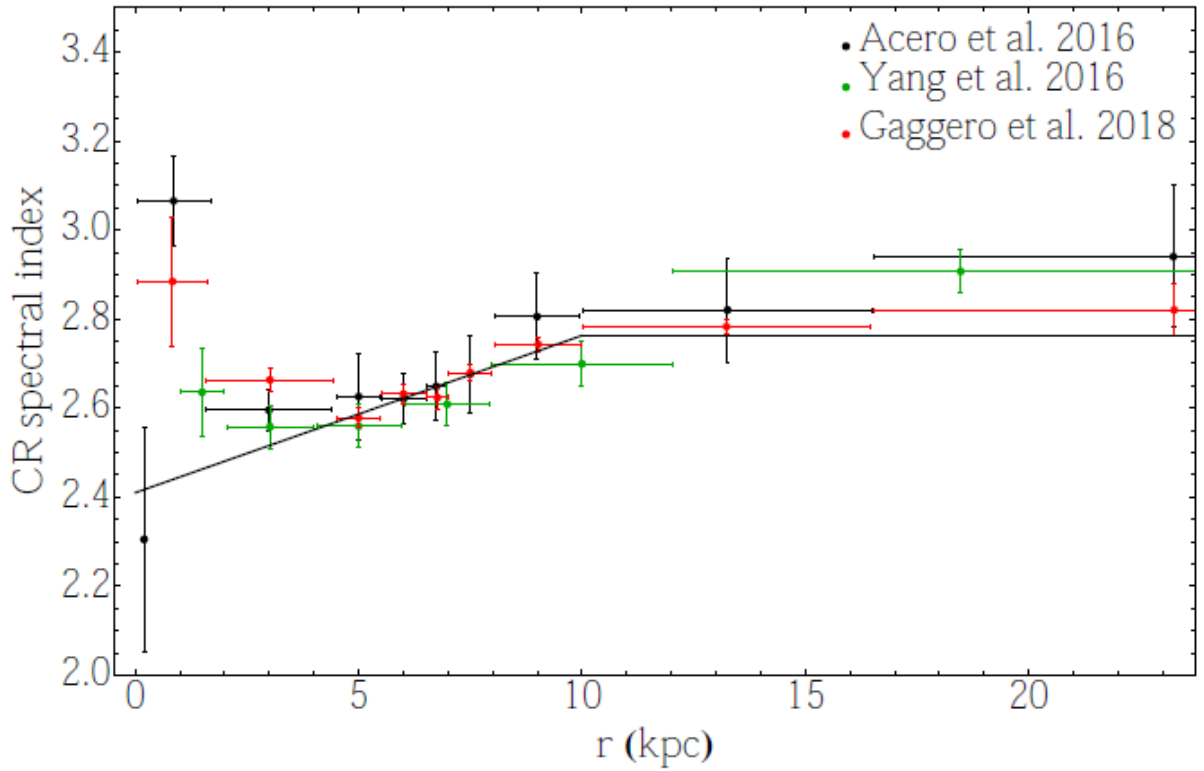

$$h(E,\vec{r}) = \left(\frac{E}{20\ GeV}\right)^{\Delta(\vec{r})};\ \Delta(\vec{r}) = 0.3\left(1 - \frac{\mathrm{r}}{\mathrm{r_{sun}}}\right)\ \text{for r} < 10\ \text{kpc}$$

- Data driven local CR spectrum;
  Dembinski, Engel, Fedynitch et al. (2018)
- The function g(r) is determined by the distribution of the CR sources $f_s\ (\vec{r})$ and by the propagation of CR in the Galaxy;
- We consider the possibility of spatially dependent CR spectral index recenty emerged from the analysis of the FermiLAT data at $\sim 20\ GeV$
  Acero et al. (2016), Yang et al. (2016), Gaggero et al. (2018)

Diffuse Galactic γ and ν emission:

Abbasi et al, Phys. Rev. D. (2020)

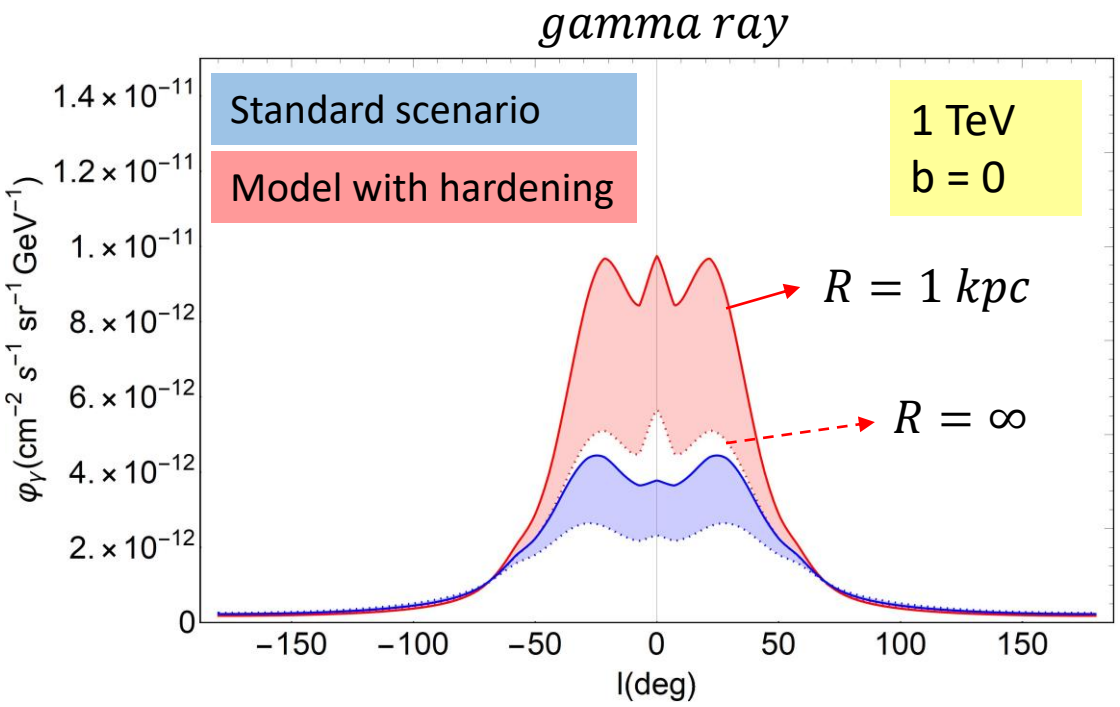

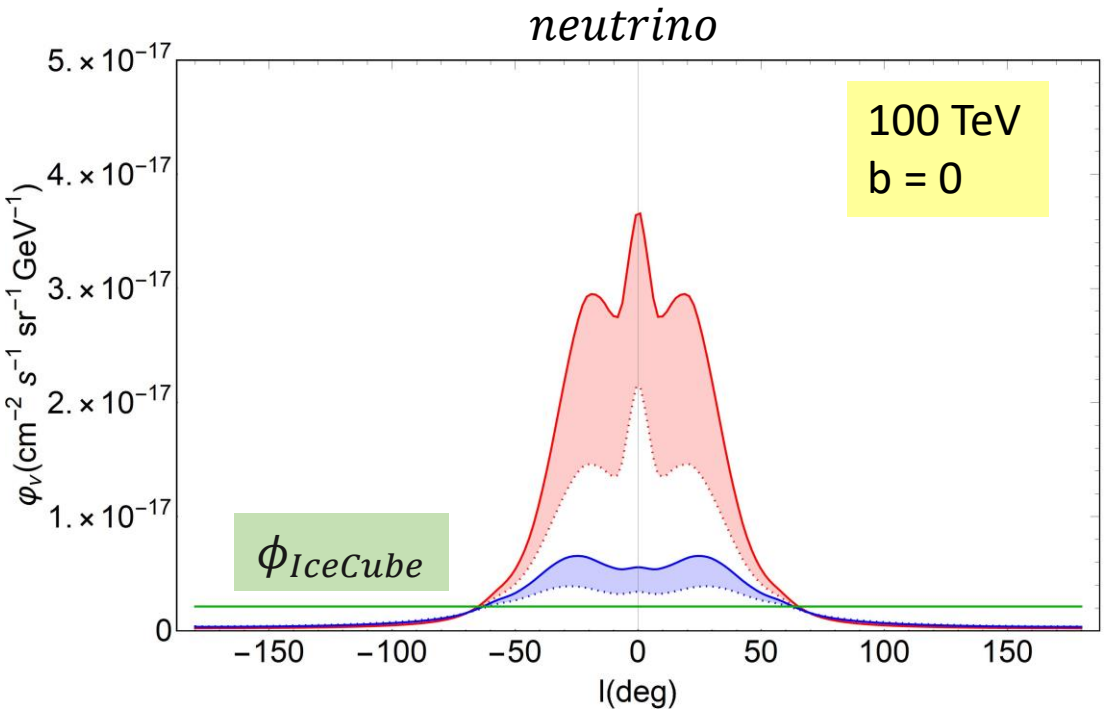

- The angle integrated γ-ray flux in the standard scenario is: $\Phi_\gamma = (7.0 - 8.0) \times 10^{-13} cm^{-2} s^{-1} GeV^{-1}$, and increases of a factor ~ 1.2 in the hardening case.
- In the region $\mathrm{l} < |60°|, \mathrm{b} < |2°|$, this factor becomes $\sim 2 (\sim 3)$ for γ (ν) respectively;
- The angle integrated neutrino flux is 3.9 % - 4.4 % (5.8 % - 8.2%) of the isotropic flux observed by IceCube (*Abbasi et al, Phys. Rev. D. (2020)*). Potentially observable in specific region of the sky.

Pagliaroli et al, JCAP (2016), Pagliaroli et al, JCAP (2018)

Diffuse Galactic γ and ν emission:

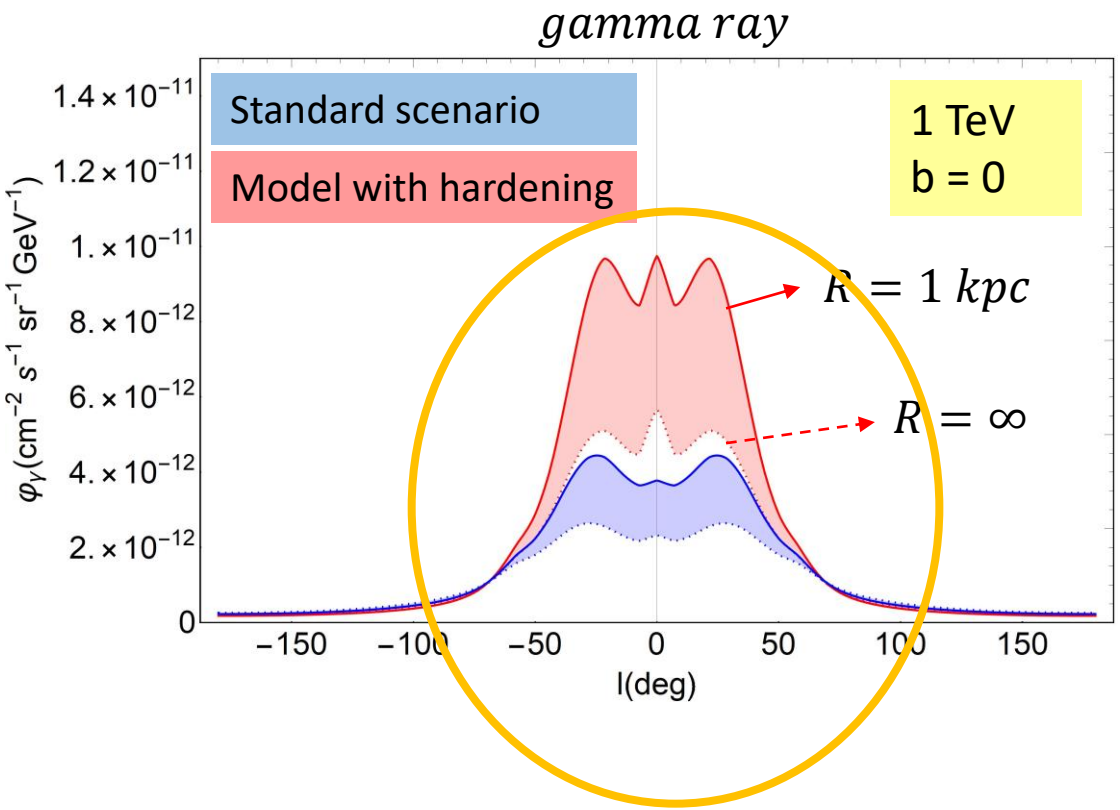

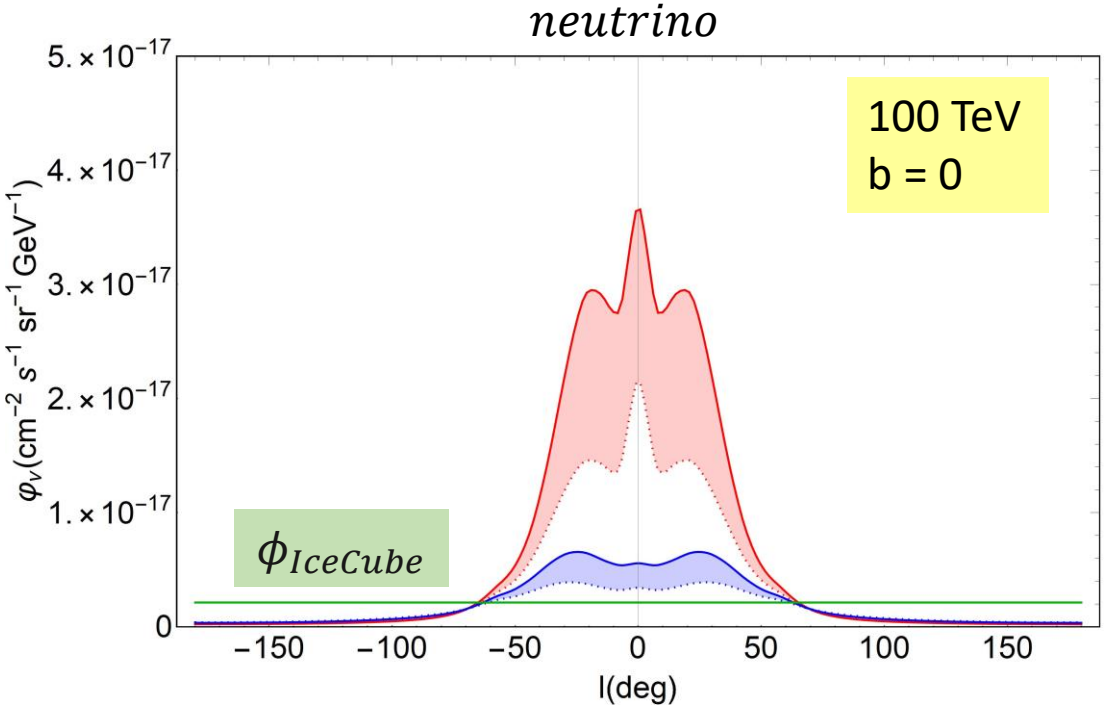

- There is a longitude region for $\mathrm{l} < |60°|$ in which the hardening case is distinguishable from the standard case without hardening;
- TeV gamma-ray observations can be used to probe our hypotheses for the CR distributions.

Comparison with observations:

$$\phi_{\gamma,tot} = \phi_{\gamma,S} + \phi_{\gamma,\mathrm{diff}} + \cancel{\phi_{\gamma,IC}}$$

$$\phi_{\gamma,S} = \phi^{r}_{\gamma,S} + \phi^{unr}_{\gamma,S}$$

$\phi_{\gamma,\mathrm{diff}}$	Different models for the Galactic gamma-ray diffuse emission
$\phi_{\gamma,tot}$	Measured by: • H.E.S.S. (1 TeV) in the sky region: $-75^{\circ} < l < 60^{\circ}, \lvert b\rvert < 2^{\circ}$; *Abramowsky et al, Phys. Rev. D (2014)* • HAWC (7 TeV) in the sky region: $0^{\circ} < l < 110^{\circ}, \lvert b\rvert < 2^{\circ}$; *Zhou et al, ICRC (2017)* • ARGO-YBJ. (0.6 TeV) in the sky region: $25^{\circ} < l < 100^{\circ}, \lvert b\rvert < 5^{\circ}$; *Bartoli et al, Astrophys. J (2018)* • Milagro (15 TeV) in the sky region: $30° < l < 110^{\circ}, \lvert b\rvert < 2^{\circ}$; *Abdo et al, ICRC (2008)*
$\phi^{r}_{\gamma,S}$	H.G.P.S. catalog: **78 VHE** sources in the H.E.S.S. observational window;

Comparison with the total observed flux:

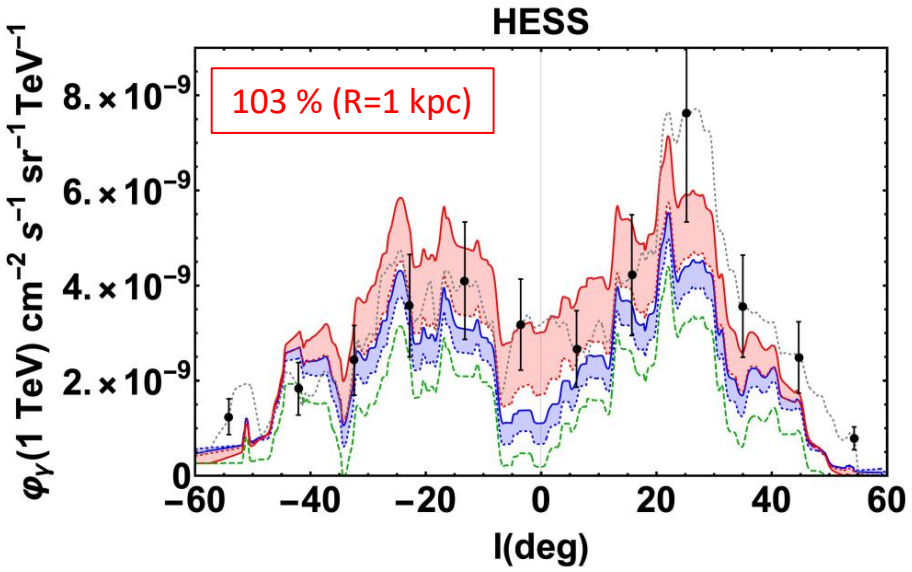

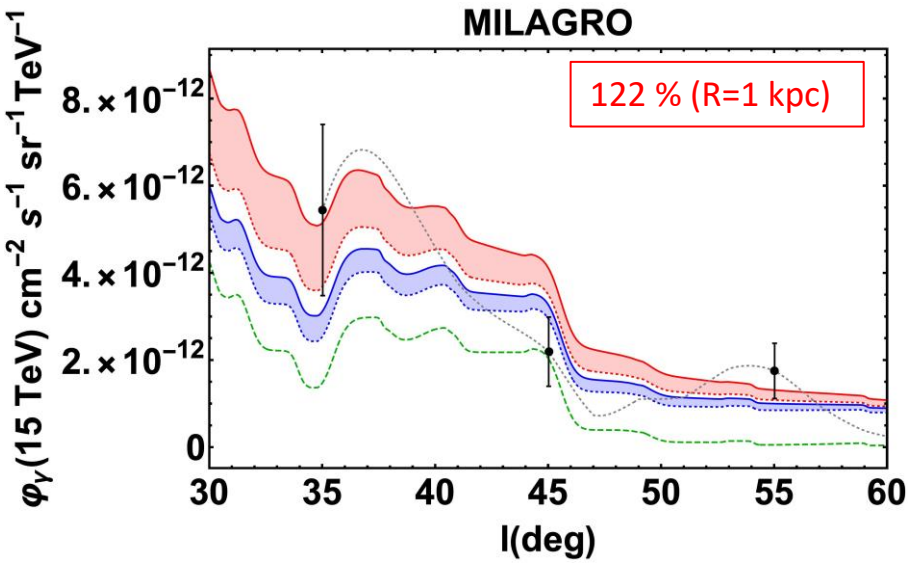

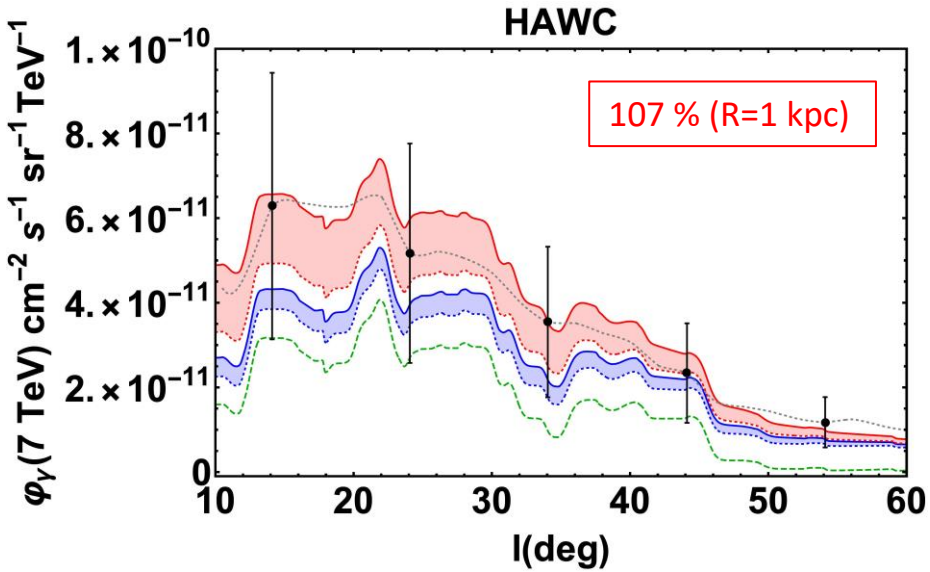

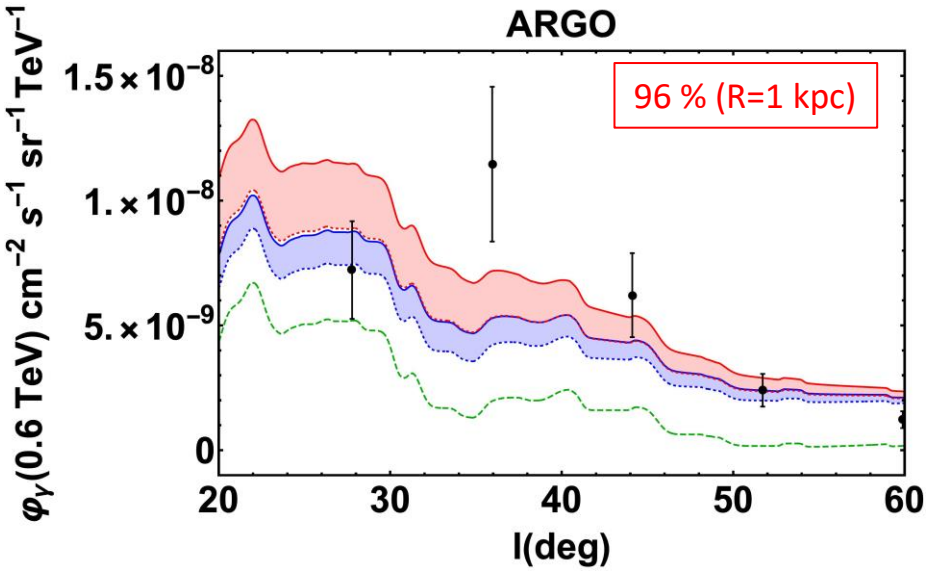

$$\phi_{\gamma,tot} > \phi^{r}_{\gamma,\,S} + \phi_{\gamma,\mathrm{diff}}$$

Resolved sources

Resolved sources + Diffuse (no Hardening)

Resolved sources + Diffuse (Hardening)

Take home message:

- The case with hardening and $R = 1\ kpc$ saturates the total observed gamma-ray flux (problem if unresolved sources are not negligible);

Population studies of TeV sources

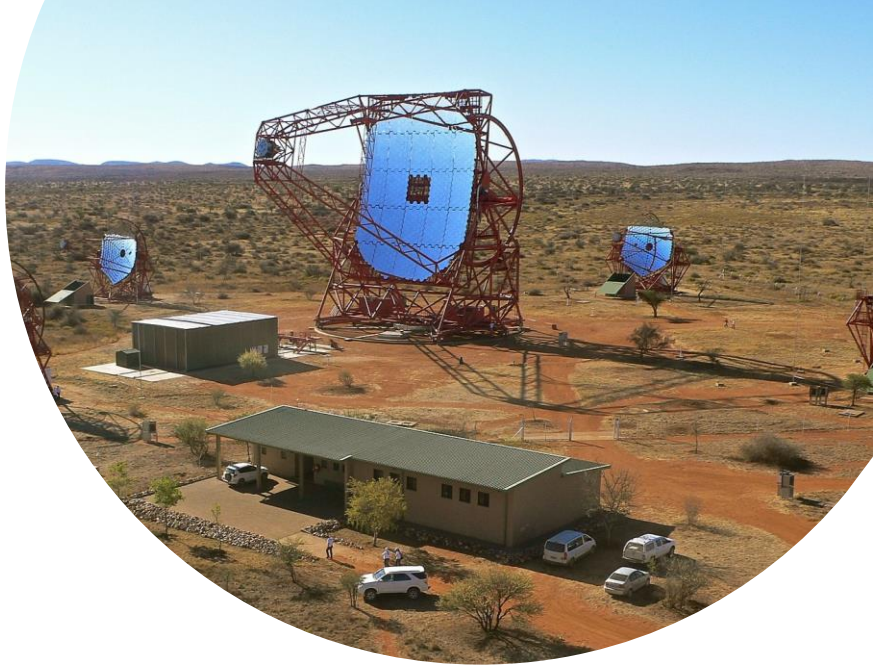

Cataldo et al. *Astrophys.J.* 904 (2020)

Study of the Pulsar wind nebulae population in the TeV range:

Cataldo et al. *Astrophys.J.* 904 (2020)

- The HGPS catalogue ($\phi > 0.1\phi_{Crab}$);

Abdalla et al, *A&A*, 612, A1 (2018)

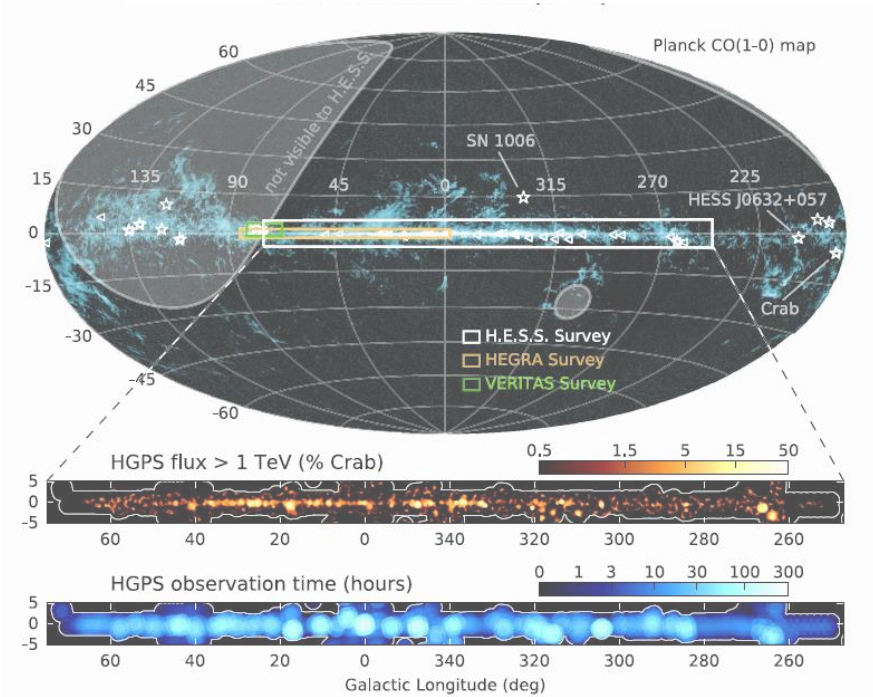

Study of the Pulsar wind nebulae population in the TeV range:

Cataldo et al. *Astrophys.J.* 904 (2020)

- The HGPS catalogue ($\phi > 0.1\phi_{Crab}$);
- Model for TeV source population:

  we assume the spatial distribution and the luminosity distribution of the sources;

$$\frac{dN}{d^3 r dL} = \rho(r)Y(L)$$

Abdalla et al, *A&A*, 612, A1 (2018)

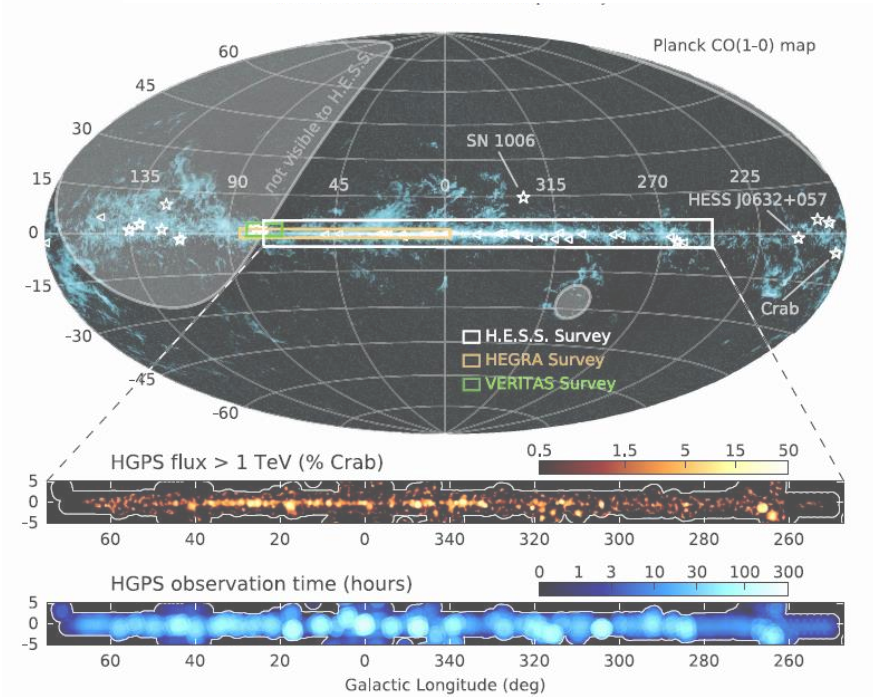

Study of the Pulsar wind nebulae population in the TeV range:

Cataldo et al. *Astrophys.J.* 904 (2020)

- The HGPS catalogue ($\phi > 0.1\phi_{Crab}$);
- Model for TeV source population:

  we assume the spatial distribution and the luminosity distribution of the sources;

$$\frac{dN}{d^3 r dL} = \rho(r)Y(L)$$

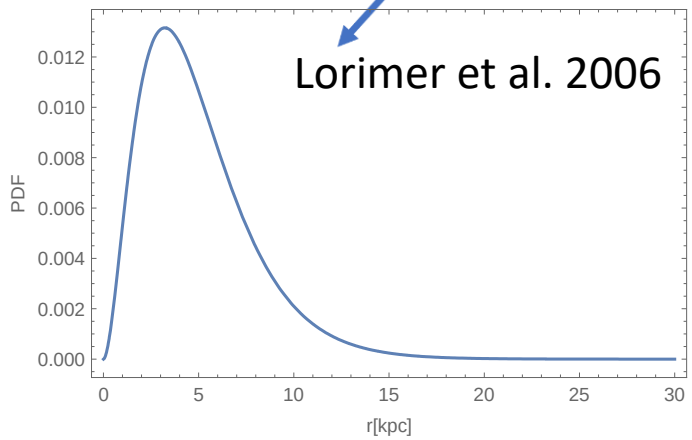

Abdalla et al, *A&A*, 612, A1 (2018)

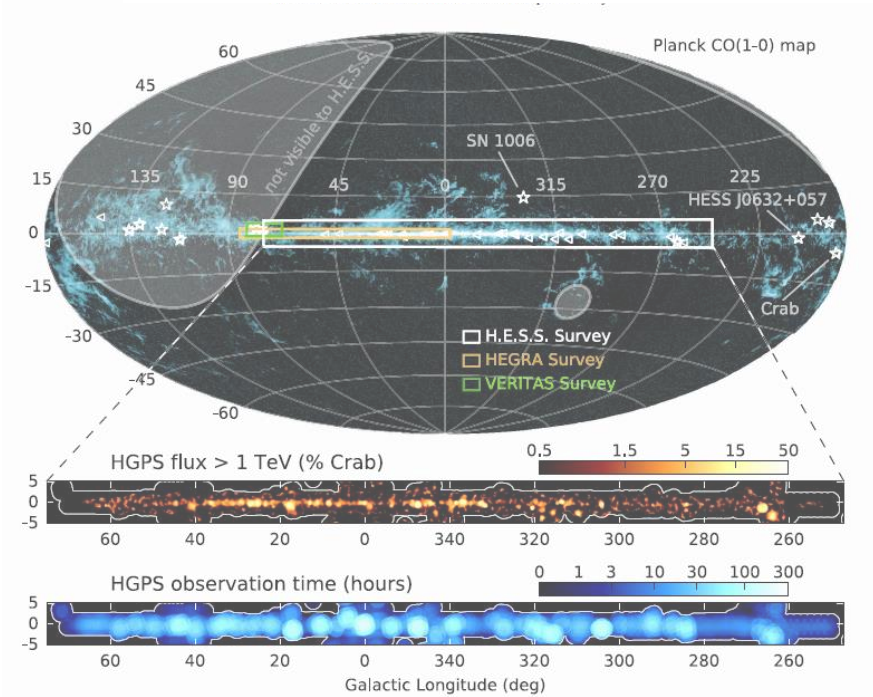

Study of the Pulsar wind nebulae population in the TeV range:

Cataldo et al. *Astrophys.J.* 904 (2020)

Abdalla et al, *A&A*, 612, A1 (2018)

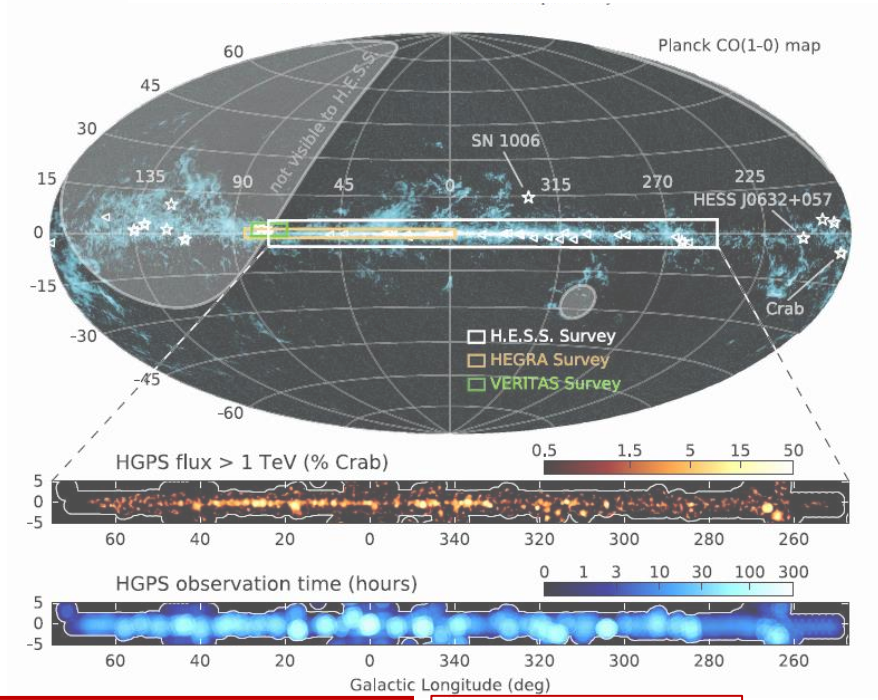

- The HGPS catalogue ($\phi > 0.1\phi_{Crab}$);
- Model for TeV source population:

  we assume the spatial distribution and the luminosity distribution of the sources;

$$\frac{dN}{d^3 r dL} = \rho(r) Y(L)$$

$$Y(L) = \frac{R\tau(\alpha-1)}{L_{\max}} \left(\frac{L}{L_{\max}}\right)^{-\alpha}$$

$\alpha = 1.5$
$\alpha = 1.8$

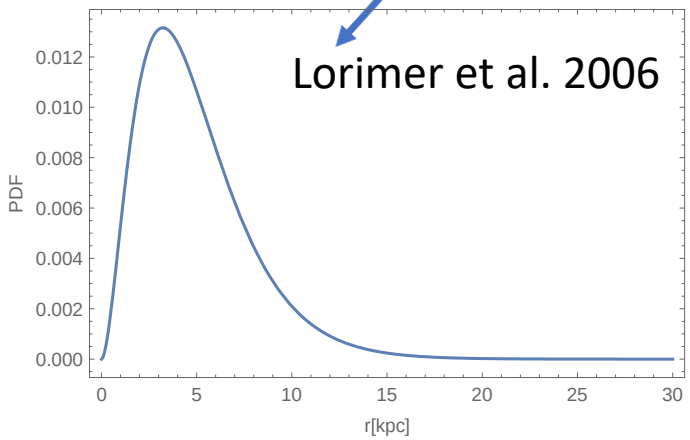

$$\alpha = 1/\gamma + 1$$

$$R = 0.019\,\mathrm{yr}^{-1}$$

For pulsar-powered sources:

$$L(t) = L_{\max}\left(1 + \frac{t}{\tau}\right)^{-\gamma}$$

Study of the Pulsar wind nebulae population in the TeV range:

Cataldo et al. *Astrophys.J.* 904 (2020)

Abdalla et al, *A&A*, 612, A1 (2018)

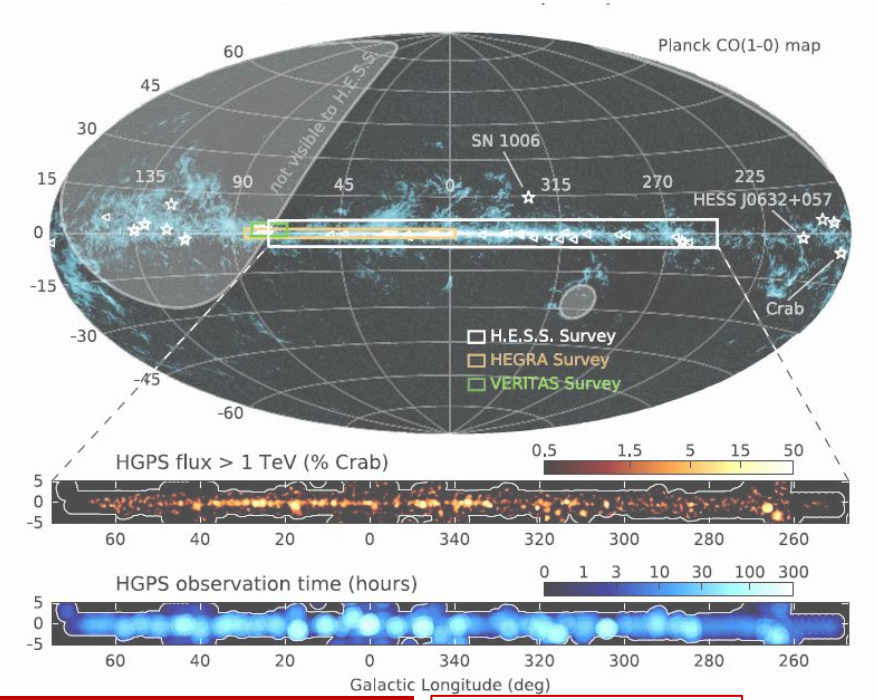

- The HGPS catalogue ($\phi > 0.1\phi_{Crab}$);
- Model for TeV source population:

  we assume the spatial distribution and the luminosity distribution of the sources;

$$\frac{dN}{d^3 r dL} = \rho(r) Y(L)$$

$$Y(L) = \frac{R\tau(\alpha-1)}{L_{\max}} \left(\frac{L}{L_{\max}}\right)^{-\alpha}$$

$\alpha = 1.5$
$\alpha = 1.8$

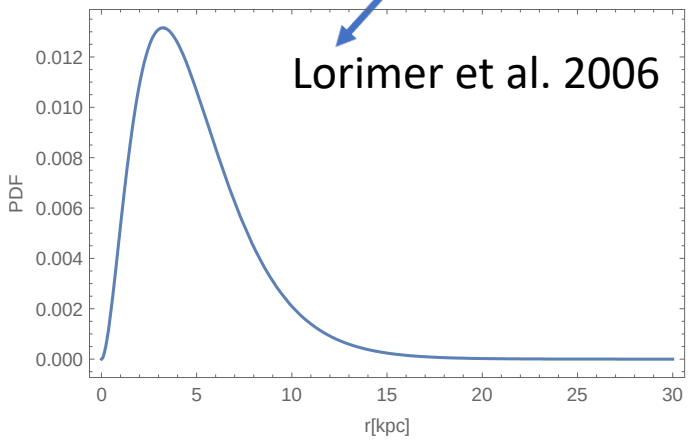

$$\alpha = 1/\gamma + 1$$

$$R = 0.019\,\mathrm{yr}^{-1}$$

For pulsar-powered sources:

$$L(t) = L_{\max}\left(1 + \frac{t}{\tau}\right)^{-\gamma}$$

We assume a **power-law** energy spectrum with index $\boldsymbol{\beta_{TeV} = 2.3}$ that is the average index for all the sources in the HGPS catalogue.

Study of the Pulsar wind nebulae population in the TeV range:

Cataldo et al. *Astrophys.J.* 904 (2020)

We fit the H.E.S.S. observational results with an unbinned likelihood

$\alpha = 1.5$

$$L_{max} = 4.0^{+3.0}_{-2.1} \times 10^{35}\ erg\ s^{-1}$$
$$\tau = 1.8^{+1.5}_{-0.6}\ kyr$$

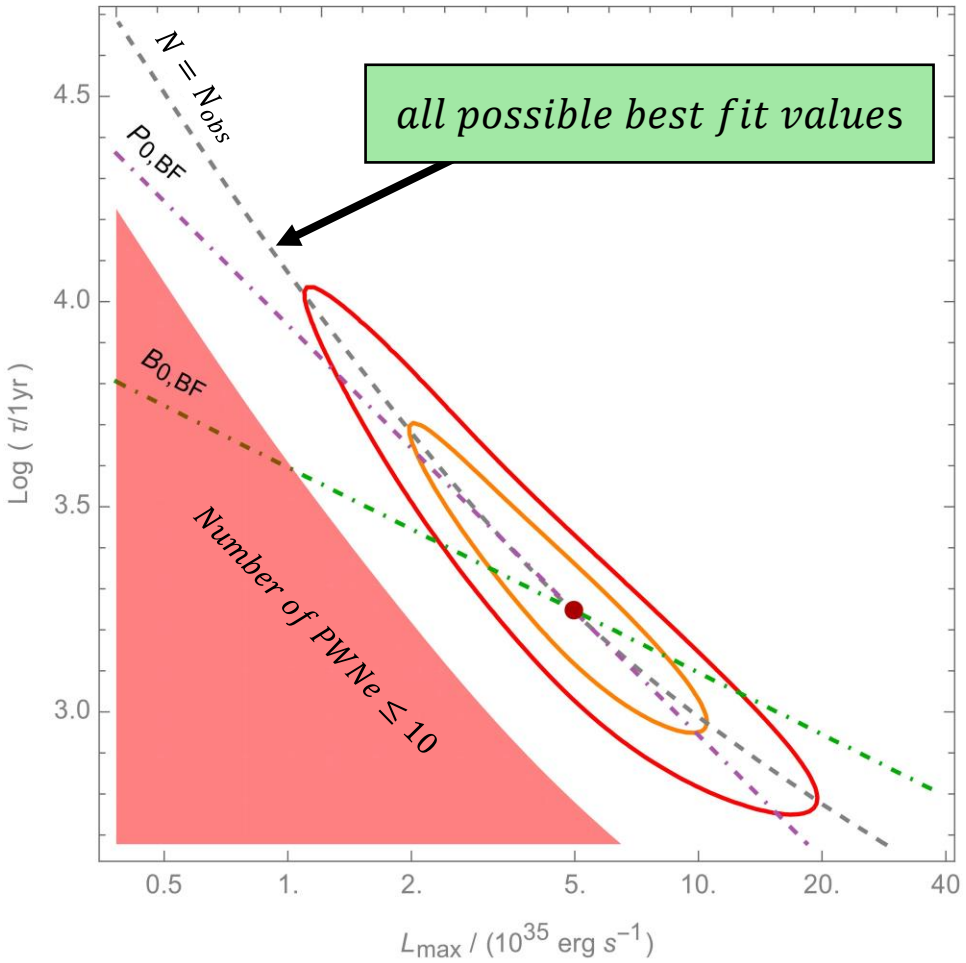

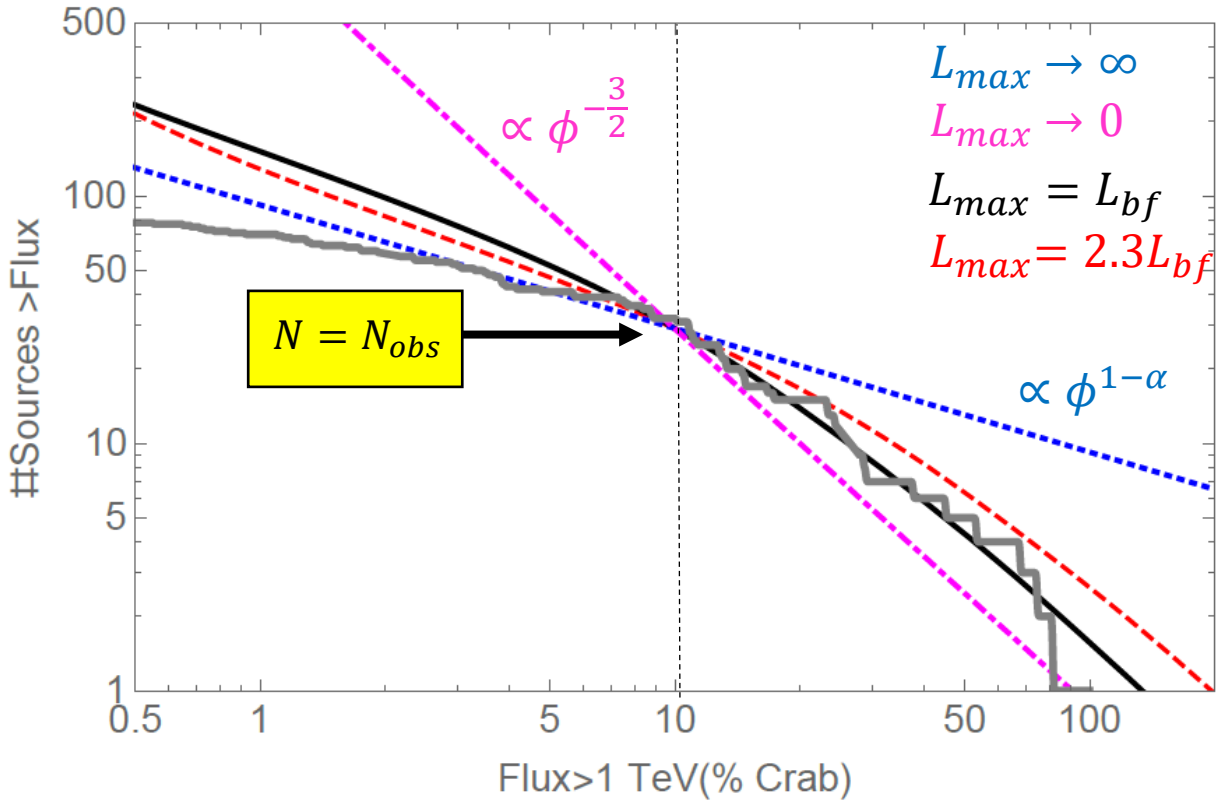

Study of the Pulsar wind nebulae population in the TeV range:

Cataldo et al. *Astrophys.J.* 904 (2020)

We fit the H.E.S.S. observational results with an unbinned likelihood

$\alpha = 1.5$

$L_{max} = 4.0^{+3.0}_{-2.1} \times 10^{35}\ erg\ s^{-1}$

$\tau = 1.8^{+1.5}_{-0.6}\ kyr$

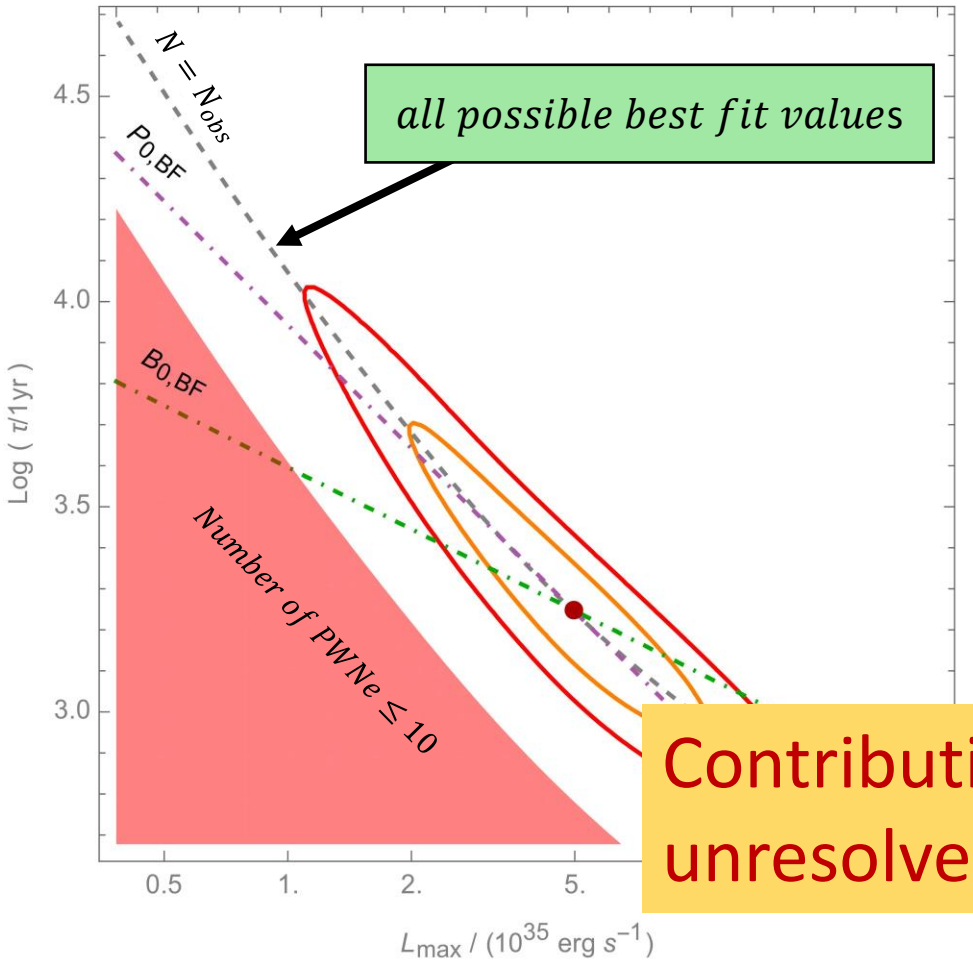

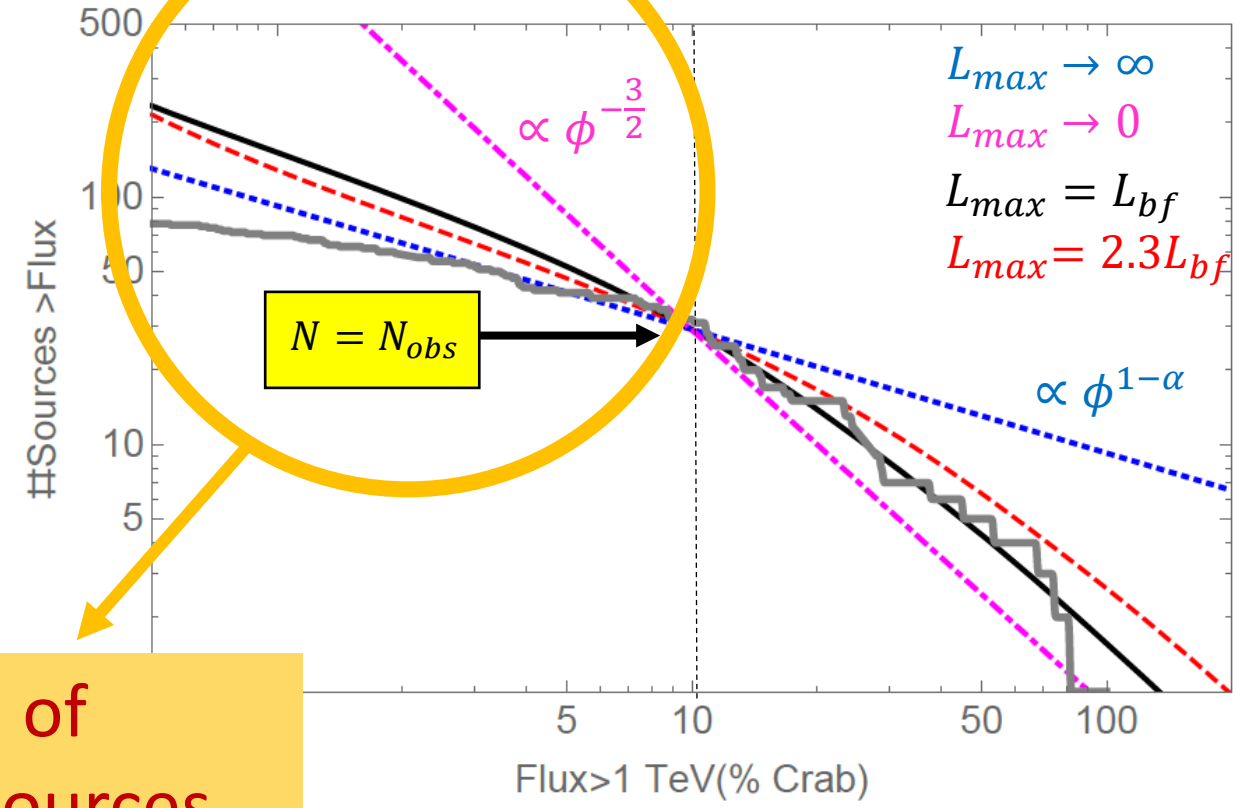

Contribution of unresolved sources

Results:

- The total TeV luminosity (1-100 TeV) of the Galaxy:

$$L_{MW} = \frac{R\tau(\alpha-1)\,L_{max}}{(2-\alpha)}\left[1-\left(\frac{L_{min}}{L_{max}}\right)^{\alpha-2}\right] = 1.7^{+0.5}_{-0.4}\times 10^{37}\ erg\ s^{-1}$$

$\left(\frac{L_{min}}{L_{max}}\right) \to 0$

- The total flux at Earth produced by all sources (1-100 TeV) (resolved and unresolved) in the H.E.S.S. OW:

$$\phi_{tot} = \frac{L_{MW}}{4\Pi\langle E\rangle}\int_{OW} d^3r\ \rho(r)\ r^{-2} = 3.8^{+1.0}_{-1.0}\times 10^{-10} cm^{-2}s^{-1}$$

$\langle E\rangle \to$ 3.25 TeV

- By subtraction we can obtain the contribution of unresolved sources in the H.E.S.S. observational window knowing that: $\phi_S^r = 2.3\times 10^{-10} cm^{-2}s^{-1}$ (cumulative flux due to all 78 sources):

$$\phi_S^{unr} = \phi_{tot} - \phi_S^r = 1.4^{+1.0}_{-0.8}\times 10^{-10}\ cm^{-2}s^{-1} \sim 60\%\ \phi_s^r$$

Comparison with the total observed flux:

Without unresolved sources we got:

$$\phi_{\gamma,tot} > \phi^{r}_{\gamma,S} + \phi_{\gamma,\mathrm{diff}}$$

103 % (hardening, R=1 kpc)
77 % (hardening, R= ∞)

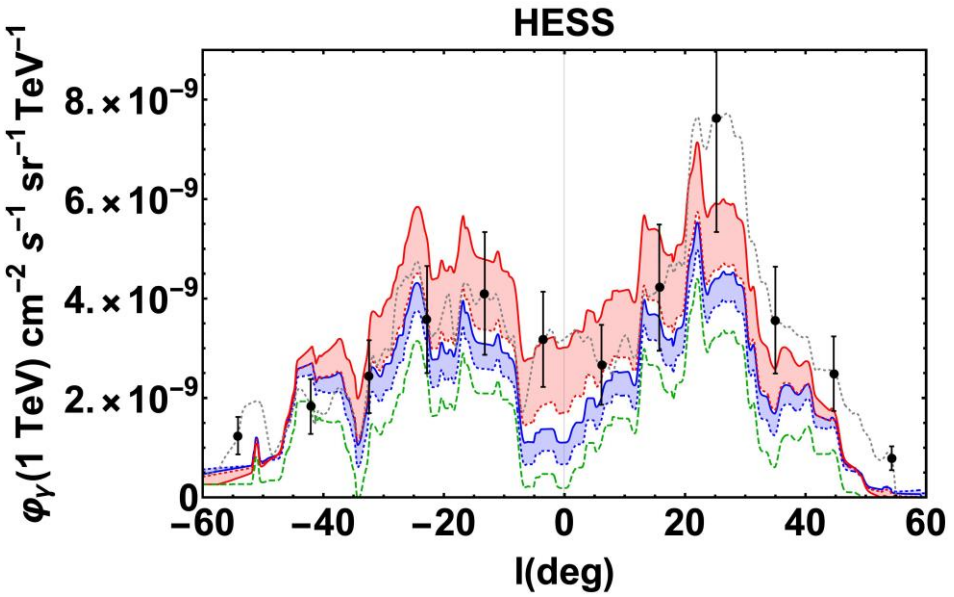

Comparison with the total observed flux:

Without unresolved sources we got:

103 % (hardening, R=1 kpc)
77 % (hardening, R= ∞)

$$\phi_{\gamma,tot} = \phi^{r}_{\gamma,S} + \phi^{unr}_{\gamma,S} + \phi_{\gamma,\mathrm{diff}}$$

121 % (hardening, R=1 kpc)
94 % (hardening, R= ∞)

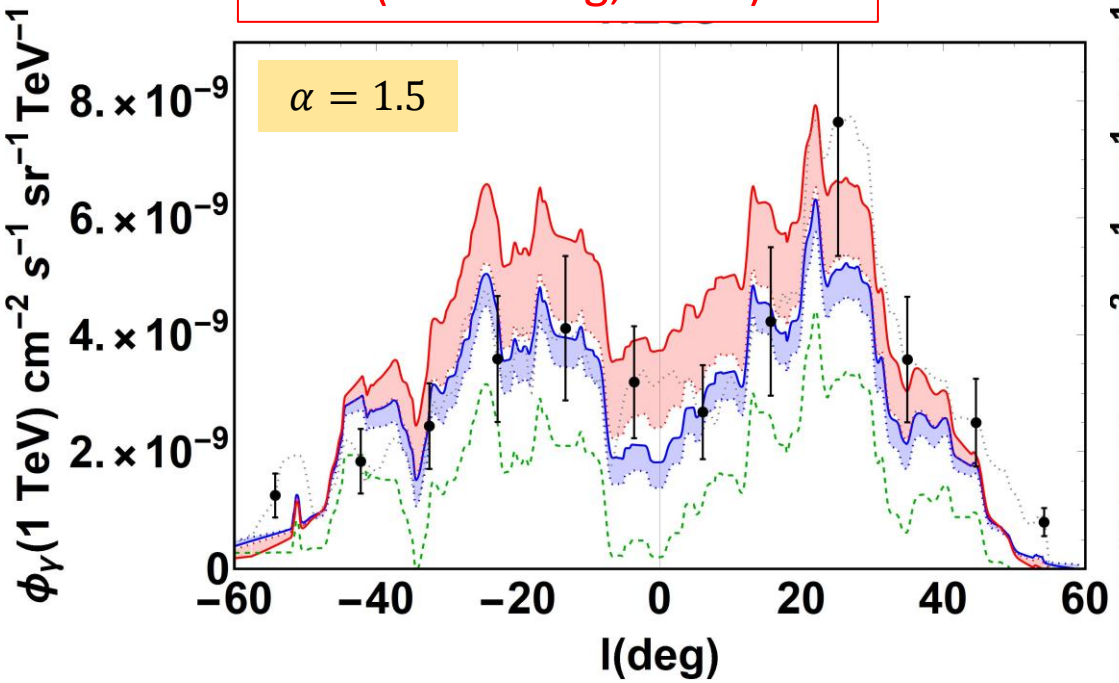

138 % (hardening, R=1 kpc)
112 % (hardening, R= ∞)

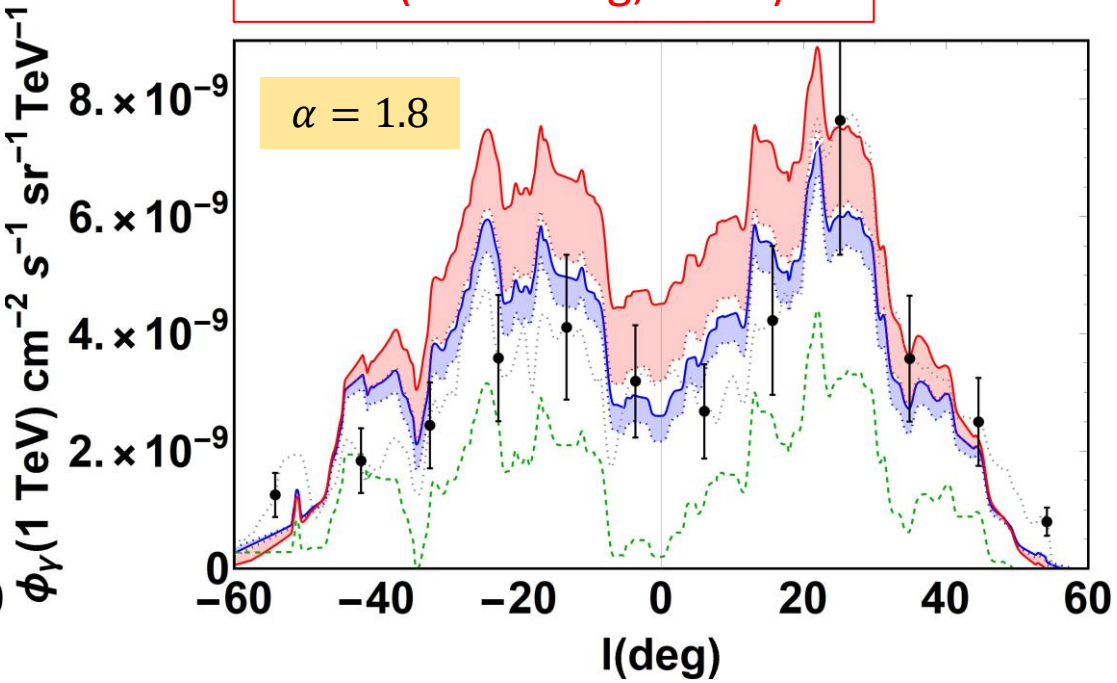

Results:

The best fit parameters L_{max} and τ_{sd} are linked to the magnetic field B_0 and the initial spin-down period P_0 of the pulsar through this relations:

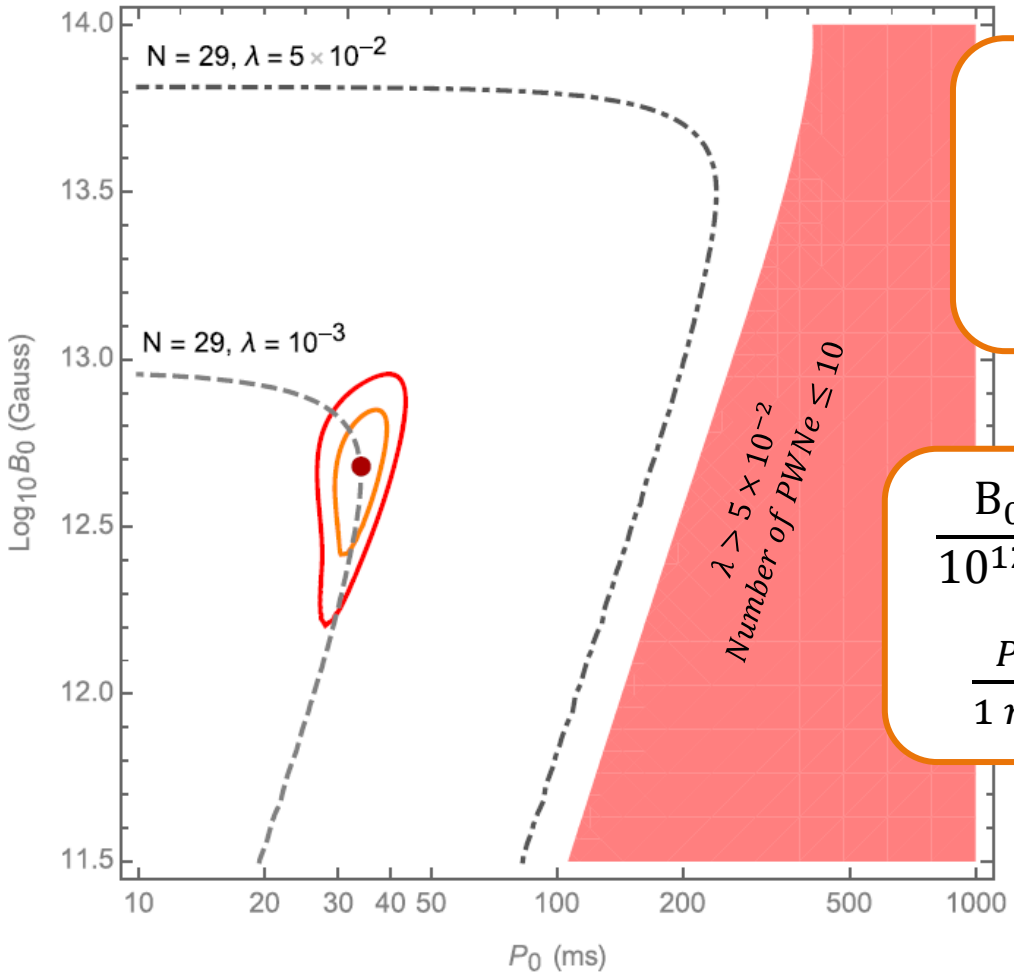

$$L_{max} = \lambda \dot{E}_0 = \lambda \frac{8\pi^4 B_0^2 R^6}{3c^3 P_0^4}$$

$$\tau_{sd} = \frac{3Ic^3 P_0^2}{4\pi^2 B_0^2 R^6}$$

For the firmly identified PWNe from the HGPS catalogue we obtained:

$$5 \times 10^{-5} \leq \lambda \leq 5 \times 10^{-2}$$

As a reference value we take $\lambda = 10^{-3}$

$$\frac{\mathrm{B_0}}{10^{12}\mathrm{G}} = 5.2 \left(\frac{\lambda}{10^{-3}}\right)^{\frac{1}{2}} \left(\frac{\tau}{10^4\ \mathrm{yr}}\right)^{-1} \left(\frac{\mathrm{L_{max}}}{10^{34}\mathrm{erg\ s^{-1}}}\right)^{-\frac{1}{2}} = 4.32^{+2.0}_{-1.9} \times \left(\frac{\lambda}{10^{-3}}\right)^{\frac{1}{2}}$$

$$\frac{P_0}{1\ ms} = 94 \left(\frac{\lambda}{10^{-3}}\right)^{\frac{1}{2}} \left(\frac{\tau}{10^4\ yr}\right)^{-\frac{1}{2}} \left(\frac{L_{max}}{10^{34} erg\ s^{-1}}\right)^{-\frac{1}{2}} = 33^{+5.4}_{-4.3} \times \left(\frac{\lambda}{10^{-3}}\right)^{\frac{1}{2}}$$

Take home message:

- Using the H.G.P.S. we are able to calculate the total Milky Way luminosity and the total flux in the H.E.S.S. observational window in the energy range 1 -100 TeV;
- The contribution of unresolved sources is not negligible being $\sim 60\,\%$ of the resolved signal measured by H.E.S.S.;
- We predict the initial spin-down period and magnetic field of the pulsar. Our results are in agreement with values obtained from gamma-ray pulsar studies.

GeV energy range

Vecchiotti et al, Communication Physics. (2022)

Total FERMI diffuse emission:

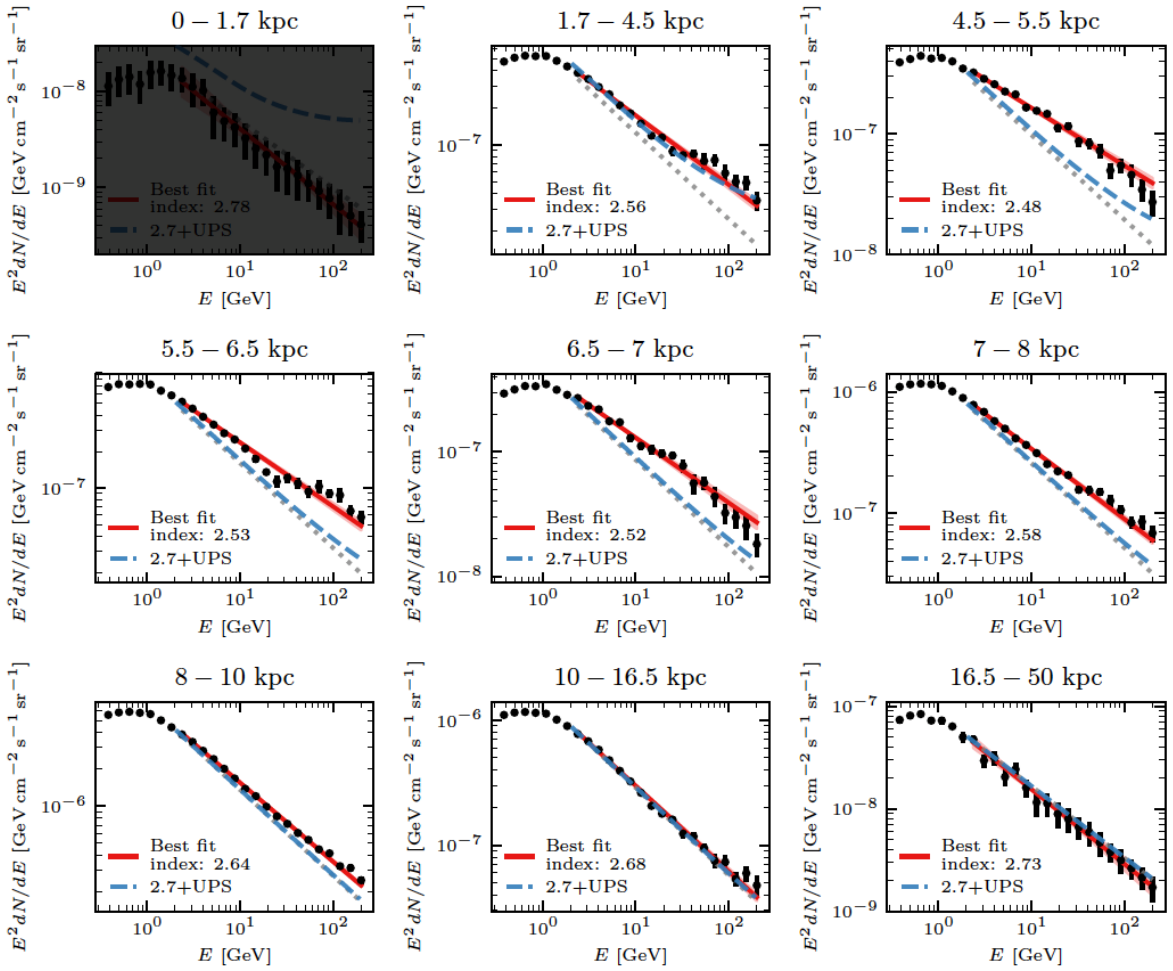

Spectral index of the CR diffuse emission (in the hypothesis that the unresolved contribution is negligible):

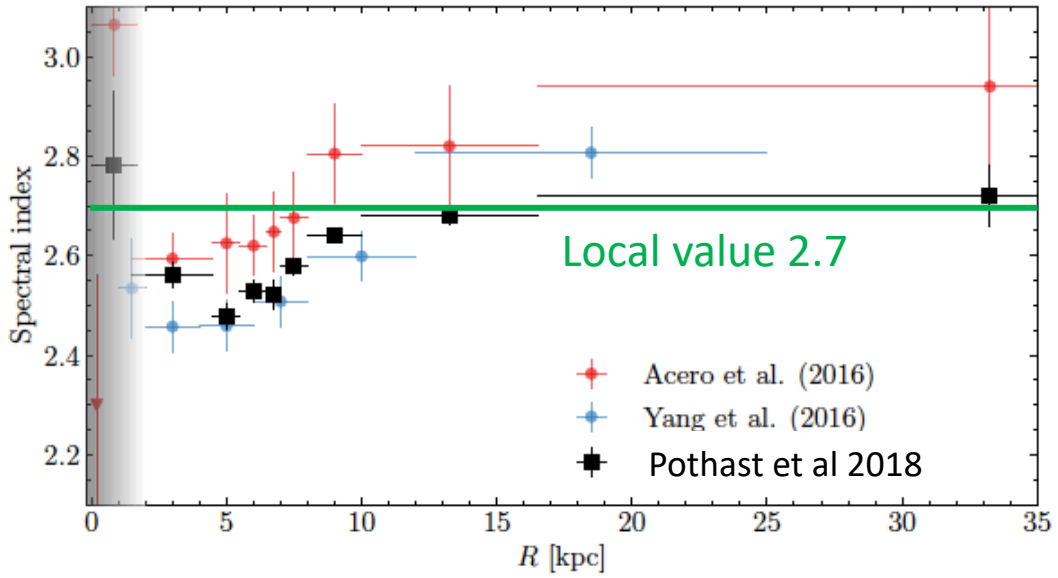

π_0 decay: $\alpha_\gamma \simeq \alpha_p - 0.1$

Indirect evidence of a progressive hardening of the CRs proton spectrum in the inner Galaxy

Total diffuse emission: 9.3 years of Fermi-LAT Pass 8 data (0.34−228.65) GeV and ($|l| < 180°, |b| < 20.25°$)

FERMI-LAT Data provided by Pothast et.al JCAP 2018

Implications of TeV PWNe at GeV energy range:

- TeV PWNe are expected to emit also at lower energies (subdominant class of sources since the Galactic GeV source population is dominated by pulsars);
- Some of them produce a signal that remains unresolved for Fermi-LAT
- Impact of unresolved TeV PWNe in the interpretation of the measured Fermi-LAT large-scale diffuse emission

$\phi_{\gamma,S}^{NR} + \phi_{\gamma,\mathrm{diff}}$ → **Measured**

Unresolved TeV PWNe and the hadronic diffuse emission add up and shape the radial and spectral behaviours of the total diffuse gamma ray emission observed by Fermi-LAT

Extrapolate to GeV range:

We define the phenomenological parameter: $R_\Phi = \frac{\Phi_{\mathrm{GeV}}}{\Phi_{\mathrm{TeV}}}$

We can calculate the total source flux and the unresolved sources in the energy range 1-100 GeV using our knowledge of the 1-100 TeV energy range:

$$\phi_{GeV}^{tot} = R_\phi \phi_{TeV}^{tot}$$

$$\frac{dN}{d\phi_{GeV}} = \frac{1}{R_\phi}\frac{dN}{d\phi_{TeV}}\left(\frac{\phi_{GeV}}{R_\phi}\right) \rightarrow \phi_{GeV}^{NR} = \int_0^{\phi_{GeV}^{th}} d\phi_{GeV}\phi_{GeV}\frac{dN}{d\phi_{GeV}} \propto \mathrm{R}_\phi^{\alpha-1}$$

Extrapolate to GeV range:

We define the phenomenological parameter: $R_\Phi = \dfrac{\Phi_{\mathrm{GeV}}}{\Phi_{\mathrm{TeV}}}$

We can calculate the total source flux and the unresolved sources in the energy range 1-100 GeV using our knowledge of the 1-100 TeV energy range:

$$\phi_{GeV}^{tot} = R_\phi \phi_{TeV}^{tot}$$

$$\frac{dN}{d\phi_{GeV}} = \frac{1}{R_\phi}\frac{dN}{d\phi_{TeV}}\left(\frac{\phi_{GeV}}{R_\phi}\right) \rightarrow \phi_{GeV}^{NR} = \int_0^{\phi_{GeV}^{th}} d\phi_{GeV}\phi_{GeV}\frac{dN}{d\phi_{GeV}} \propto \mathrm{R}_\phi^{\alpha-1}$$

We need a spectral assumption (motivated by observation):

$$\varphi_{\mathrm{PWN}}(E) = \varphi_0 \begin{cases} \left(\dfrac{E}{E_b}\right)^{-\beta_{GeV}} & E \le E_b \\ \left(\dfrac{E}{E_b}\right)^{-\beta_{TeV}} & E > E_b \end{cases}$$

$$R_\phi, E_b, \beta_{TeV} \rightarrow \beta_{GeV}$$

Parameter space:

Properties of 12 objects firmly identified as PWNe by both HGPS (*Abdalla et al, A&A, 612, A1 (2018)*) and 4FGL-DR2 (*Abdollahi et Al, Astrophys. J. Suppl. 247 (2020)*)

- $R_\phi = [250 - 1500]$;
- $E_0 = [0.1 - 1]$ TeV;
- $\beta_{TeV} = [1.9 - 2.5]$;
- $\beta_{GeV}(R_\Phi, E_0, \beta_{TeV}) = [1.06 - 2.19]$

Cumulative spectrum of sources with known distance;

Average value (red line):
$\beta_{TeV} = 2.4, E_b \sim 0.8\,TeV, R_\phi \sim 770, \rightarrow \beta_{GeV} \sim 1.9$

Cumulative spectrum (1 kpc)

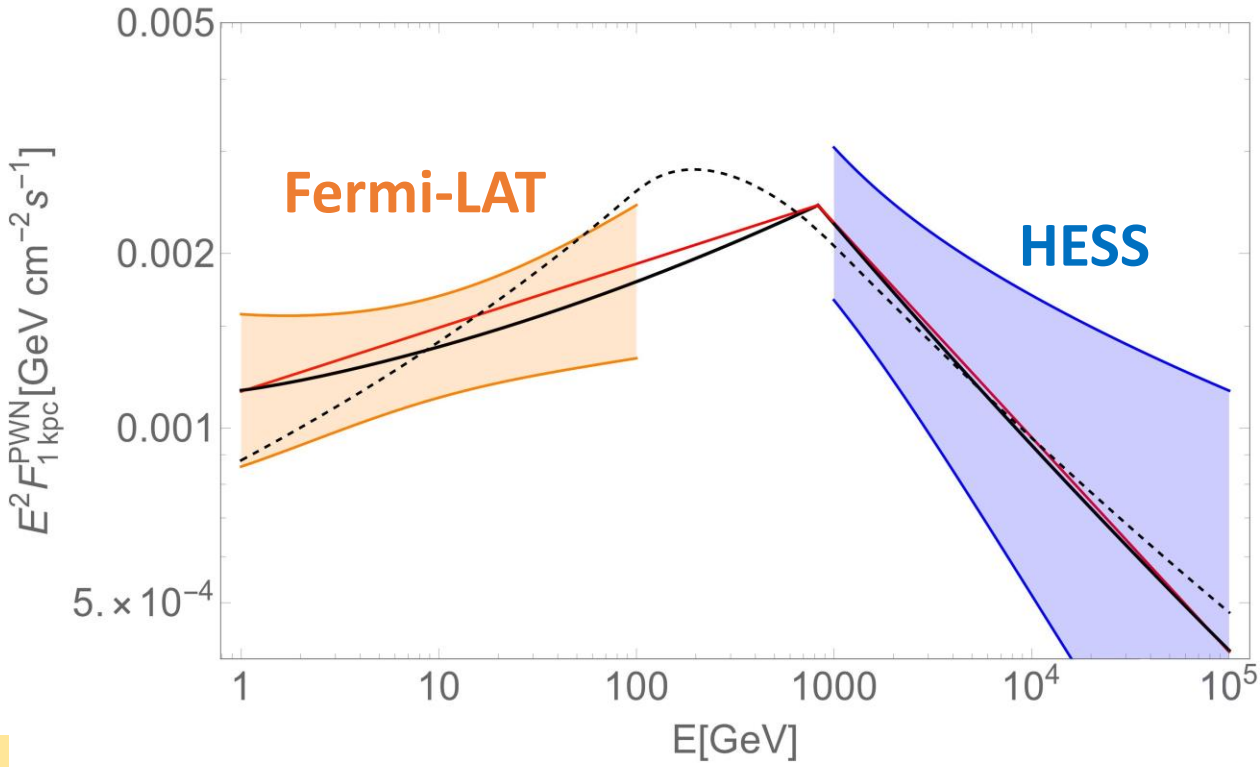

Unresolved PWNe by FermiLAT:

$\alpha = 1.8$

$$\frac{\phi_{NR}}{\phi_{PWN}} = (32\,\% - 46\,\%)$$

$\alpha = 1.5$

$$\frac{\phi_{NR}}{\phi_{PWN}} = (10\,\% - 24\,\%)$$

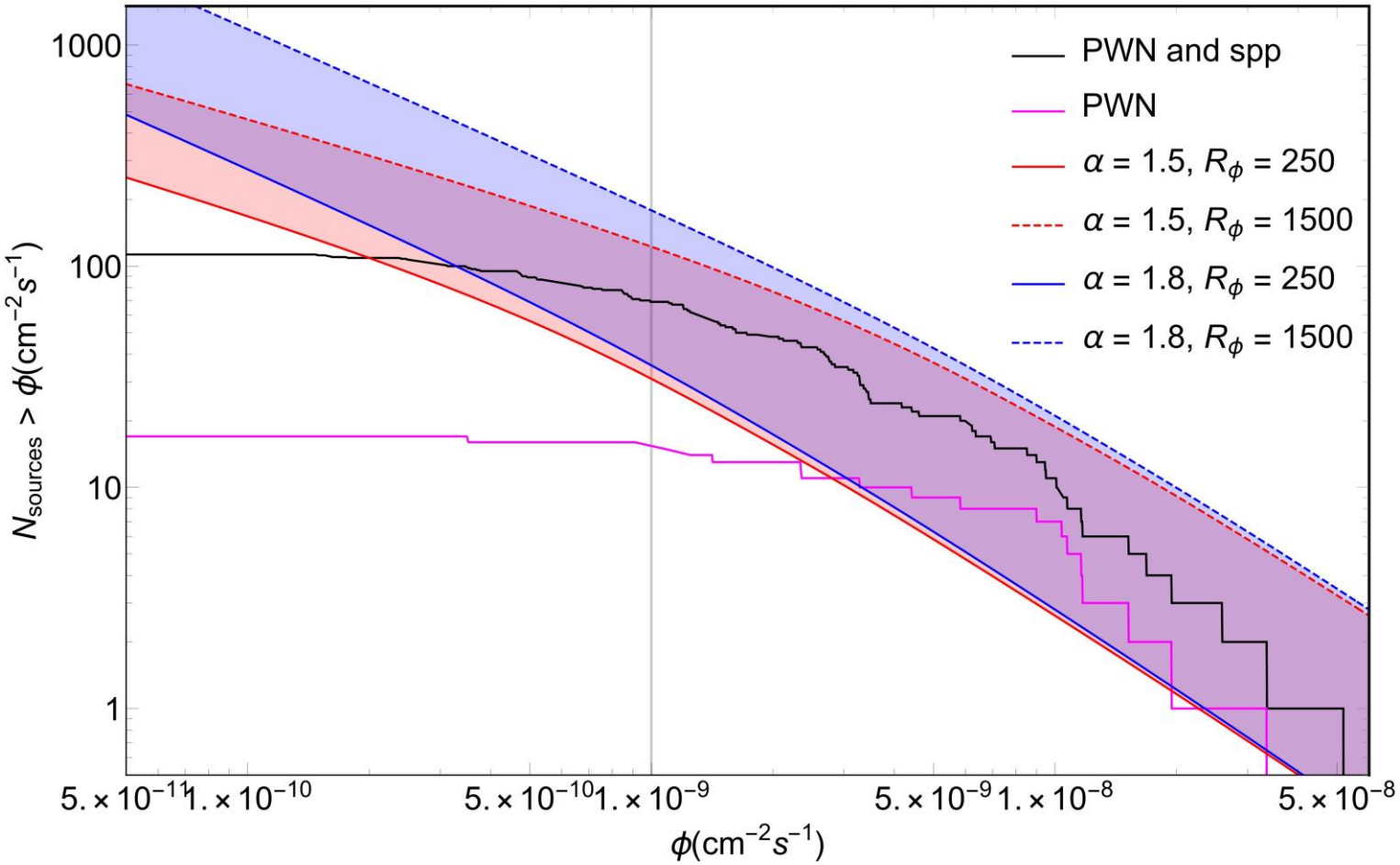

$$\Phi^{\rm th}_{\rm GeV} = 10^{-9}\,{\rm cm}^{-2}\,{\rm s}^{-1}$$ *Acero et.al. 2015*

Unresolved PWNe by FermiLAT:

$$\alpha = 1.8$$

$$\frac{\phi_{NR}}{\phi_{PWN}} = (32\,\% - 46\,\%)$$

$$\alpha = 1.5$$

$$\frac{\phi_{NR}}{\phi_{PWN}} = (10\,\% - 24\,\%)$$

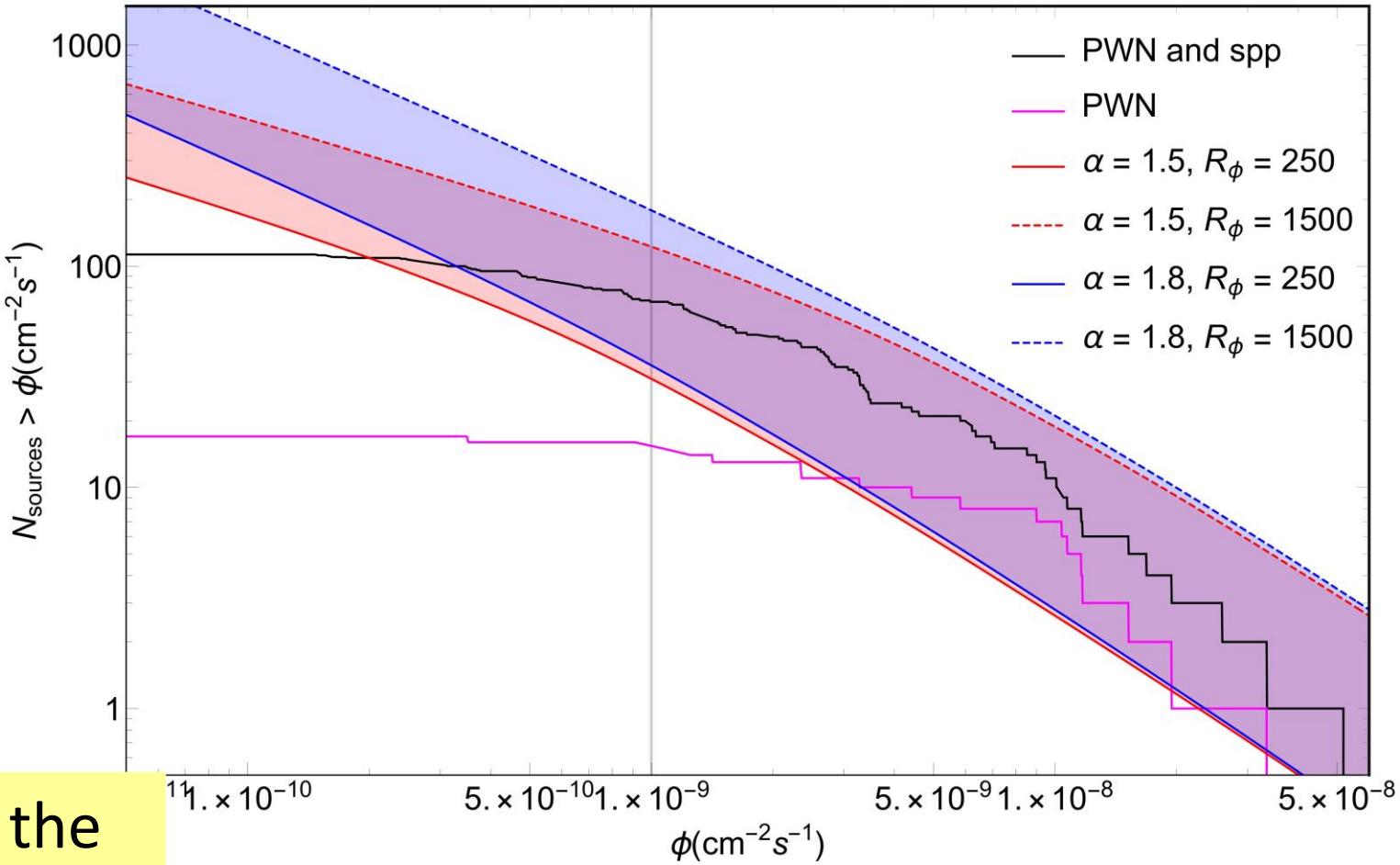

A non-negligible fraction of the TeV PWNe population cannot be resolved by Fermi-LAT

$$\Phi_{\rm GeV}^{\rm th} = 10^{-9}\,{\rm cm}^{-2}\,{\rm s}^{-1}$$ *Acero et.al. 2015*

Reinterpreting the diffuse emission observed by Fermi:

The unresolved PWNe account up to the 36 % of the total diffuse emission in the ring 1.7-4.5 kpc.

Reinterpreting the diffuse emission observed by Fermi-LAT:

The unresolved PWNe account up to the 36 % of the total diffuse emission in the ring 1.7-4.5 kpc.

Diffuse emission (Power-Law):

$$\Gamma_1 = 2.56$$

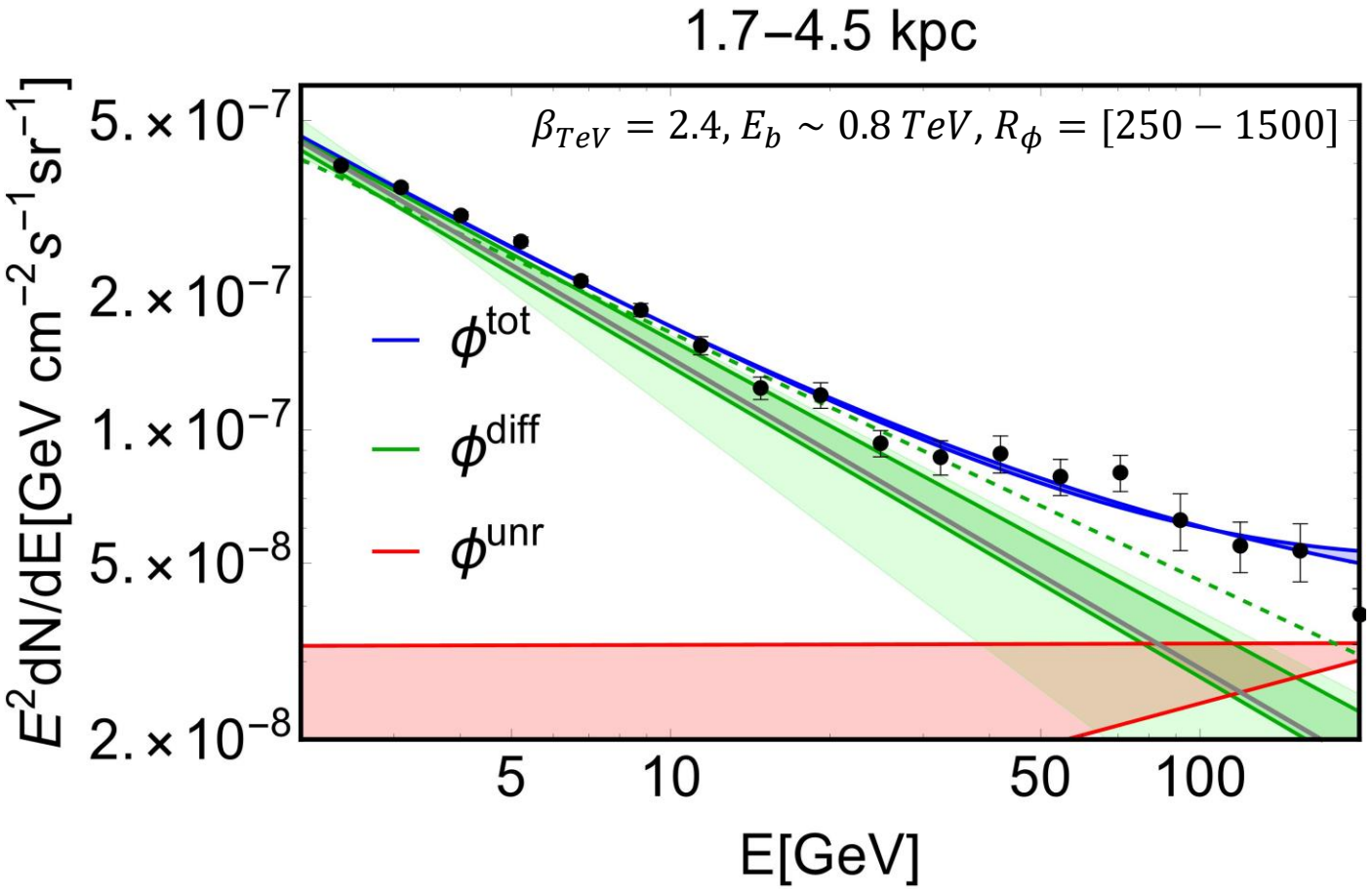

Reinterpreting the diffuse emission observed by Fermi-LAT:

The unresolved PWNe account up to the 36 % of the total diffuse emission in the ring 1.7-4.5 kpc.

Diffuse emission (Power-Law):

$$\Gamma_1 = 2.56$$

Diffuse emission (Power-Law)
+ Uresolved PWNe

$$\Gamma_{BF} = 2.64 - 2.71$$

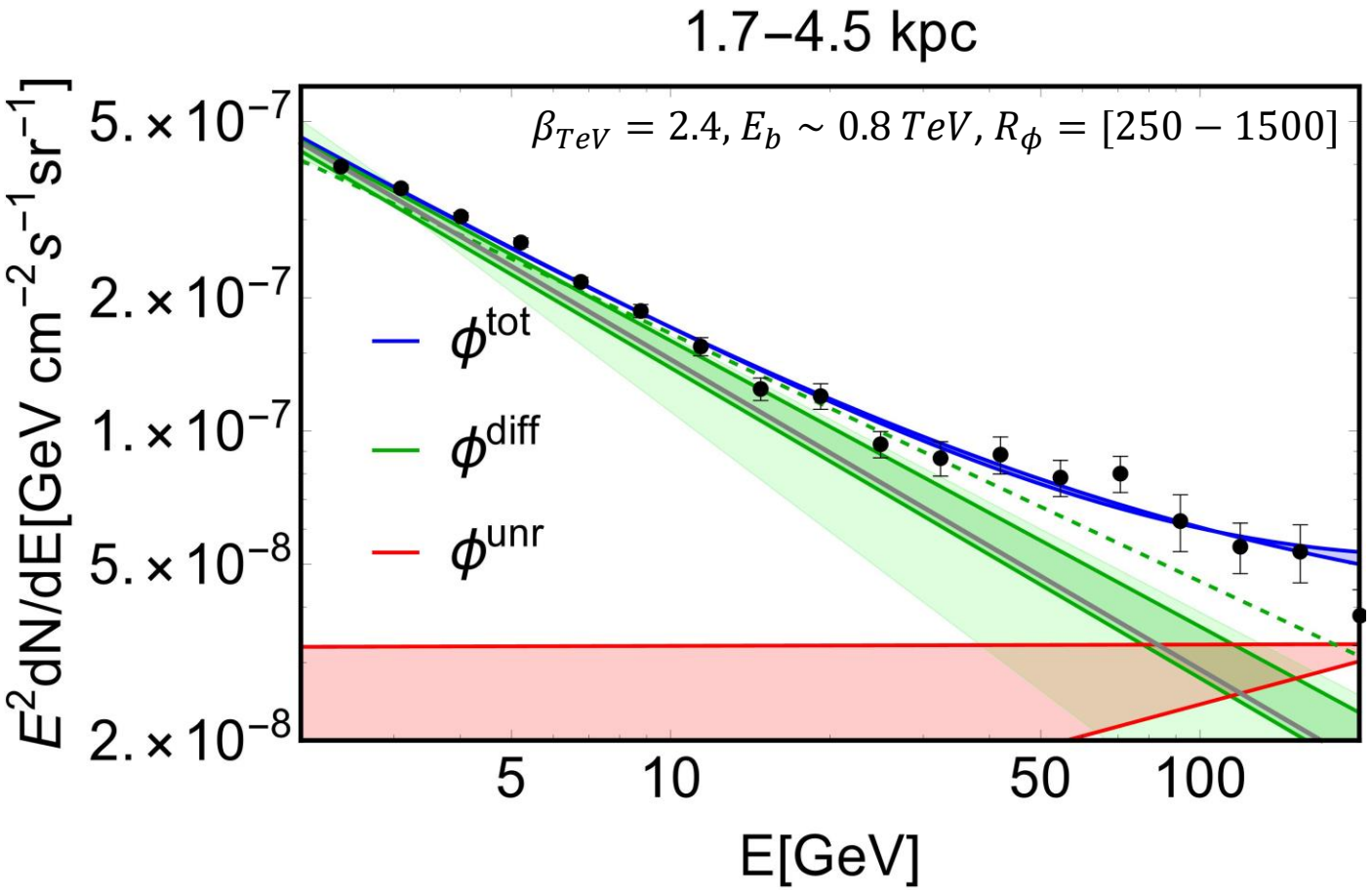

Spectral index and gamma-ray emissivity ($\alpha = 1.8$):

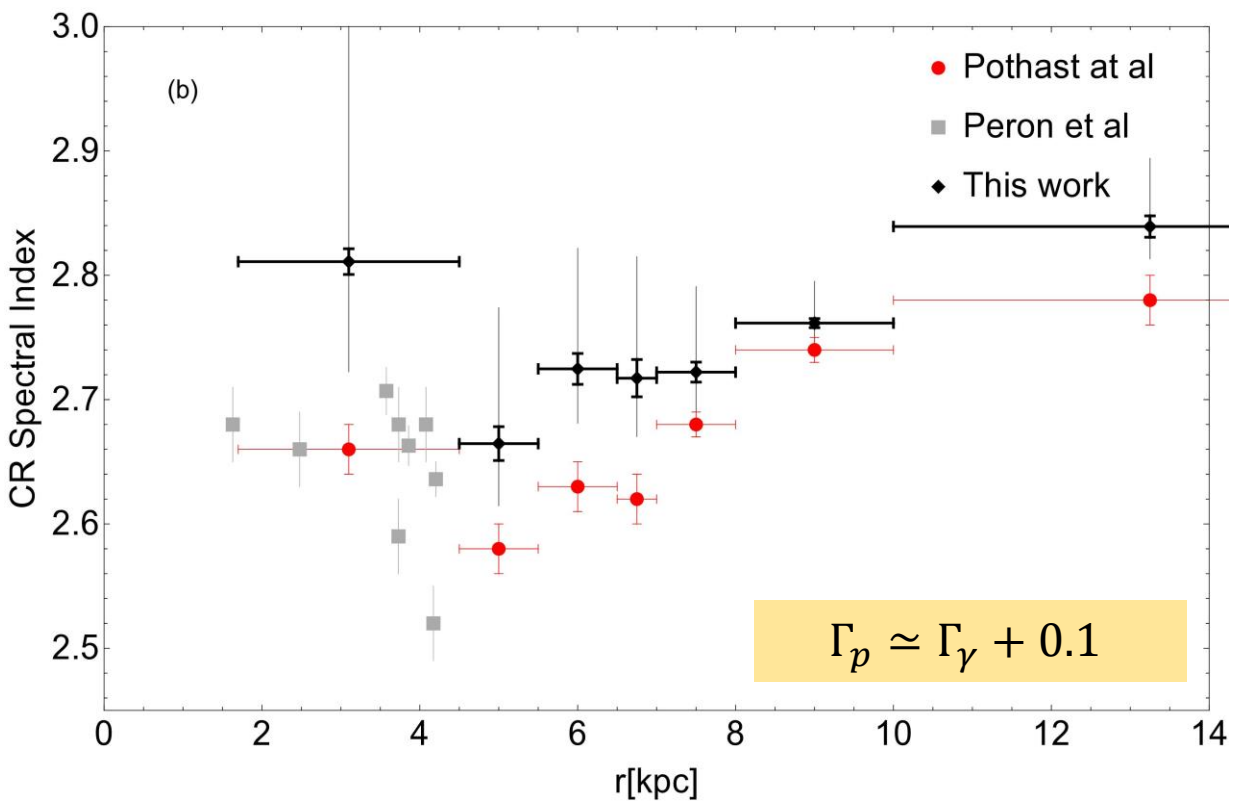

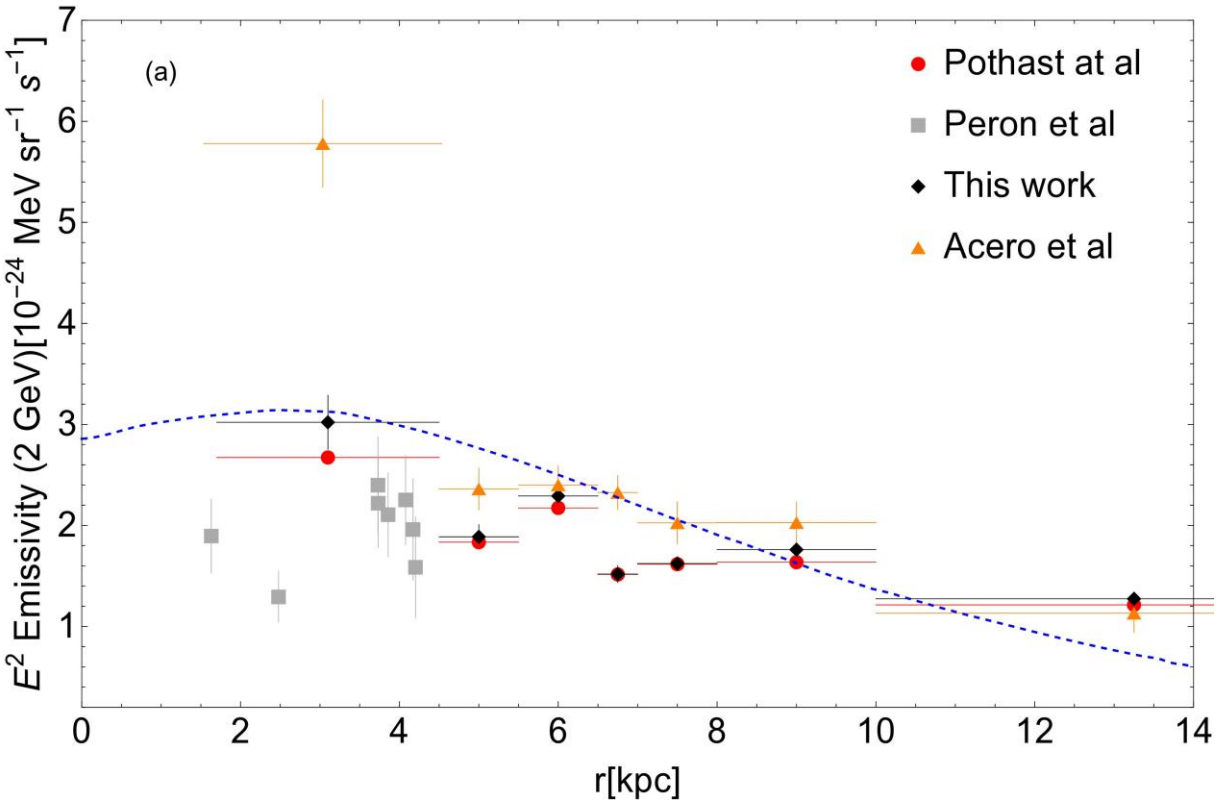

- PWNe contribution accounts for a part of the spectral index variation observed by Fermi-LAT in particular in the inner Galaxy;

Take home message:

- A non-negligible fraction of the TeV PWNe population cannot be resolved by Fermi-LAT

- TeV unresolved PWNe contribution could account for a part of the spectral index variation observed by Fermi-LAT in particular in the inner Galaxy;

Sub PeV energy range

Vecchiotti et al, Astrophys. J. (2022)

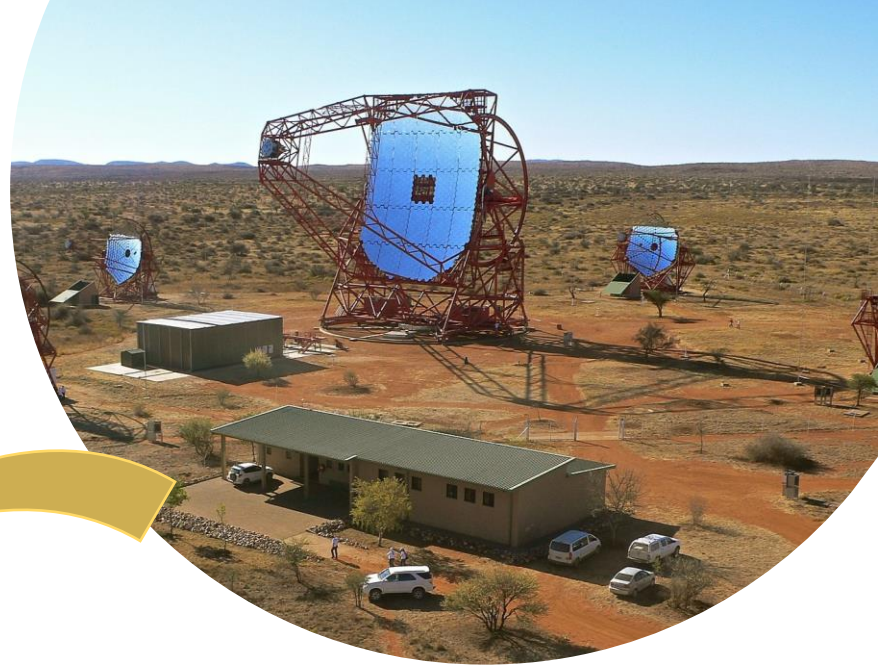

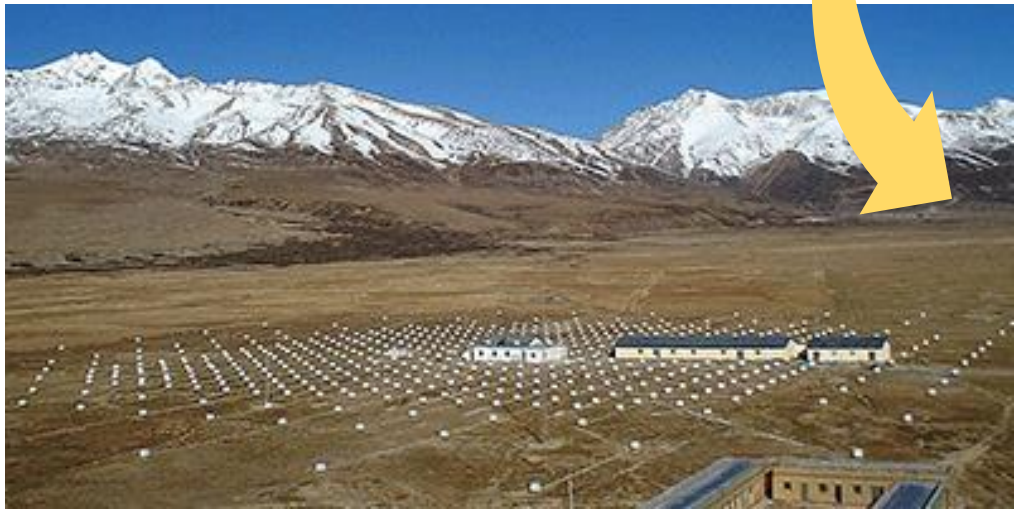

Tibet ASγ :

Amenomori, M., et al. 2021, Phys. Rev. Lett., 126, 141101,326

$\phi_{\gamma,\mathrm{diff}}^{Tibet}$ → First measurement of the Galactic diffuse γ-ray emission in the sub-PeV energy range.

→ They exclude the contribution from the known TeV sources (within 0.5 degrees) listed in the TeV source catalog.

Tibet ASγ :

Amenomori, M., et al. 2021, Phys. Rev. Lett., 126, 141101,326

$\phi_{\gamma,\mathrm{diff}}^{Tibet}$ → First measurement of the Galactic diffuse γ-ray emission in the sub-PeV energy range.

→ They exclude the contribution from the known TeV sources (within 0.5 degrees) listed in the TeV source catalog.

The Tibet measurements are contaminated by the presence of Unresolved Sources

$$\phi_{\gamma,\mathrm{diff}}^{Tibet} = \phi_{\gamma,S}^{UnRes} + \phi_{\gamma,\mathrm{diff}}$$

Population study (H.E.S.S.)→ we obtain general information on the sources

Models: Assumptions on the CR spatial and energy distributions.

Diffuse Galactic gamma-ray emission:

Definition: Hardening ≡ spatially dependent CR spectral index

$25° < l < 100°, |b| < 5°$

- Tibet
- Argo

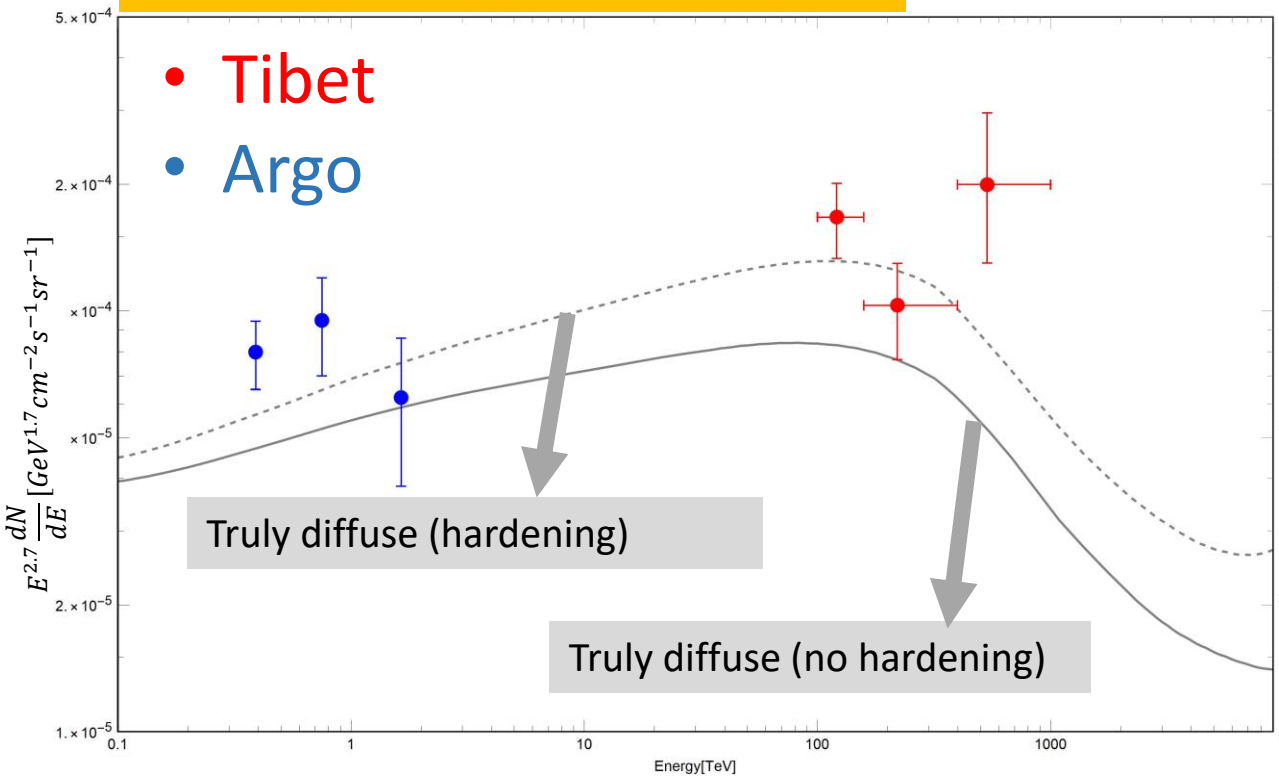

$50° < l < 200°, |b| < 5°$

- Tibet
- Casa Mia

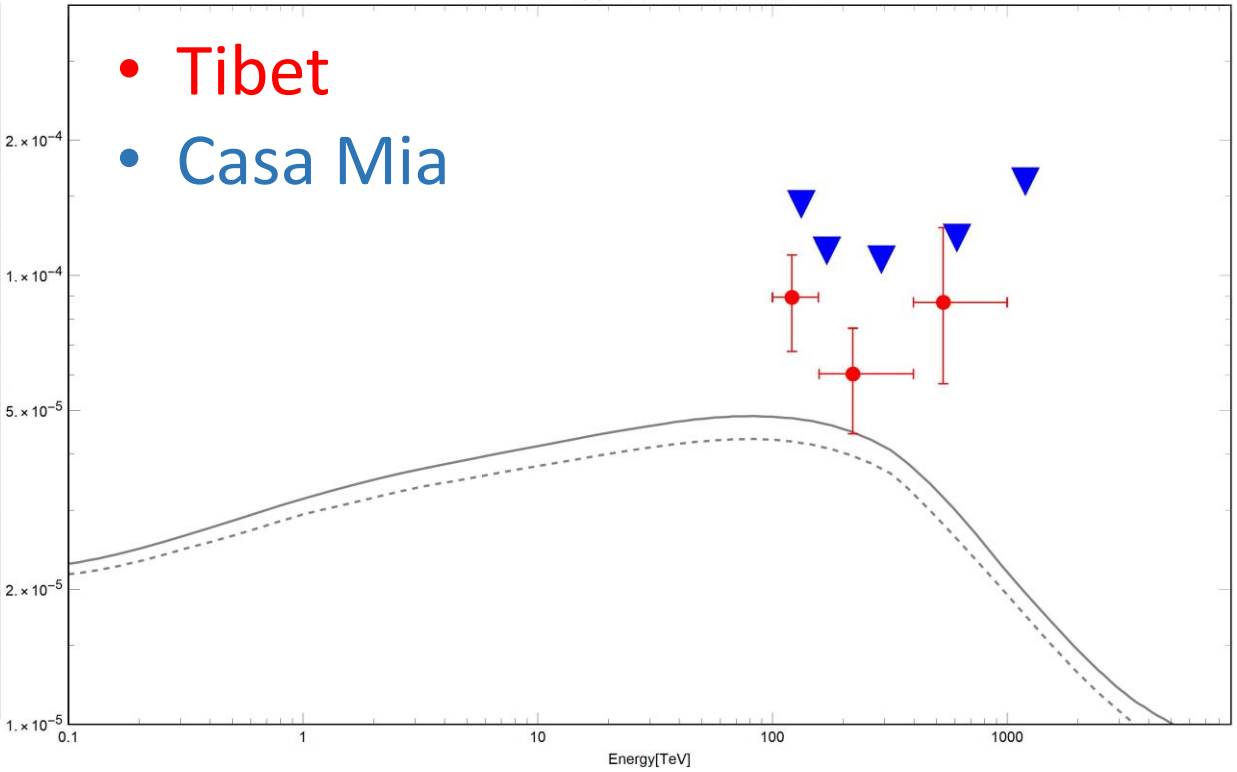

Similar results are obtained using the models described in Lipari & Vernetto, Phys. Rev. D (2018)

Unresolved Source component:

We have $\Phi_{1-100\ TeV}$ → we need $\phi(E)$:

- Spectral assumption: power-law with an exponential cut-off.

$$\varphi(E) = \left(\frac{E}{1\ TeV}\right)^{-\beta_{TeV}} Exp\left(-\frac{E}{E_{cut}}\right)$$

$\beta_{TeV} = 2.3$ from the HGPS catalogue;

Unresolved Source component:

We have $\Phi_{1-100\ TeV}$ → we need $\phi(E)$:

- Spectral assumption: power-law with an exponential cut-off.

$$\varphi(E) = \left(\frac{E}{1\ TeV}\right)^{-\beta_{TeV}} Exp\left(-\frac{E}{E_{cut}}\right)$$

$\beta_{TeV} = 2.3$ from the HGPS catalogue;

$E_{cut} = 500\ TeV$ still not well constrained but motivated by recent observations of Tibet, HAWC and LHAASO;

Amenomori, M., Bao, Y. W., Bi, X. J., et al. 2019, Phys.323Rev. Lett., 123, 051101

Abeysekara, A., Albert, A., Alfaro, R., et al. 2020, Physical316Review Letters, 124

Cao, Z., Aharonian, F. A., An, Q., et al. 2021, Nature, 594,33033

Unresolved Source component:

We have $\Phi_{1-100\ TeV}$ → we need $\phi(E)$:

- Spectral assumption: power-law with an exponential cut-off.

$$\varphi(E) = \left(\frac{E}{1\ TeV}\right)^{-\beta_{TeV}} Exp\left(-\frac{E}{E_{cut}}\right)$$

$\beta_{TeV} = 2.3$ from the HGPS catalogue;

$E_{cut} = 500\ TeV$ still not well constrained but motivated by recent observations of Tibet, HAWC and LHAASO;

Amenomori, M., Bao, Y. W., Bi, X. J., et al. 2019, Phys.323Rev. Lett., 123, 051101

Abeysekara, A., Albert, A., Alfaro, R., et al. 2020, Physical316Review Letters, 124

Cao, Z., Aharonian, F. A., An, Q., et al. 2021, Nature, 594,33033

We introduce a flux detection threshold based on the performance of H.E.S.S.

$\phi_{th} = 0.01\phi_{crab} - 0.1\phi_{crab}$

We calculate the unresolved source contribution.

Tibet ASγ : We add the contribution of unresolved sources to the truly diffuse emission without the hypothesis of CR spectral hardening.

Tibet ASγ : We add the contribution of unresolved sources to the truly diffuse emission without the hypothesis of CR spectral hardening.

Definition: Hardening ≡ spatially dependent CR spectral index

$$25° < l < 100°, |b| < 5°, E_{cut} = 500\ TeV$$

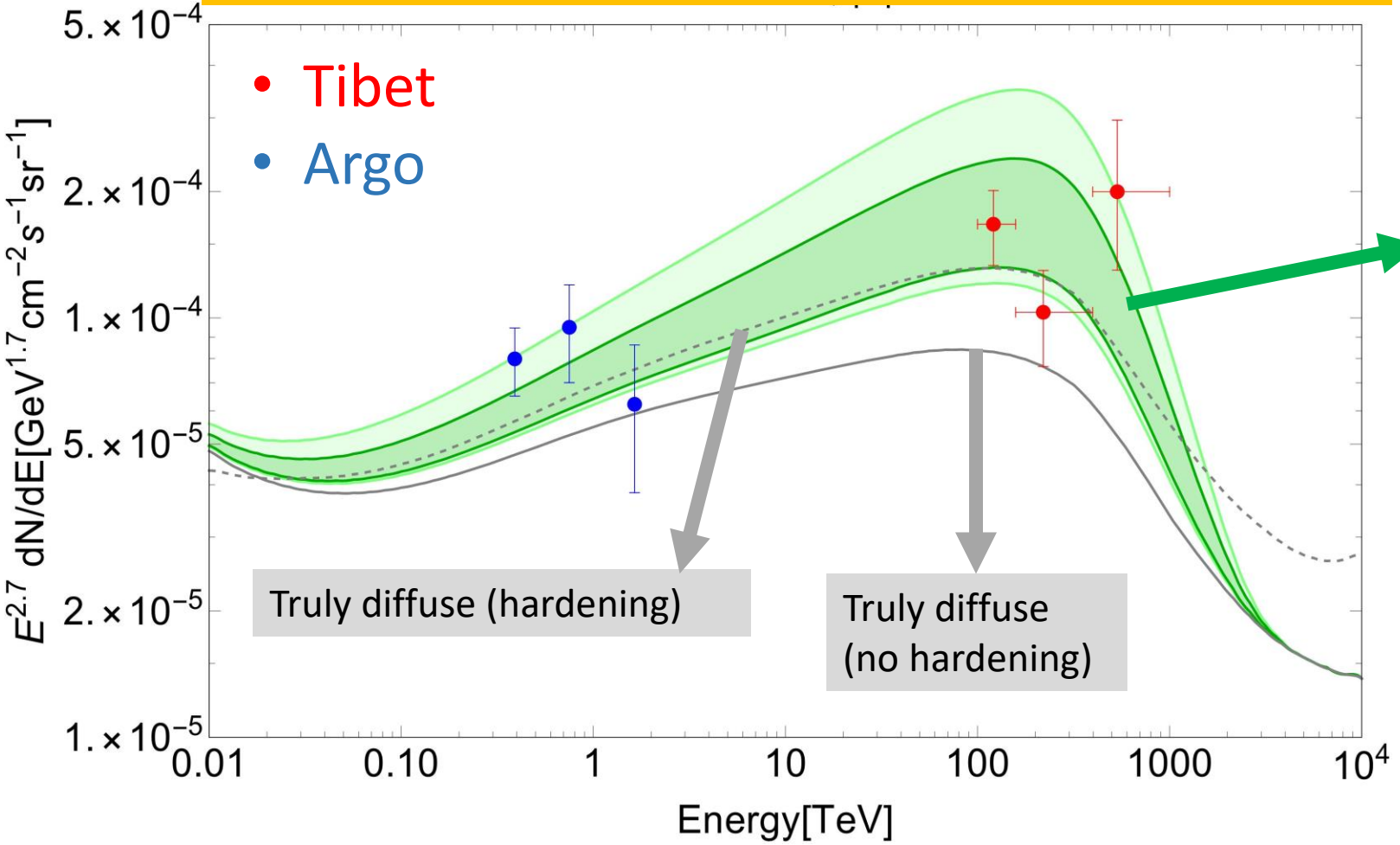

Luminosity index: $\alpha = 1.5$

Unresolved sources +
Truly diffuse (no hardening)

Tibet ASγ : We add the contribution of unresolved sources to the truly diffuse emission without the hypothesis of CR spectral hardening.

Definition: Hardening ≡ spatially dependent CR spectral index

$$50° < l < 200°, |b| < 5°, E_{cut} = 500\ TeV$$

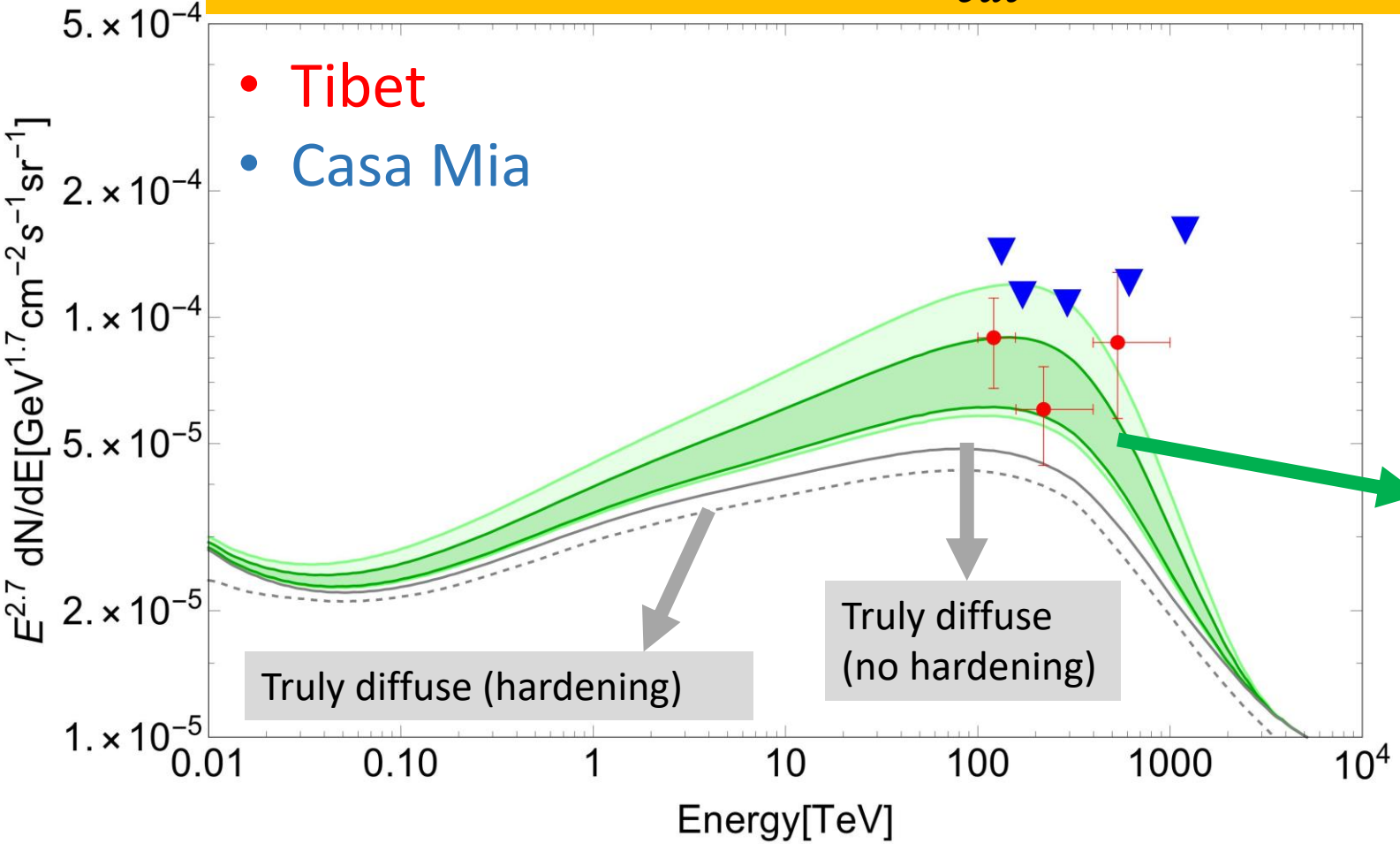

Luminosity index: $\alpha = 1.5$

Unresolved sources +
Truly diffuse (no hardening)

Take home message:

- In the **PeV** energy range the inclusion of the **unresolved PWNe** contribution produces a better description of the Tibet data than CR spectral hardening;

Looking at different sky regions is fundamental because it allows us to distinguish between the two effects.

Conclusions and outlook:

- The diffuse gamma-ray and neutrino emission can provide important information about CR spatial and energy distribution in the Galaxy;
- We modeled the gamma diffuse emission. We considered four different hypotheses for the CR distribution;
- We test these models with TeV observations. We conclude that the spatially-dependent CR spectral hardening hypothesis with R=1 kpc is in tension with gamma-ray observation in the TeV energy range if the contribution of unresolved sources is non-negligible;

Conclusions and outlook:

- The diffuse gamma-ray and neutrino emission can provide important information about CR spatial and energy distribution in the Galaxy;
- We modeled the gamma diffuse emission. We considered four different hypotheses for the CR distribution;
- We test these models with TeV observations. We conclude that the spatially-dependent CR spectral hardening hypothesis with R=1 kpc is in tension with gamma-ray observation in the TeV energy range if the contribution of unresolved sources is non-negligible;

- We performed a population study of the HGPS catalog in order to infer the general properties of TeV sources (e.g. to determine their luminosity distribution, the total luminosity, the total flux, etc) and to estimate unresolved source component.
- The contribution of unresolved sources is not negligible and it is about ∼60 % of the resolved signal measured by H.E.S.S.;

Conclusions and outlook:

- We show that a non-negligible fraction of TeV PWNe cannot be resolved by Fermi-LAT;
- We performed a Galactocentric ring analysis of the measured large-scale diffuse emission including the contribution of both unresolved TeV PWNe and the hadronic diffuse emission;
- We show that the inclusion of unresolved TeV PWNe could account for a part of the spectral index variation observed by Fermi-LAT, in particular in the inner Galaxy;

Conclusions and outlook:

- We show that a non-negligible fraction of TeV PWNe cannot be resolved by Fermi-LAT;
- We performed a Galactocentric ring analysis of the measured large-scale diffuse emission including the contribution of both unresolved TeV PWNe and the hadronic diffuse emission;
- We show that the inclusion of unresolved TeV PWNe could account for a part of the spectral index variation observed by Fermi-LAT, in particular in the inner Galaxy;

- We calculate the unresolved component in the sub-PeV energy range using our knowledge of the TeV source population.
- We add the contribution of unresolved sources to the truly diffuse emission without the hypothesis of CR spectral hardening;
- In the sub-PeV energy range the inclusion of the unresolved PWNe contribution produces a better description of the Tibet data than CR spectral hardening;

Conclusions and outlook:

- Study of **Molecular Clouds** emission.

  Vecchiotti et al, RICAP 2022, EPJ Web Conf (2023)

- Introduce a **theoretical model** to describe the **gamma-ray emission from PWNe.**

- Calculate the **neutrino emission from Galactic sources.**

Backup slides

Diffuse Galactic γ and ν emission:

$$\phi_{\gamma,tot} = \phi_{\gamma,S} + \phi_{\gamma,\mathrm{diff}} + \cancel{\phi_{\gamma,IC}}$$

$$\varphi_\gamma^{diff}(E_\gamma, \hat{n}_\gamma) = \int_{E_\gamma}^{\infty} dE \frac{d\sigma(E, E_\gamma)}{dE_\gamma} \int_0^{\infty} dl\, \varphi_{CR}(E, \bar{r}_{Sun} + l\hat{n}_\gamma)\, n_H(\bar{r}_{Sun} + l\hat{n}_\gamma)$$

Differential inelastic cross section of pp interaction from the SYBILL code *[Kelner,Aharonian,Bugayov (2006)]*

Cosmic-ray energy and spatial distribution

Interstellar gas distribution in the Galaxy [*Galprop*]

4 models for the diffuse fluxes **for 4 assumptions of the CR distribution** in the Galaxy.

Interstellar gas distribution in the Galaxy [*Galprop*]

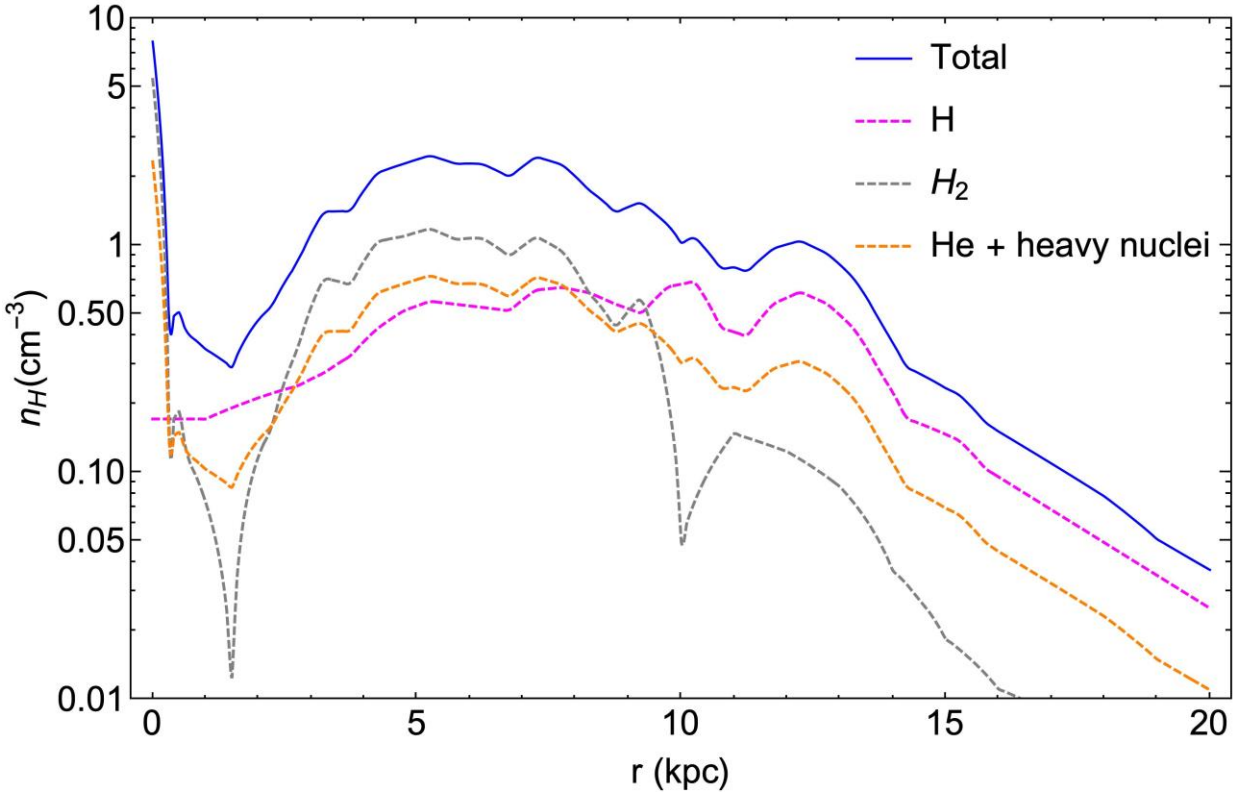

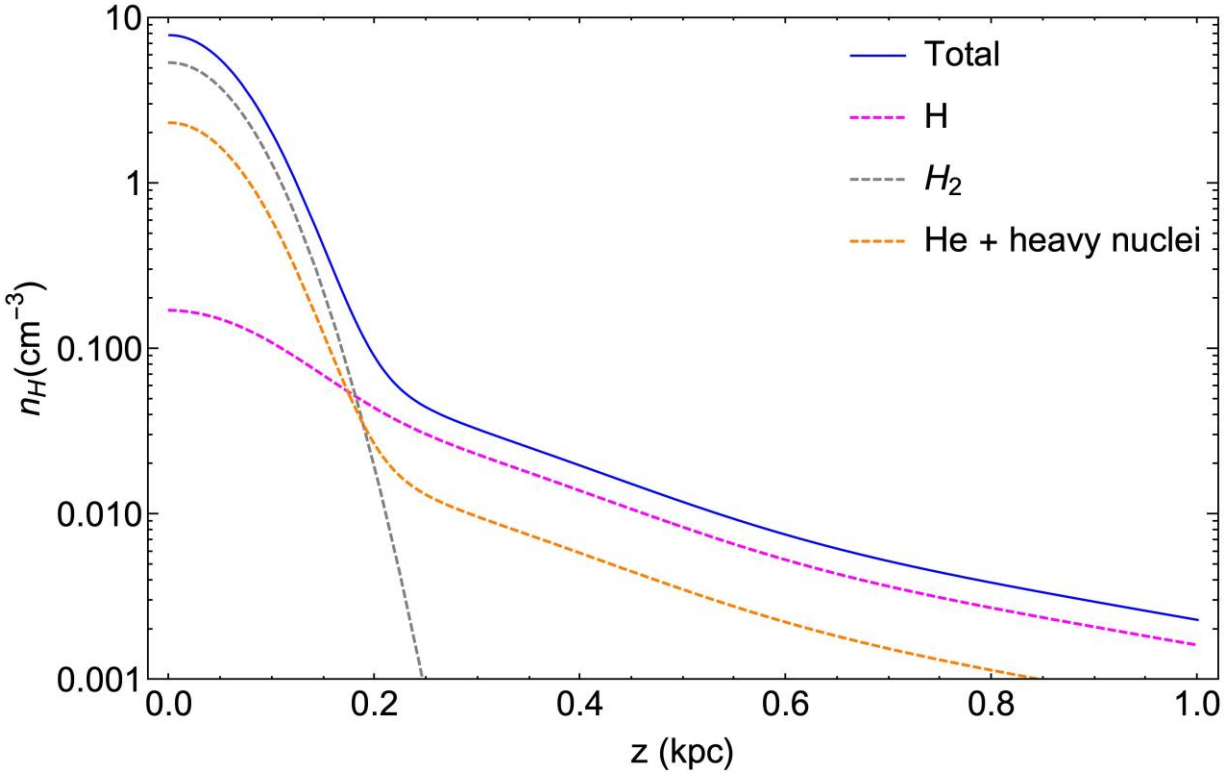

CR local spectrum

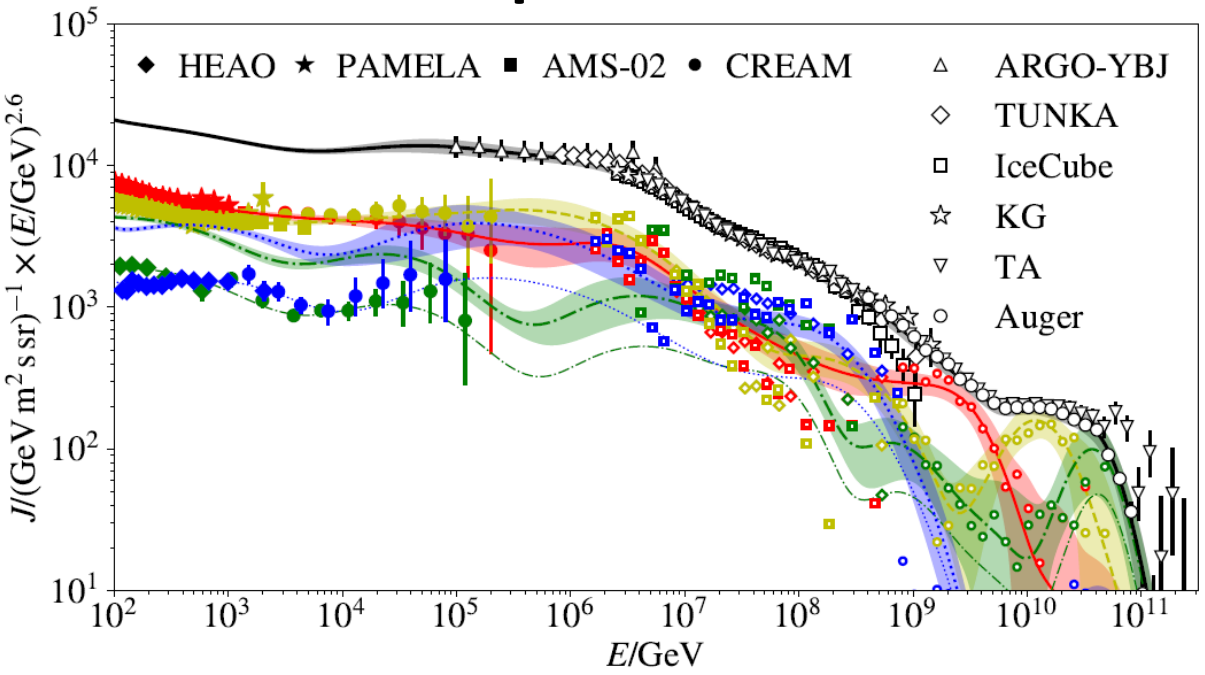

At energies of few PeV, the CR spectrum is affected by large uncertainties:

- It is a transition region between different detection techniques;
- Transition from Galactic to extragalactic CRs.
- CRs compositions;

The diffuse emission is determined by the total nucleon flux that depends on the CR composition.

$$\varphi_{CR,Sun}(E) = \sum_A A^2 \frac{d\phi_A}{dE_A d\Omega_A}(AE)$$

CR nucleons spectrum

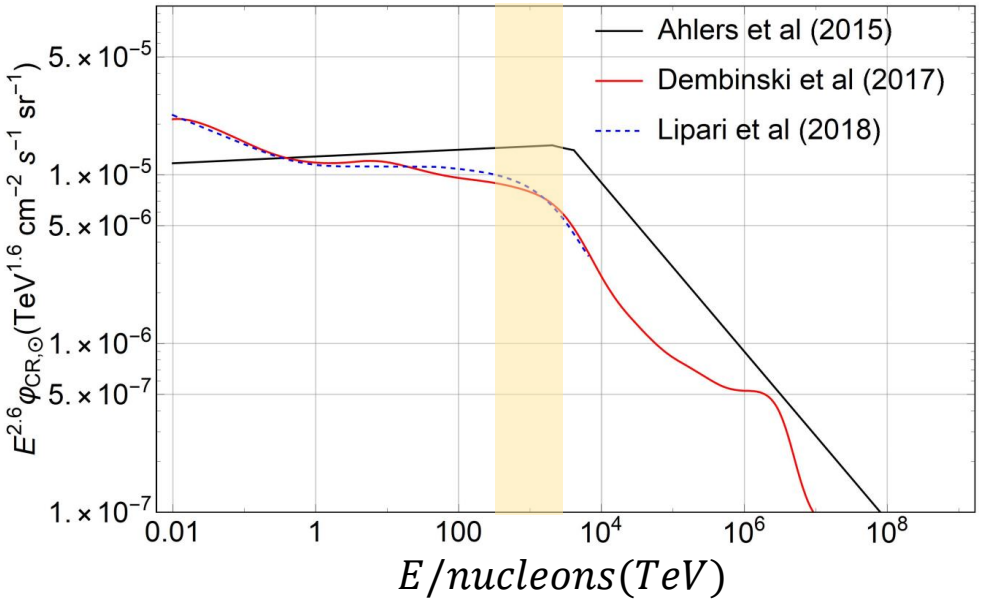

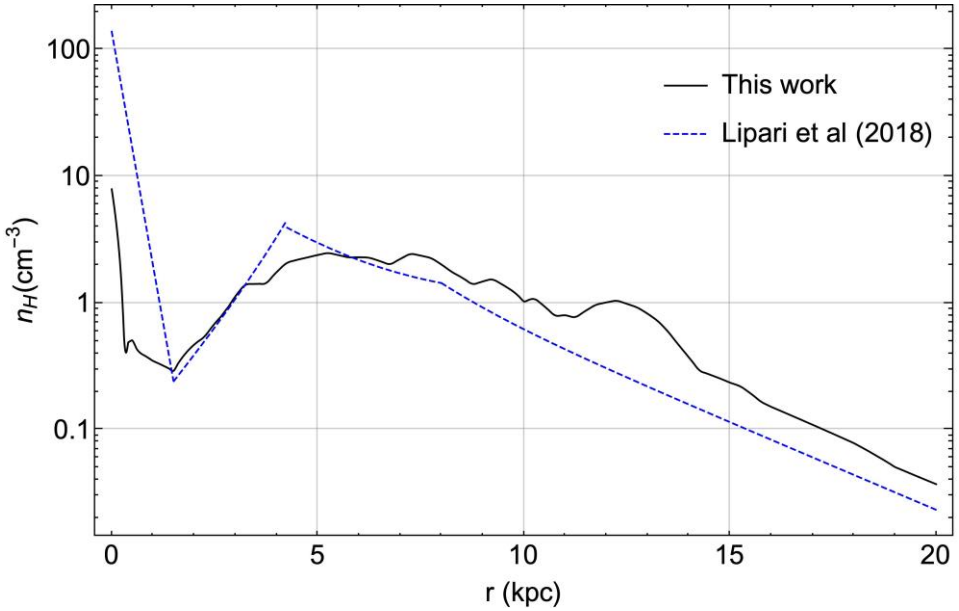
This work
Lipari et al (2018)
n_H(cm^{-3})
r (kpc)

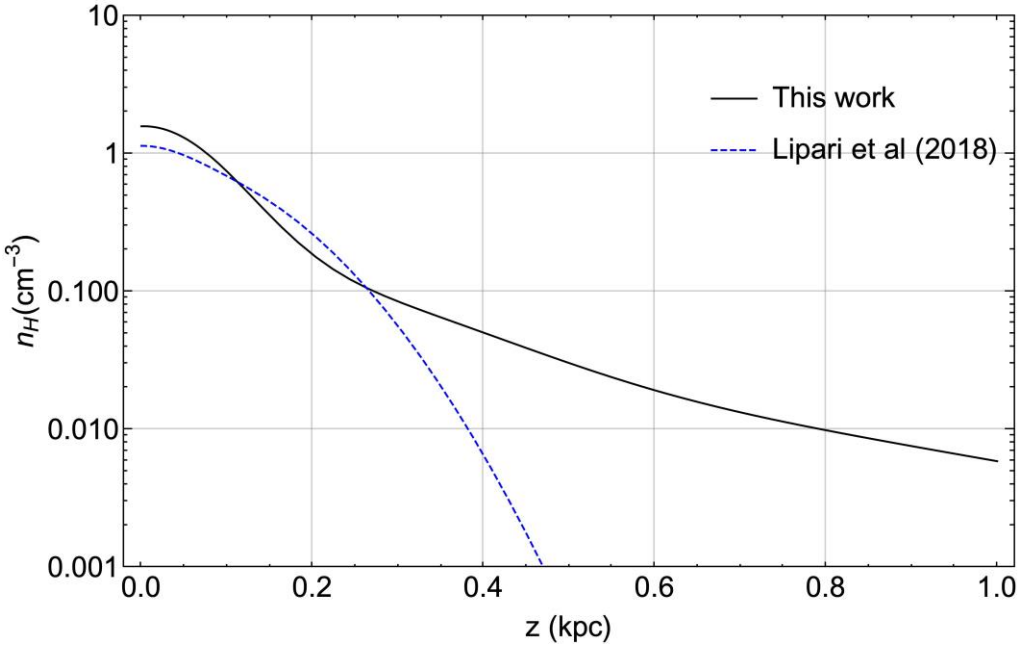
This work
Lipari et al (2018)
n_H(cm^{-3})
z (kpc)

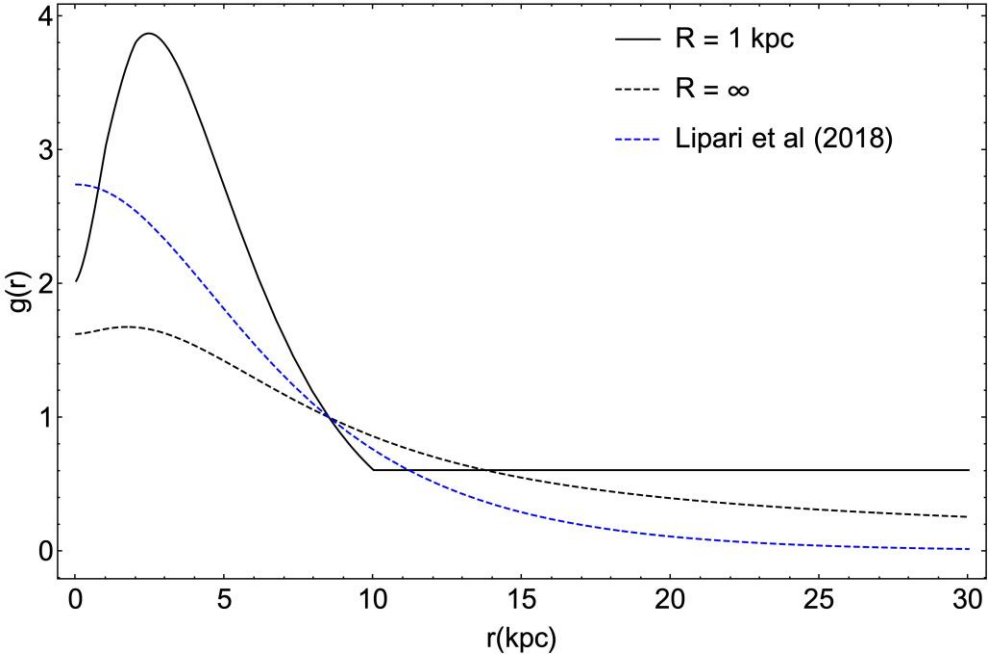
R = 1 kpc
R = ∞
Lipari et al (2018)
g(r)
r(kpc)

Diffuse Galactic neutrino emission:

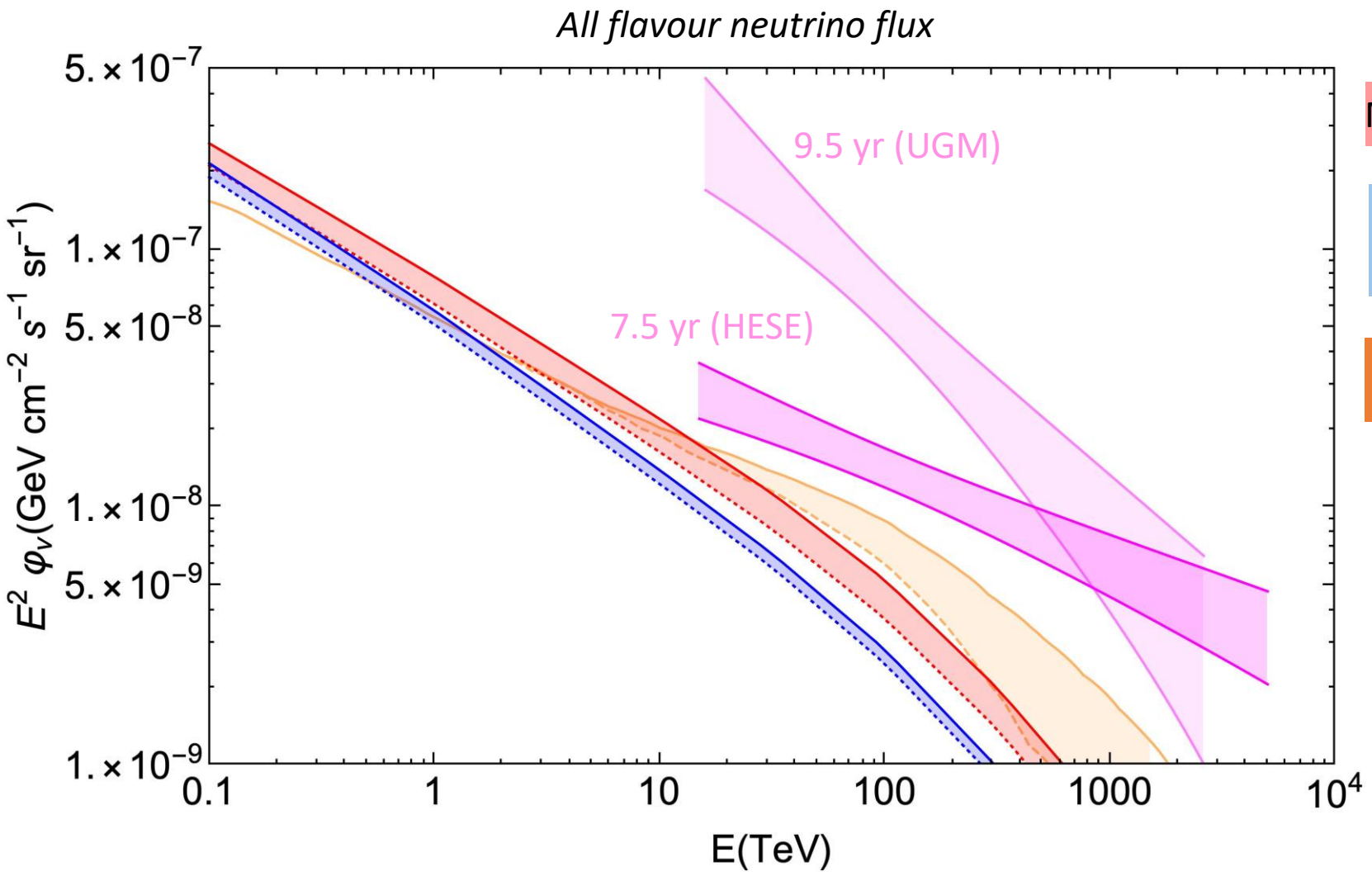

Model with hardening

Model without hardening

KRA_γ ($\frac{E_{cut}}{n} = 5 - 50\ PeV$)

Diffuse Galactic γ and ν emission:

Model without hardening

$R = 1\ kpc$

$R = \infty$

Model with hardening

$R = 1\ kpc$

$R = \infty$

$gamma\ ray$

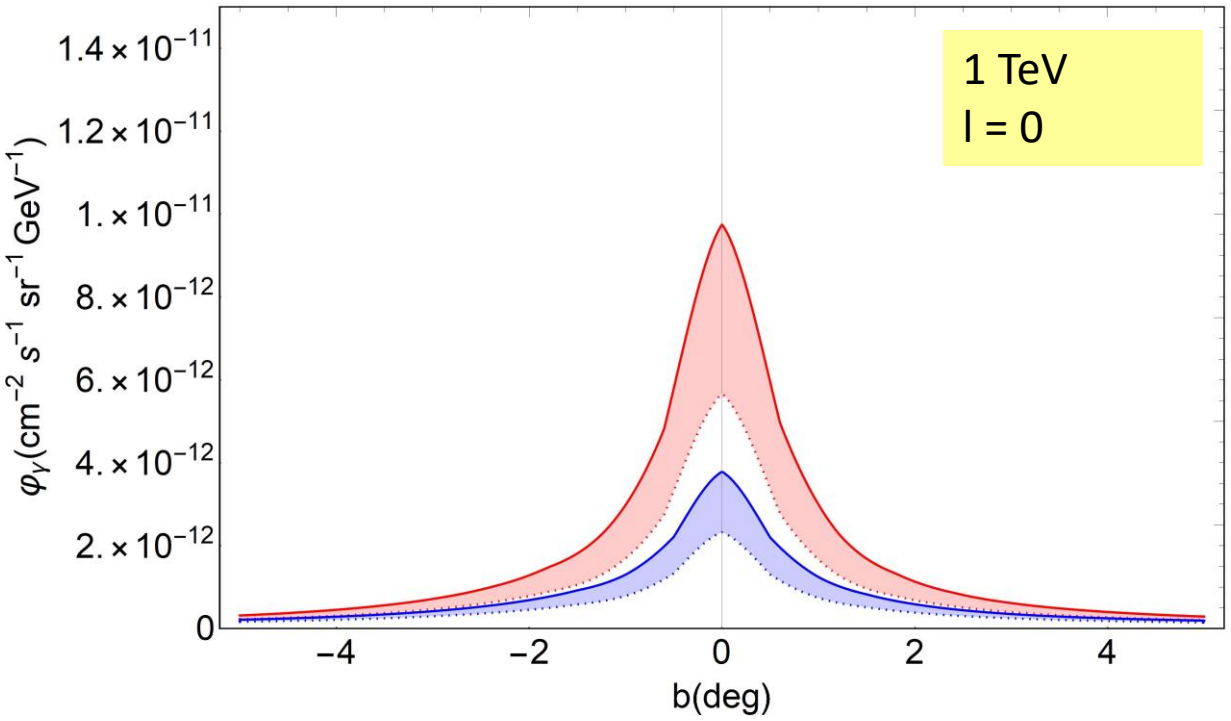

$neutrino$

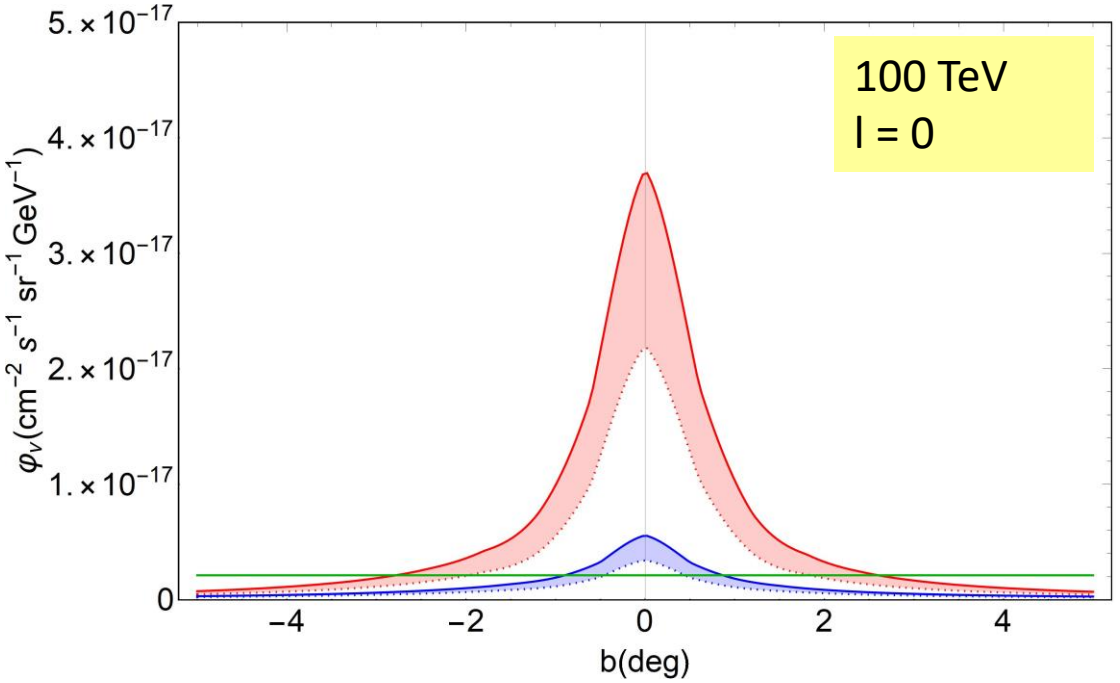

Comparison with the total observed flux:

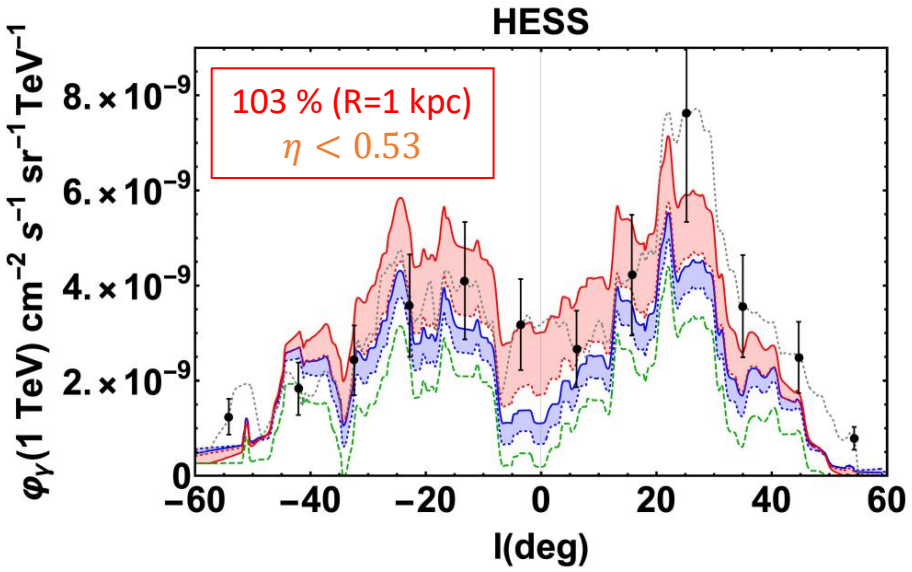

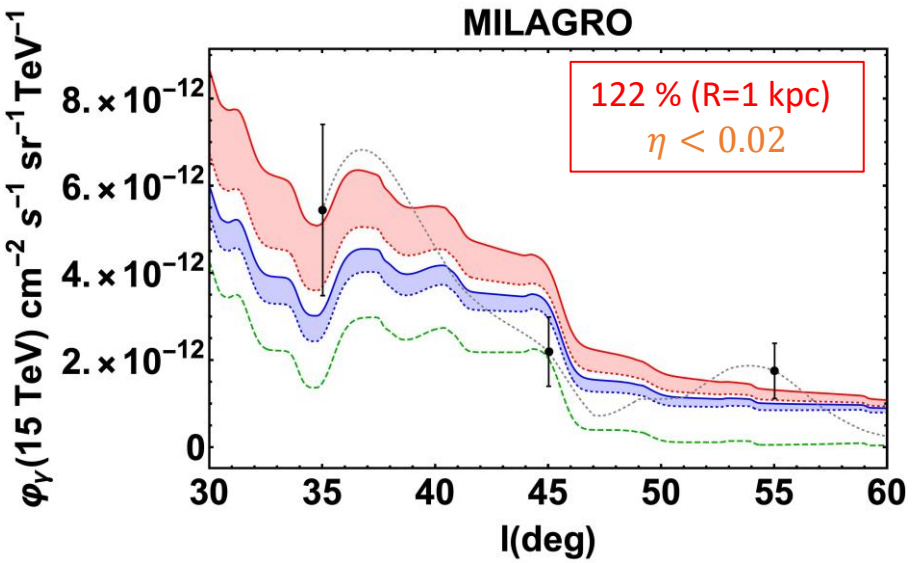

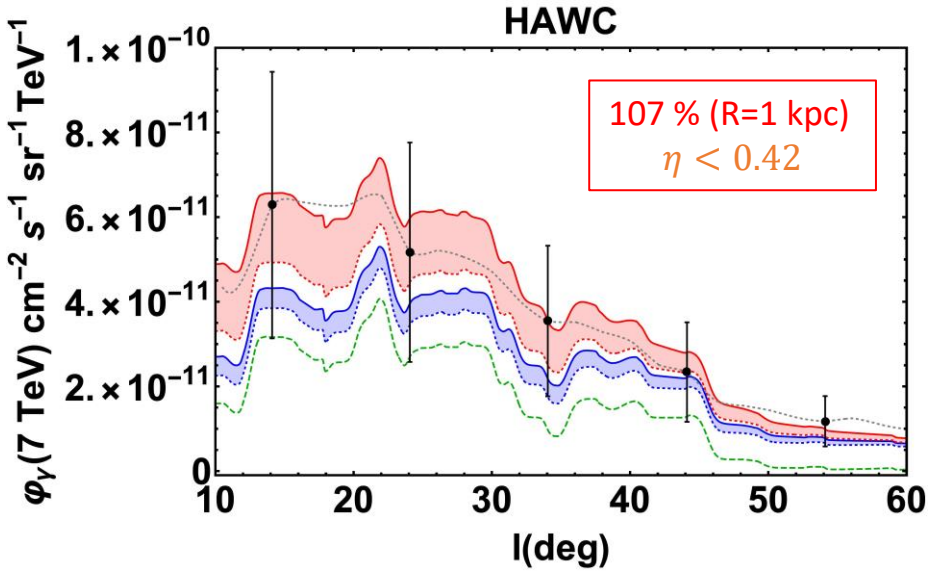

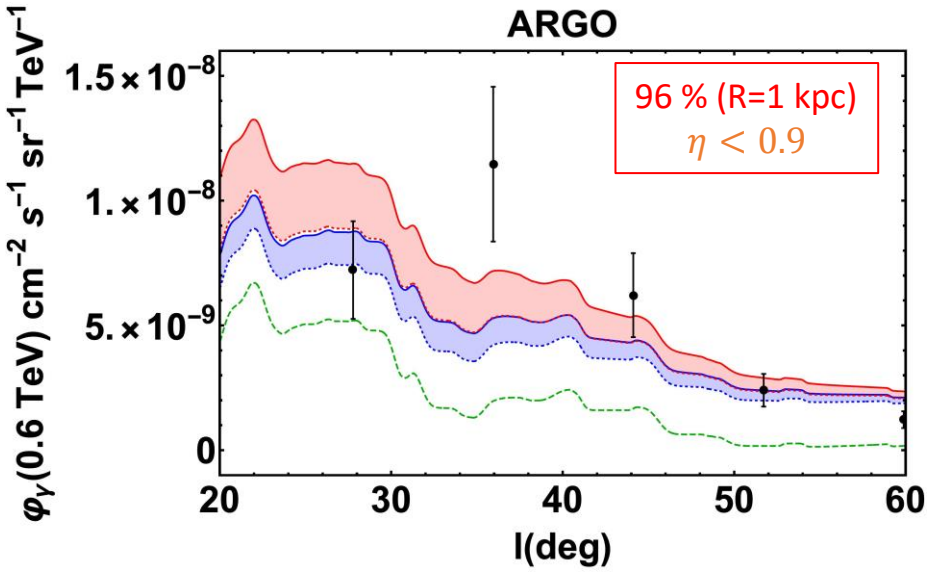

$$\phi_{\gamma,tot} > \phi^{r}_{\gamma,\,S} + \phi_{\gamma,\mathrm{diff}}$$

Resolved sources

Resolved sources + Diffuse (no Hardening)

Resolved sources + Diffuse (Hardening)

The case with hardening and smearing radius $R = \infty$ is used to set an upper limit on the parameter $\eta = \phi^{unr}/\phi^{r}$

Unresolved sources:

Are unresolved sources negligible?

H.E.S.S. resolves a relatively small region of the Galaxy (even if the sources are assumed to be very luminous);

We can performe an analytical estimate for η assuming that all the sources have the same spectrum described by a power law with spectral index 2.3 and are as luminous as the CRAB nebula. We get $\eta \sim 0.7 \gg 0.53$.

Unresolved sources produce a non-negligible signal that has to be properly estimated

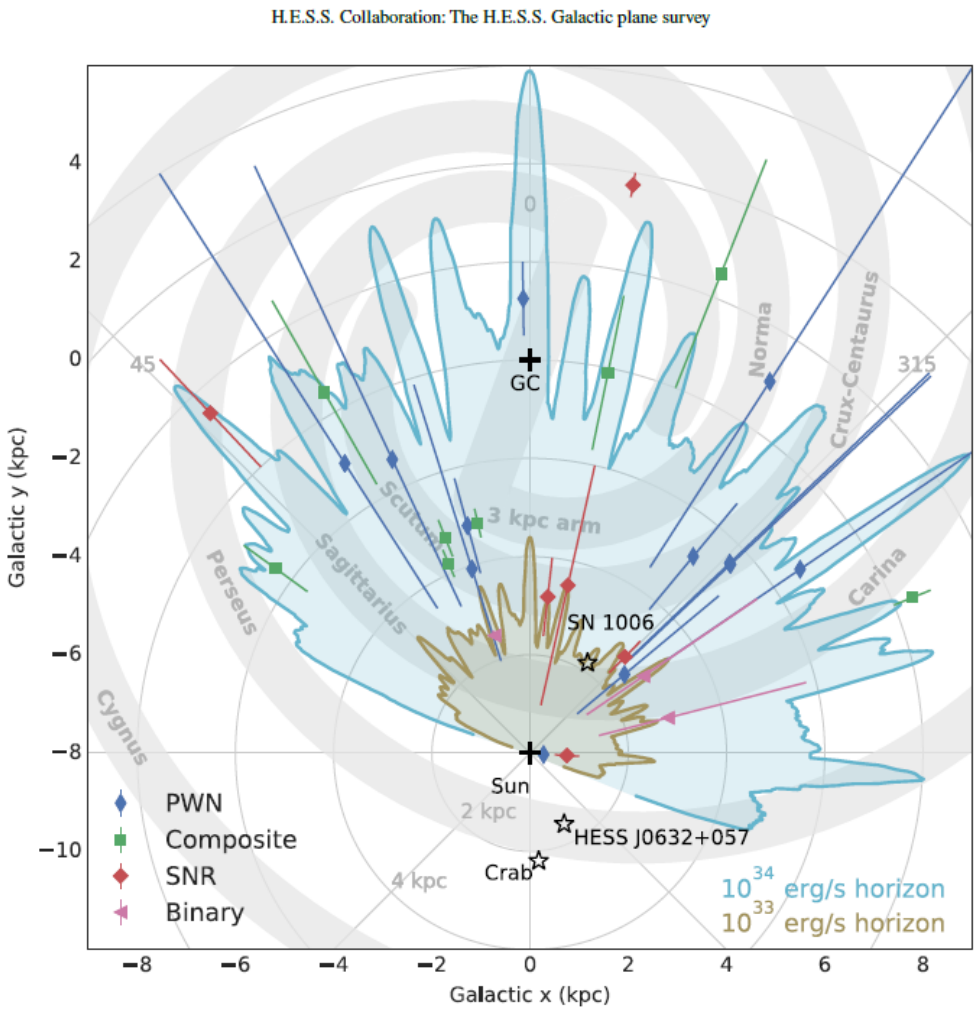

H.E.S.S. sensitivity:

- For $0.01\phi_{Crab} \leq \phi \leq 0.1\phi_{Crab}$ the H.E.S.S. sensitivity depends on the angular size of the sources.

- For $\phi \geq 0.1\phi_{Crab}$ all the sources are resolved independently of their angular size. Above this threshold the catalogue is complete.

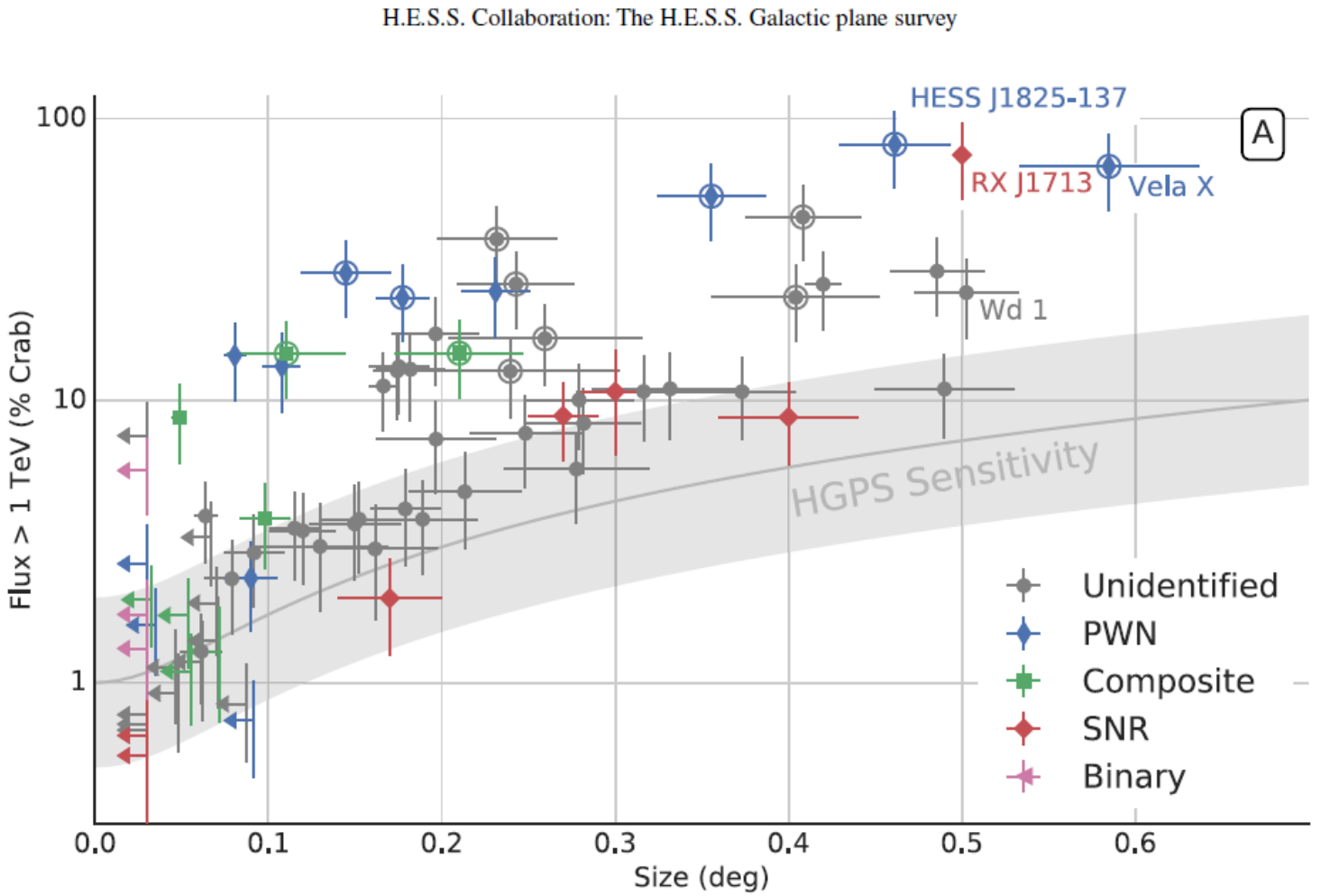

H.E.S.S.:

H.E.S.S. provides observation of the γ-ray sky in the window: $-110^{\circ} < l < 60^{\circ}$ and $|b| < 3^{\circ}$ above 1 TeV.

The HGPS catalogue:

- includes **78 VHE** sources in the H.E.S.S. observational window;
- provides the integrated flux above 1 TeV of each sources ϕ.

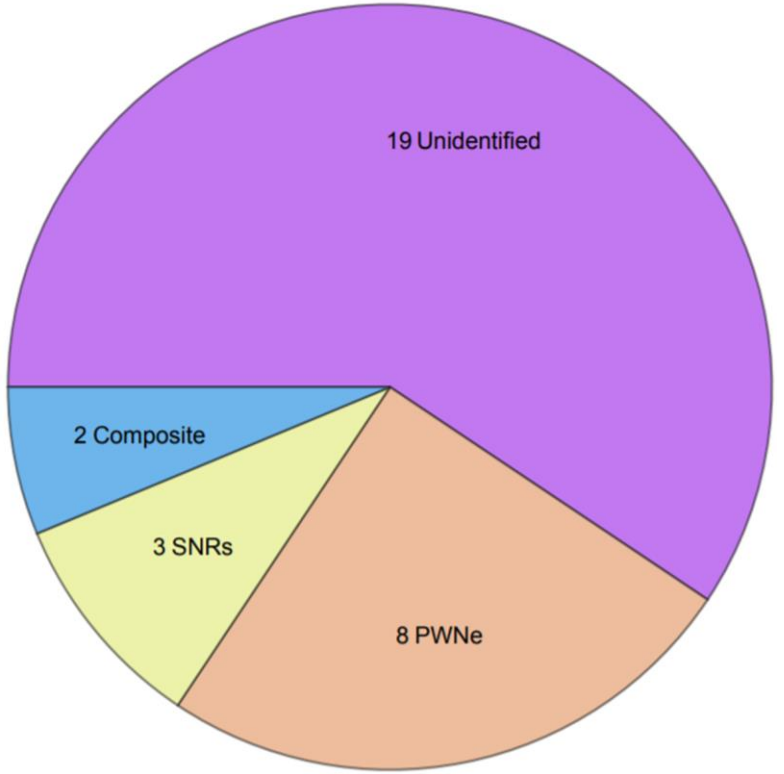

In our analysis:

We focus on the brightest sources with flux:

$$\phi > 0.1\phi_{Crab} = 0.1\ (2.26 \times 10^{-11} cm^{-2} s^{-1})$$

- The catalogue above this threshold is considered complete (no unresolved sources): **32 sources**.

Inverse Compton:

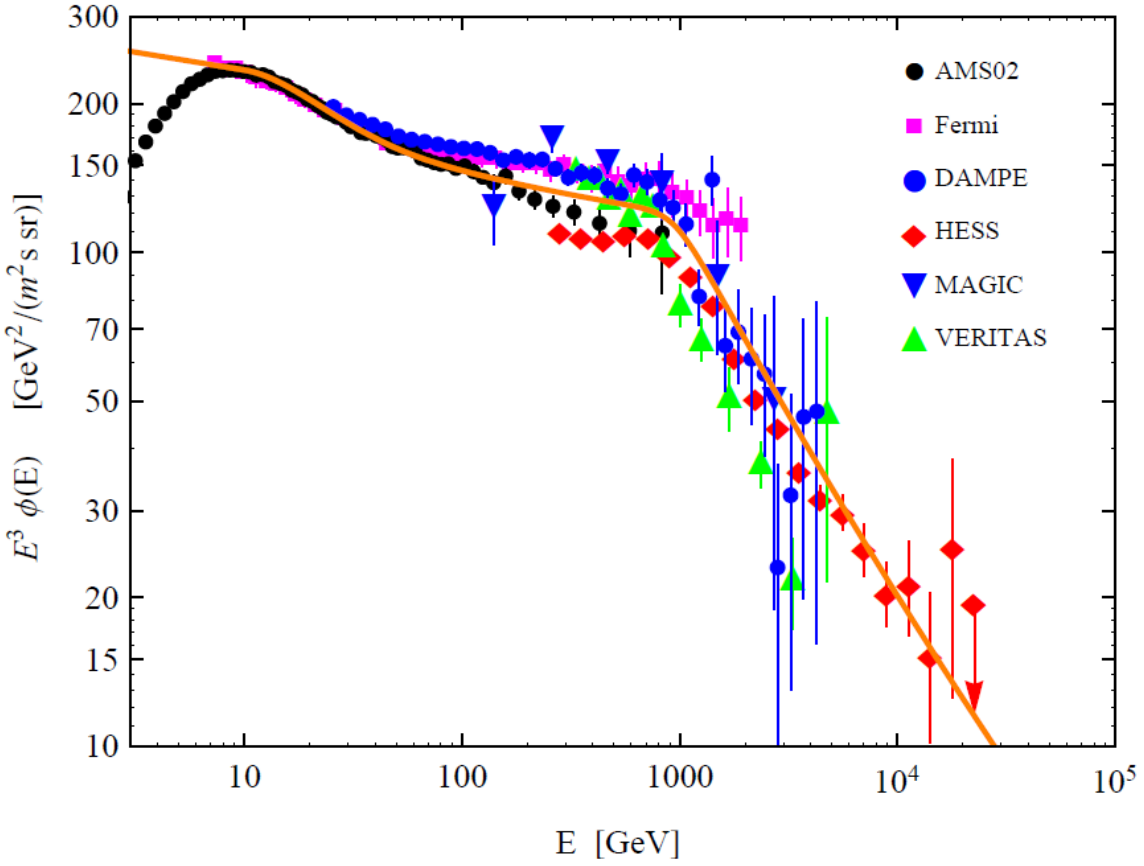

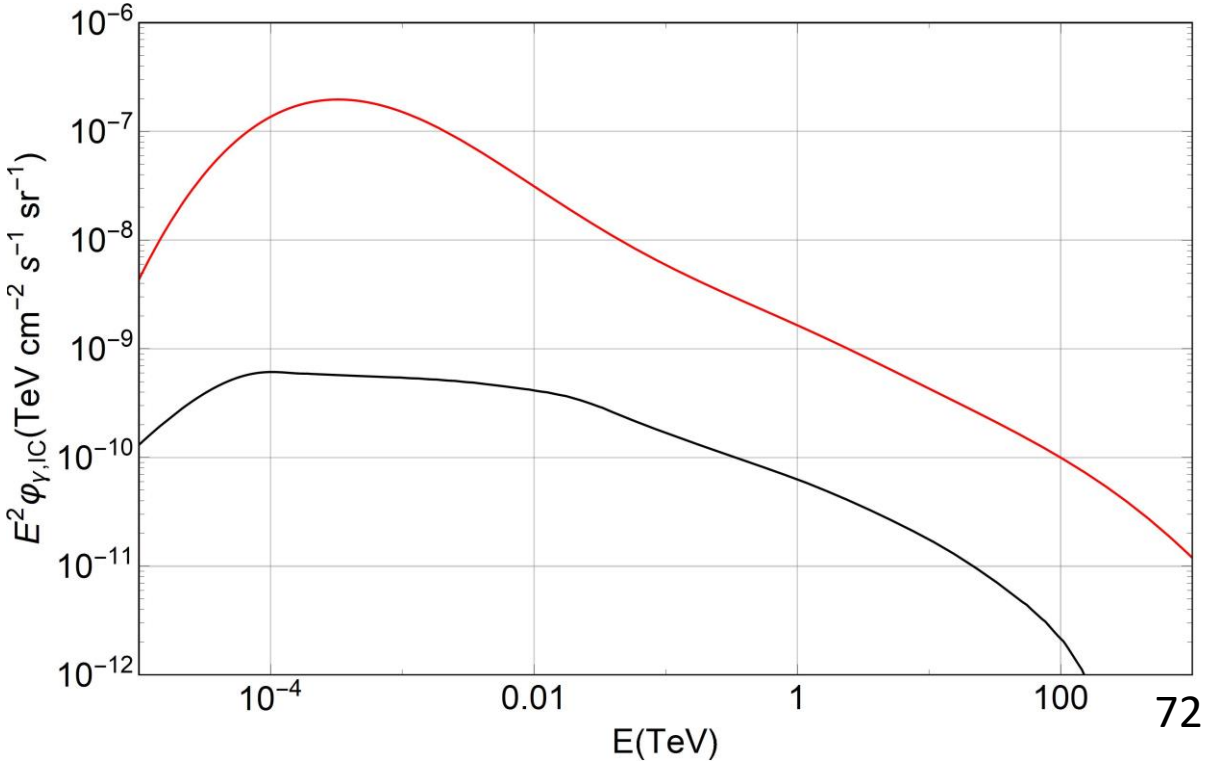

Model:

The power-law for the luminosity distribution can be automatically obtained assuming a fading source population (like PWNe, TeV Halos) create at a constant rate R.

The spin-down power is described by: $\dot{E}(t) = \dot{E}_0 \left(1 + \frac{t}{\tau}\right)^{-\gamma}$

Considering that a fraction $\boldsymbol{\lambda(t)}$ of the spin-down power is converted into gamma-rays then the intrinsic luminosity decreases according to:

$$L(t) = \lambda(t)\dot{E}(t) = \lambda \dot{E}_0 \left(1 + \frac{t}{\tau}\right)^{-\gamma} \text{ where } \gamma = 2(\delta + 1);$$

L_{max}

$$\lambda(t) = \lambda \left(\frac{\dot{E}(t)}{\dot{E}_0}\right)^{\delta}$$

Abdalla et al, *A&A*, 612, A2 (2018)

Then:

$$Y(L) = \frac{\bar{r}\,\tau\,(\alpha - 1)}{L_{\max}} \left(\frac{L}{L_{\max}}\right)^{-\alpha}$$

Where $R = 0.019\ yr^{-1}$ is the SN's rate and $\alpha = \left(\frac{1}{\gamma} + 1\right)$. Therefore, for $\gamma = 2$, we have $\alpha = 1.5$.

And instead of the parameter N we have the spin-down timescale of the Pulsar τ.

Model:

The power-law for the luminosity distribution can be automatically obtained assuming a fading source population (like PWNe, TeV Halos) create at a constant rate R .

The spin-down power is described by: $\dot{E}\,(t) = \dot{E}_0 \left(1 + \frac{t}{\tau}\right)^{-\frac{n+1}{n-1}}$

Considering that a fraction $\boldsymbol{\lambda(t)}$ of the spin-down power is converted into gamma-rays then the intrinsic luminosity decreases according to:

$$L(t) = \lambda(t)\dot{E}(t) = \lambda \dot{E}_0 \left(1 + \frac{t}{\tau}\right)^{-\gamma} \text{ where } \gamma = -\frac{n+1}{n-1}(\delta + 1);$$

L_{max}

$$\lambda(t) = \lambda \left(\frac{\dot{E}(t)}{\dot{E}_0}\right)^{\delta}$$

Abdalla et al, *A&A*, 612, A2 (2018)

Then:

$$Y(L) = \frac{\bar{r}\,\tau\,(\alpha - 1)}{L_{\max}} \left(\frac{L}{L_{\max}}\right)^{-\alpha}$$

Where $\mathrm{R} = 0.019\ yr^{-1}$ is the SN's rate and $\alpha = \left(\frac{1}{\gamma} + 1\right)$ therefore for $\gamma = 2$ we have $\alpha = 1.5$.

And instead of the parameter $\mathcal{N}$ we have the spin-down timescale of the Pulsar τ.

Likelihood:

$$\log L = -\mu_{tot} + \sum_i \log(\mu_i)$$

- μ_{tot} represents the number of expected sources;
- μ_i is the probability to observe an object with coordinates (b_i, l_i) and measured flux ϕ_i.

The source distribution per unit of flux is:

$$\mu(b, l, \phi) = \int dr\, 4\pi r^4 \rho(r, l, b) Y(4\pi r^2 \langle E \rangle \phi)$$

While is given by:

$$\mu_i = \int d\phi \mu(b_i, l_i, \phi_i) P(\phi_i, \phi, \delta\phi_i)$$

Where $P(\phi_i, \phi, \delta\phi_i)$ respresents the probability that the measured flux ϕ_i is obtained for the real flux ϕ.

We assume a Gaussian.

The $\chi^2 = -2logL$ was used for obtaining the best fit values and the allowed regions for the parameters.

Cumulative distribution:

The flux distribution can be calculated as:

$$\frac{dN}{d\Phi} = \int dr\ 4\pi r^4 \langle E \rangle\ Y(4\pi r^2 \langle E \rangle \Phi)\ \overline{\rho}(r)$$

- $\bar{\rho}(r)$ is the sources spatial distribution integrated over the longitude and latitude intervals probed by H.E.S.S.;
- The above integral is performed in the range $\mathrm{d}/\theta_{max} \leq \mathrm{r} \leq D(L,\phi) =$ where $\theta_{max} = 0.7^{o}$ is the maximal angular dimension that can be probed by H.E.S.S. and the d is the physical dimention of the source. While $D(L,\phi) = (L/4\,\pi\,\langle E \rangle\,\phi)^{\frac{1}{2}}$;
- We calculate analytically the flux distribution for the 2 limits cases $L_{max} \to \infty$ and $L_{max} \to 0$:

$$\frac{dN}{d\Phi} = R\,\tau\,(\alpha-1)\,L_{\max}^{\alpha-1}\,\Phi^{-\alpha} \int_0^{\infty} dr\ (4\pi\langle E \rangle)^{1-\alpha}\ r^{4-2\alpha}\ \overline{\rho}(r)$$

$$\frac{dN}{d\Phi} \simeq (4\pi\langle E \rangle)^{1-\alpha}\ \overline{\rho}(0)\ R\,\tau\,(\alpha-1)\,L_{\max}^{\alpha-1}\,\Phi^{-\alpha} \int_0^{D(L_{\max},\Phi)} dr\ r^{4-2\alpha} = \overline{\rho}(0)\ R\,\tau \left(\frac{\alpha-1}{5-2\alpha}\right) \left(\frac{L_{\max}}{4\pi\langle E \rangle}\right)^{\frac{3}{2}} \Phi^{-\frac{5}{2}}$$

Resolved and Unresolved sources:

The resolved flux can be calculated from:

$$\phi_{res} = \int dr\, r^2 \bar{\rho}(r) \int d\phi Y(4\pi r^2 \langle E \rangle \phi)$$

$$\phi_{res} = \int dr\, r^2 \bar{\rho}(r) \int dL\, 4\pi r^2 \langle E \rangle Y(L)$$

$$\phi_{res} = \phi_{th} \int dr \bar{\rho}(r) \int dL \overline{D}(L)^2 Y(L)$$

- $\bar{\rho}(r)$ is the sources spatial distribution integrated over the longitude and latitude intervals probed by H.E.S.S.;
- The above integral is performed in the range $\mathrm{d}/\theta_{max} \leq \mathrm{r} \leq D(L, \phi)$ where $\theta_{max} = 0.7^{\mathrm{o}}$ is the maximal angular dimension that can be probed by H.E.S.S. and the d is the physical dimention of the source. While $D(L, \phi) = (L/4\pi \langle E \rangle \phi)^{\frac{1}{2}}$;
- The luminosity integral is performed in the range $L_{min}(r) \leq \mathrm{L} \leq L_{max}$ where $L_{min} = 4\pi r^2 \langle E \rangle \phi_{th}$

Results:

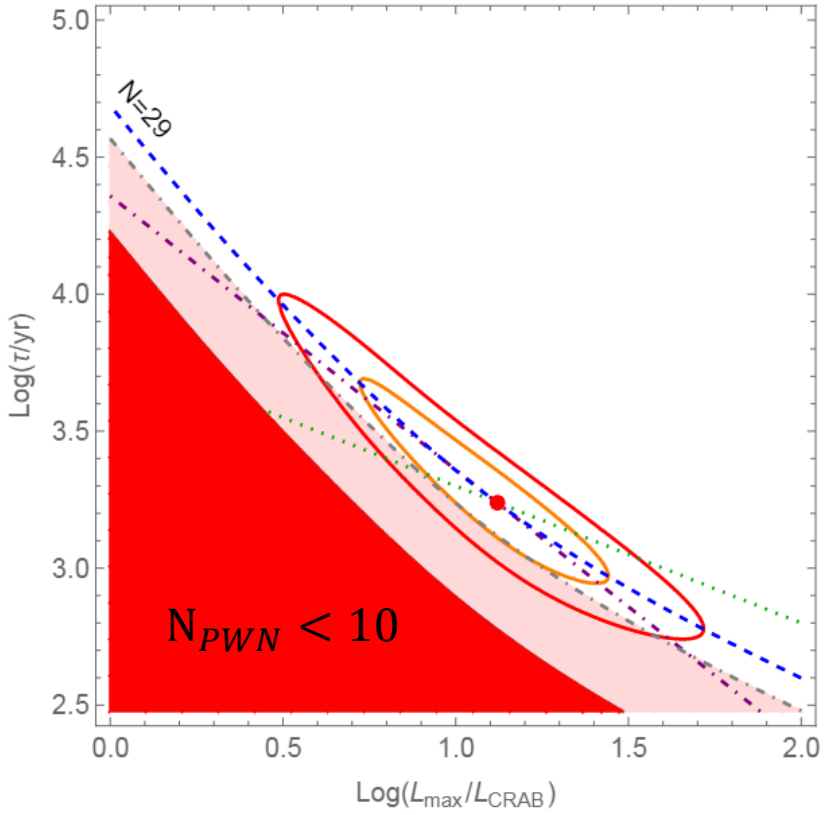

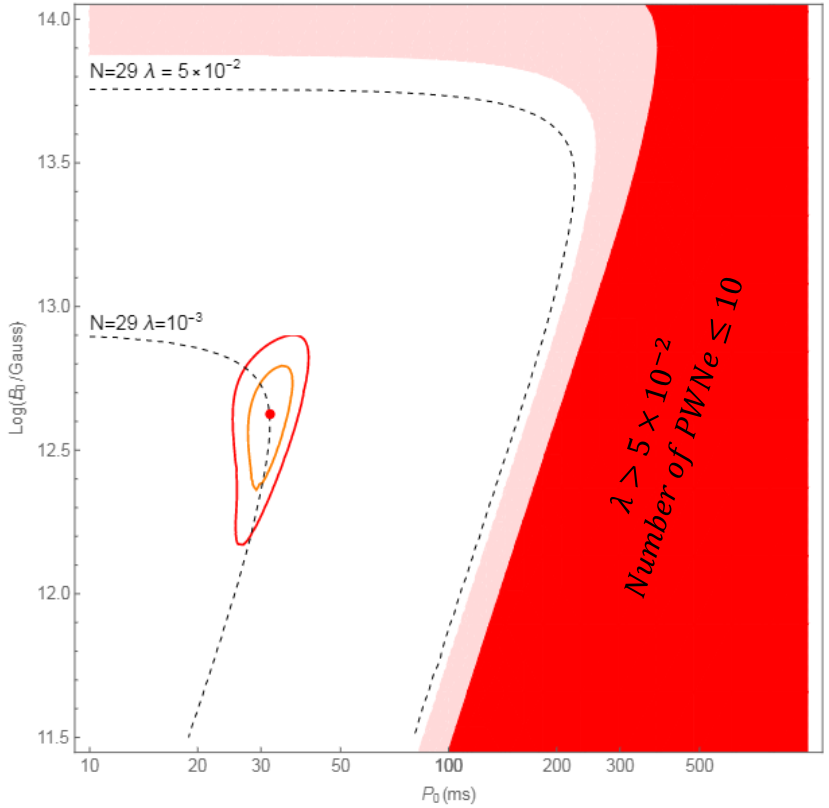

The gray lines correspond to a fixed number of sources above the adopted flux threshold $0.1\phi_{CRAB}$.
It can be shown analytically that $N(\phi)$ scales as:

- $N(\phi) \propto \tau \, L_{max}^{\frac{3}{2}} = B_0 P_0^{-4} \lambda^{\frac{3}{2}}$ $(L_{max} \rightarrow 0)$
- $N(\phi) \propto \tau \, L_{max}^{\alpha-1} = B_0^{2\alpha-4} P_0^{6-4\alpha} \lambda^{\alpha-1}$ $(L_{max} \rightarrow \infty)$

Best fit results for $\alpha = 1.8$:

$$L_{max} = 6.8 \times 10^{35}\ erg\ s^{-1}$$
$$\tau = 0.5\ kyr$$

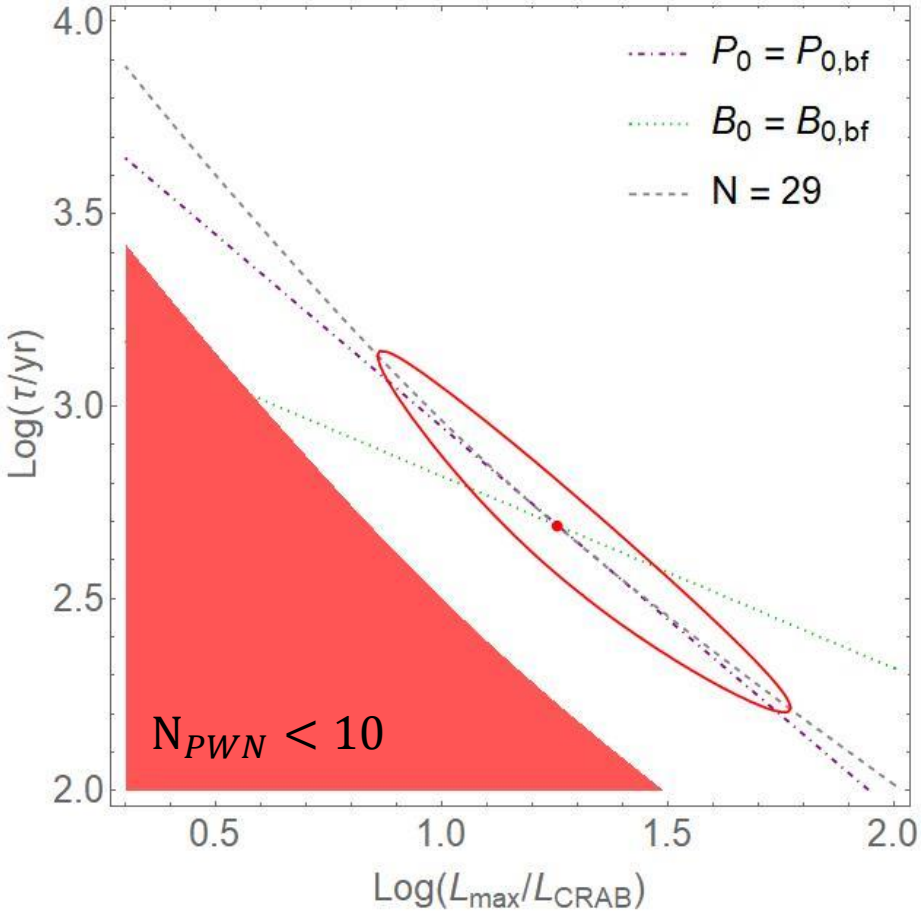

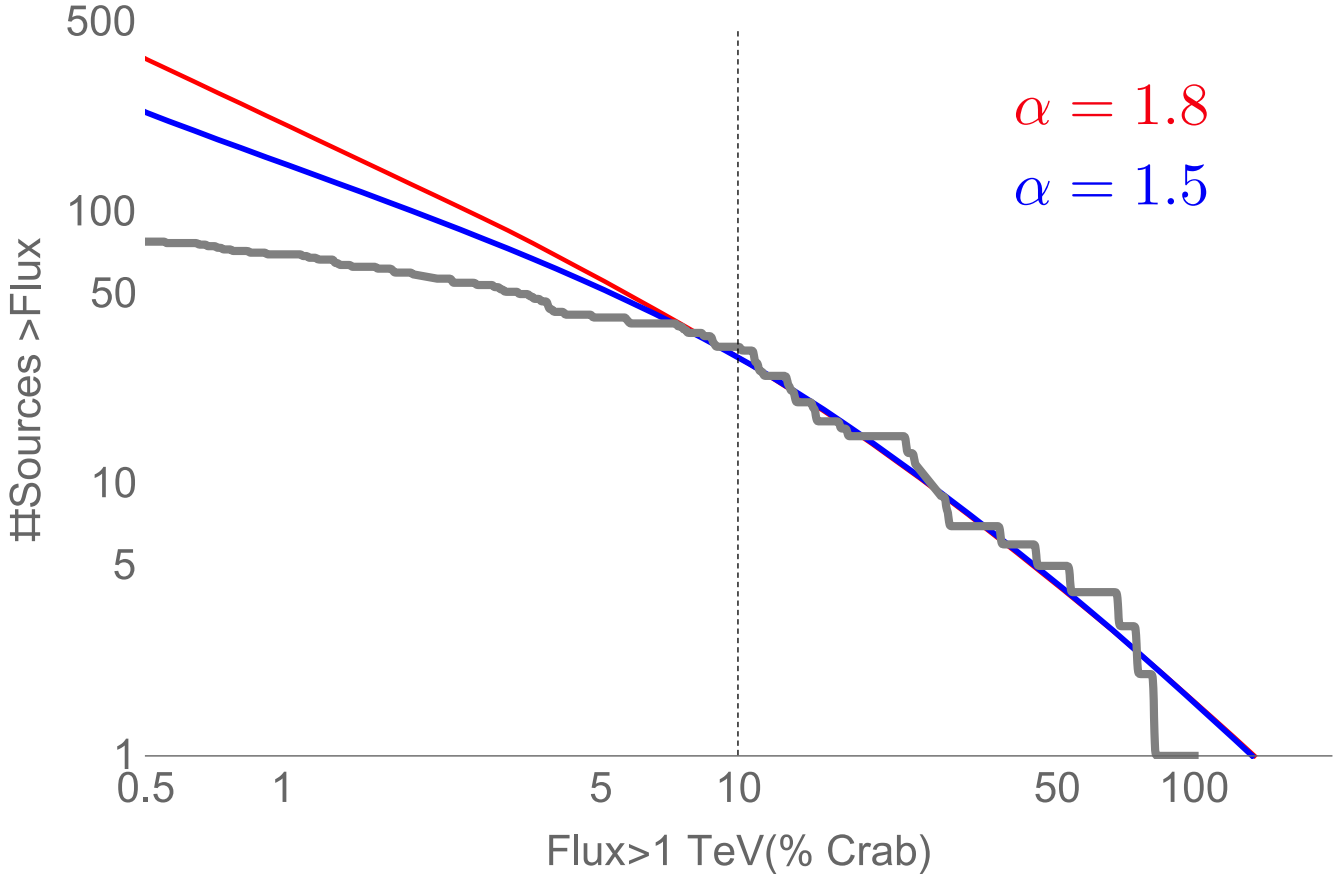

Robustness of the results:

	$\log_{10}\frac{L_{\rm max}}{\rm erg\,s^{-1}}$	$\mathcal{N}$	$\log_{10}\frac{L_{\rm MW}}{\rm erg\ s^{-1}}$	$\Phi_{\rm tot}$	$\tau_{\rm sd}$	$\Delta\chi^2$
Ref.	$35.69^{+0.21}_{-0.28}$	17^{+14}_{-6}	$37.22^{+0.12}_{-0.13}$	$3.8^{+1.2}_{-1.0}$	$1.8^{+1.5}_{-0.6}$	–
SNR	$35.69^{+0.22}_{-0.25}$	18^{+15}_{-7}	$37.23^{+0.12}_{-0.13}$	$3.8^{+1.0}_{-1.0}$	$1.8^{+1.6}_{-0.7}$	1.4
$H = 0.1\,\rm kpc$	$35.65^{+0.22}_{-0.27}$	$15^{+14.5}_{-6}$	$37.13^{+0.12}_{-0.13}$	$4.1^{+1.3}_{-1.0}$	$1.6^{+1.5}_{-0.6}$	−7.3
$H = 0.05\,\rm kpc$	$35.34^{+0.26}_{-0.19}$	28^{+19}_{-13}	$37.08^{+0.12}_{-0.13}$	$4.4^{+1.3}_{-0.9}$	$2.9^{+2.0}_{-1.4}$	−10.5
$d = 20$ pc	$35.69^{+0.20}_{-0.26}$	17^{+16}_{-6}	$37.23^{+0.12}_{-0.13}$	$3.9^{+1.2}_{-1.0}$	$1.9^{+1.9}_{-0.7}$	−0.4
$d = 40$ pc	$35.67^{+0.20}_{-0.25}$	20^{+20}_{-8}	$37.28^{+0.12}_{-0.13}$	$4.4^{+1.2}_{-1.1}$	$2.2^{+2.0}_{-0.8}$	−1.8
$\alpha = 1.3$	$35.61^{+0.18}_{-0.27}$	$25^{+24}_{-8.5}$	$37.17^{+0.12}_{-0.13}$	$3.5^{+1.1}_{-0.9}$	$4.3^{+4.3}_{-1.5}$	0.0
$\alpha = 1.8$	$35.83^{+0.29}_{-0.24}$	7^{+6}_{-4}	$37.39^{+0.11}_{-0.13}$	$5.9^{+1.8}_{-1.5}$	$0.5^{+0.4}_{-0.2}$	0.5
$N_{\rm obs} = 32$	$35.71^{+0.22}_{-0.24}$	18^{+14}_{-7}	$37.26^{+0.12}_{-0.12}$	$4.2^{+1.3}_{-1.0}$	–	–

- Results are stable with respect to assumptions;
- The total TeV luminosity and flux are constrained within a factor ~ 2:

$\boldsymbol{L_{MW} = (1.2 - 2.5) \times 10^{37}\ erg\ s^{-1}}$, $\boldsymbol{\phi_{tot} = (3.5 - 5.9) 10^{-10} cm^{-2} s^{-1}}$

Effect of dispersion in our Model:

We also consider the effects of dispertion of initial period P_0 and magnetic field B_0 around the references values $\tilde{P}_0$ and $\tilde{B}_0$. This turn into a dispertion in $L_{max}(\mathrm{P_0}, \mathrm{B_0})$ and $\tau(\mathrm{P_0}, \mathrm{B_0})$.
We obtain the following luminosity distribution after integrating on $\mathrm{P_0}$ and B_0 distribution:

$$Y(L) = \frac{R\,\tilde{\tau}\,(\alpha - 1)}{\tilde{L}} \left(\frac{L}{\tilde{L}}\right)^{-\alpha} G\left(\frac{L}{\tilde{L}}\right)$$

Where $\tilde{L}(\tilde{P}_0, \tilde{B}_0)$ and $\tilde{\tau}(\tilde{P}_0, \tilde{B}_0)$ are the spin-down time scale and maximum luminosity for the reference values $\tilde{P}_0$ and $\tilde{B}_0$ and $G(x)$ is:

$$G(x) \equiv \int dp\, h(p)\, p^{6-4\alpha} \int db\, g(b)\, b^{2\alpha-4}\, \theta\left(p^{-4}\, b^2 - x\right)$$

Probability distribution for the initial period and it is assumed to be a gaussian distribution in $Log_{10}(p)$ where $p = P/\tilde{P}_0$

Probability distribution for the magnetic field and it is assumed to be a gaussian distribution in $Log_{10}(b)$ where $b = B_0/\tilde{B}_0$

Results:

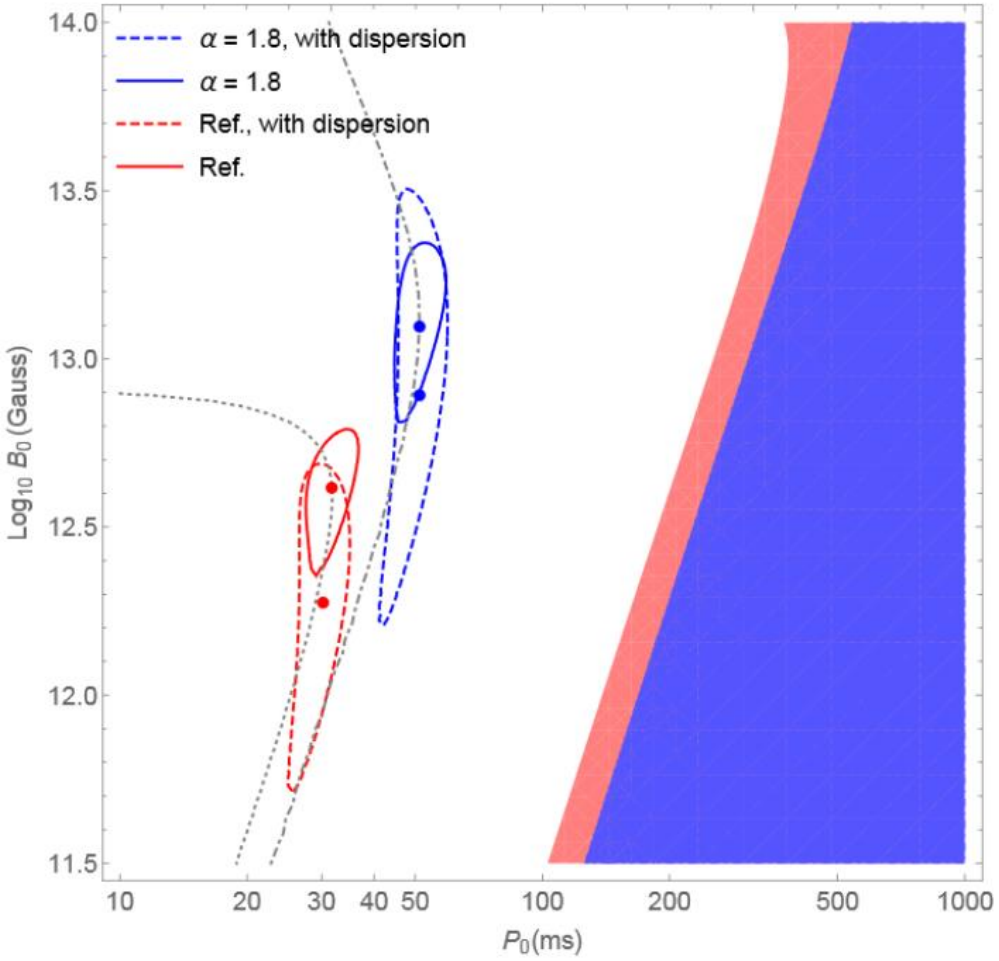

The best fit value of P_0 does not change, while B_0 is slightly reduced as a consequence of the high-luminosity tail of the new source luminosity.

$\alpha = 1.8$

$$B_0 = 12.7^{+9.6}_{-5.8} 10^{12} G \times \left(\frac{\lambda}{10^{-3}}\right)^{\frac{1}{2}}$$

$$P_0 = 51^{+8.1}_{-6.4}\, ms \times \left(\frac{\lambda}{10^{-3}}\right)^{\frac{1}{2}}$$

Table of the 12 sources observed by both Fermi and HESS:

Table 1: *In the table are shown the 12 PWNe observed by both FermiLAT (4FGL-DR2) and H.E.S.S. (HGPS). In addition we show also the Crab although is it is not observed by H.E.S.S.. In the first columns is reported the calculated value of R_ϕ. In the second one the power-law spectral index (it is specified when the spectral form is different than a simple power-law) in the GeV energy range taken from the 4FGL-DR2 catalogue. In the last column is reported the power-law spectral index (it is specified when the spectral form is different than a simple power-law) in the TeV energy range taken from the HGPS catalogue.*

H.E.S.S.-association	R_ϕ	β_{GeV}	β_{TeV}	D(kpc)	τ_c(kyr)
Crab	1481.24	1.38 (1 GeV) (log-par)	2.30	2.0	0.94
HESS J0835-455	754.938	2.18	1.89	0.29	11.3
HESS J1303-631	447.05	1.81	2.33	6.7	11.0
HESS J1356-645	63.47	1.41	2.20	2.4	7.31
HESS J1420-607	999.354	1.99	2.20	5.6	13.0
HESS J1616-508	1223.36	2.05	2.32	6.8	8.13
HESS J1632-478	799.56	1.76	2.51	-	-
HESS J1746-285	98950.	0.96 (1 GeV) (log-par)	2.17	-	-
HESS J1825-137	582.721	1.73	2.38	3.9	21.4
HESS J1837-069	1612.13 (483.598)	2.04 (1.84)	2.54	6.6	22.7
HESS J1841-055	1149.91	1.98	2.47	-	-
HESS J1857+026	2390.84	2.12	2.57	-	20.6
HESS J1514-591	686.30	1.83	2.05	5.2	1.56

If we assume a simple power-law:

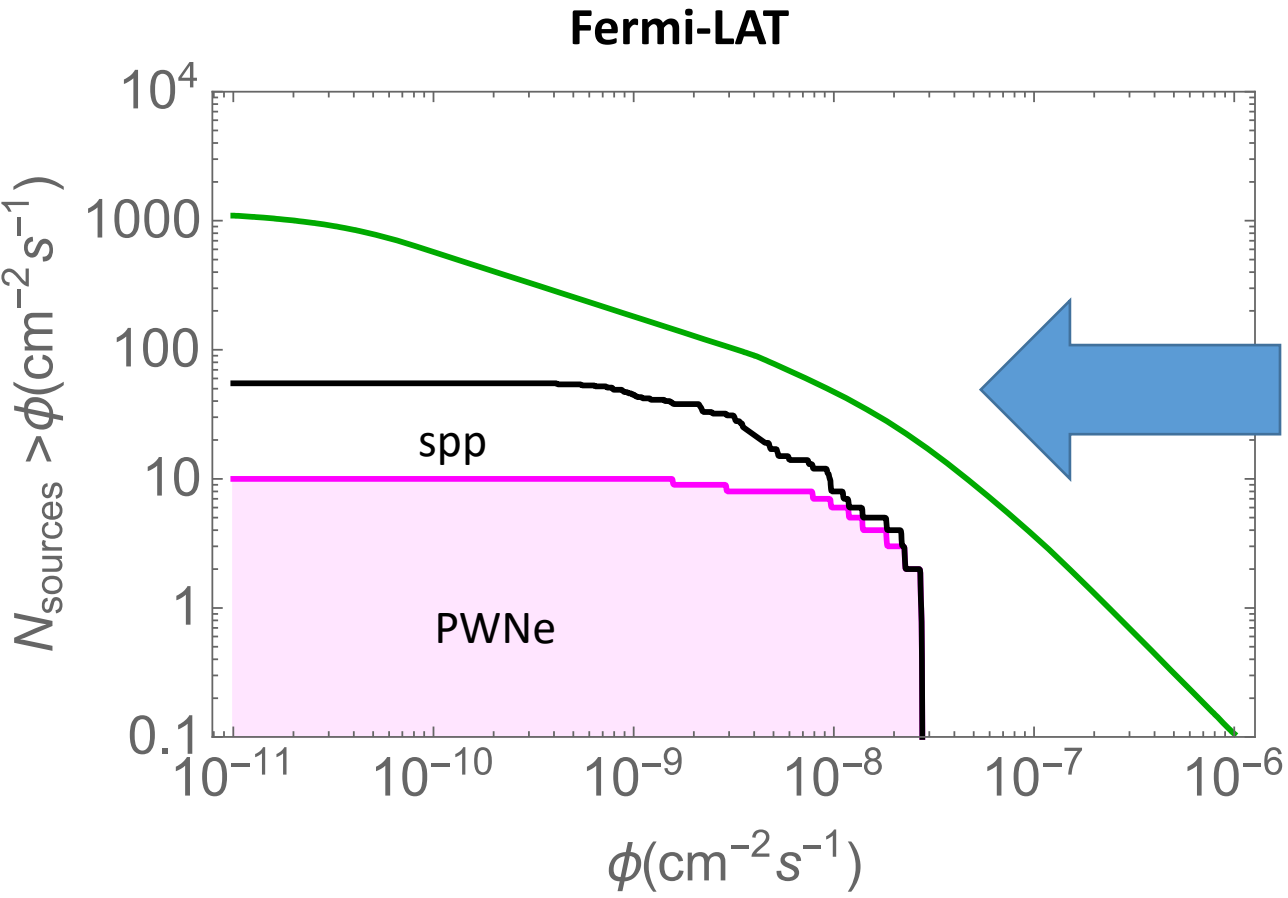

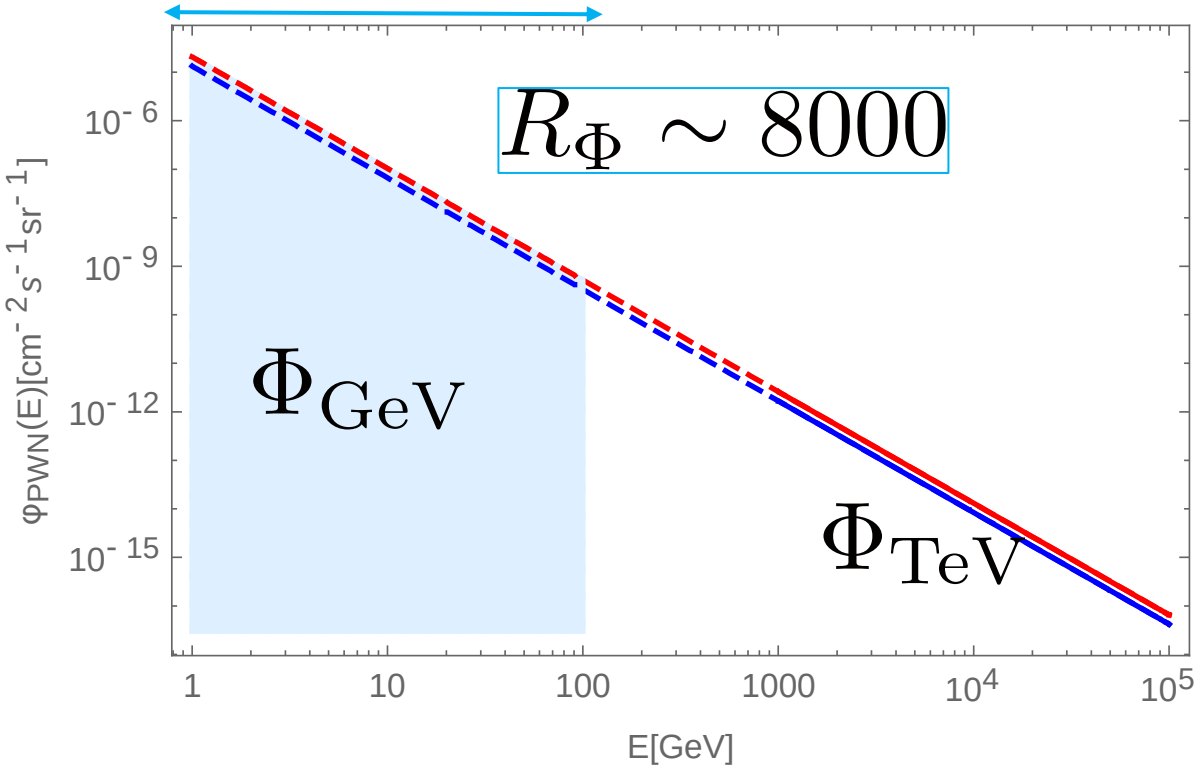

Expected cumulative distribution of Fermi-LAT PWNe under the assumption of spectral index $\beta_{\mathrm{GeV}} = 2.3$

Effects of parameter space:

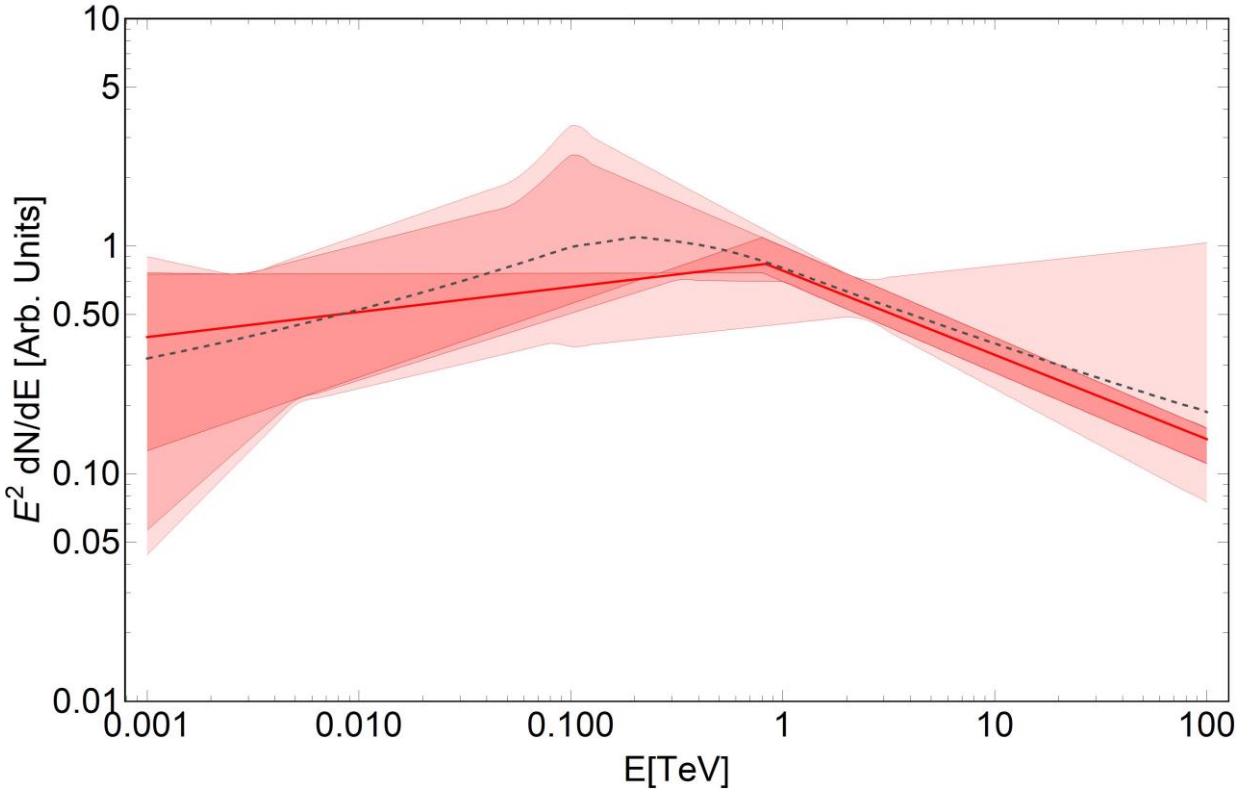

The unresolved source flux is either large or has a hard spectrum:

$R_\phi = 250\ (E_0 = 0.8\,TeV, \beta_{TeV} = 2.4) \rightarrow \beta_{GeV} = 1.67$

$R_\phi = 1500 (E_0 = 0.8\,TeV, \beta_{TeV} = 2.4) \rightarrow \beta_{GeV} \sim 2$

This behavior is because the flux in the TeV energy range is fixed (constrained by the population study of the H.G.P.S catalog).

The unresolved flux is affected by large uncertainties at few GeV that become smaller as the energy increase because of the constraint in the TeV energy range

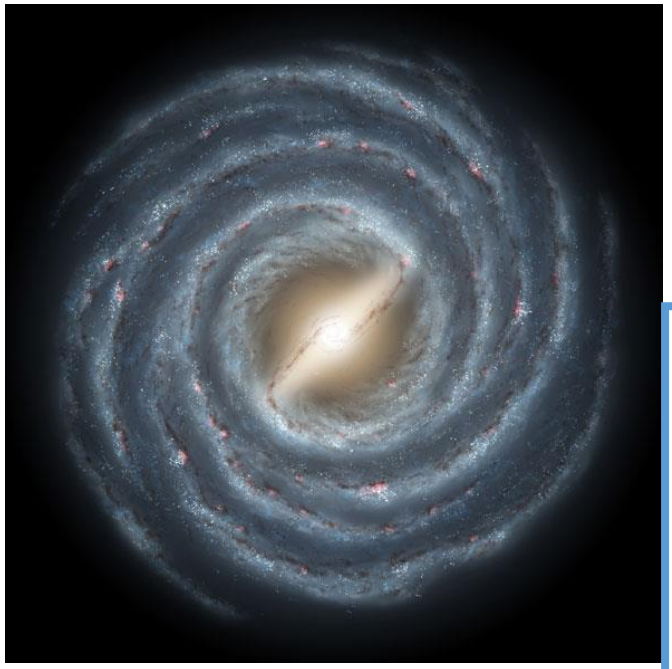

PWNe contribution in galactocentric rings

	$\Phi^{\rm diff}_{\rm GeV}$ $(cm^{-2}\ s^{-1})$	$\Phi^{\rm NR}_{\rm GeV}$ $(cm^{-2}\ s^{-1})$		$\Phi^{\rm NR}_{\rm GeV}$ $(cm^{-2}\ s^{-1})$	
		$R_\Phi = 250,\ \alpha = 1.8$	$R_\Phi = 1500,\ \alpha = 1.8$	$R_\Phi = 250,\ \alpha = 1.5$	$R_\Phi = 1500,\ \alpha = 1.5$
$1.7 - 4.5$ kpc	3.86×10^{-7}	3.35×10^{-8} (8.6%)	1.40×10^{-7} (36%)	1.60×10^{-8} (4.1%)	3.92×10^{-8} (10%)
$4.5 - 5.5$ kpc	3.11×10^{-7}	1.91×10^{-8} (6.1%)	8.00×10^{-8} (26%)	8.30×10^{-9} (2.7%)	2.00×10^{-8} (6.4%)
$5.5 - 6.5$ kpc	5.09×10^{-7}	2.13×10^{-8} (4.2%)	8.93×10^{-8} (17%)	8.33×10^{-9} (1.6%)	2.02×10^{-8} (3.9%)
$6.5 - 7.0$ kpc	2.57×10^{-7}	1.15×10^{-8} (4.5%)	4.81×10^{-8} (19%)	3.96×10^{-9} (1.5%)	9.48×10^{-9} (3.7%)
$7.0 - 8.0$ kpc	7.7×10^{-7}	2.67×10^{-8} (3.5%)	1.12×10^{-7} (14%)	7.53×10^{-9} (1.0%)	1.83×10^{-8} (2.4%)
$8.0 - 10.0$ kpc	3.84×10^{-6}	4.89×10^{-8} (1.3%)	2.05×10^{-7} (5.3%)	1.08×10^{-8} (0.3%)	2.69×10^{-8} (0.7%)
$10.0 - 16.5$ kpc	7.68×10^{-7}	1.51×10^{-8} (1.9%)	6.37×10^{-8} (8.3%)	6.37×10^{-9} (0.8%)	1.65×10^{-8} (2.1%)
$16.5 - 50.0$ kpc	4.44×10^{-8}	3.87×10^{-10} (0.8%)	2.07×10^{-9} (4.7%)	2.43×10^{-10} (0.5%)	6.98×10^{-10} (1.6%)
$0.0 - 50.0$ kpc	6.89×10^{-6}	1.79×10^{-7} (2.6%)	7.53×10^{-7} (11%)	6.28×10^{-8} (1.0%)	1.54×10^{-7} (2.2%)

9 Galactocentric rings

Total diffuse emission: 9.3 years of Fermi-LAT Pass 8 data (0.34−228.65) GeV and (|l|<180◦) and |b|<20.25◦

Diffuse emission due to unresolved PWNe (1-100) GeV with $\alpha = 1.8$

Diffuse emission due to unresolved PWNe (1-100) GeV with $\alpha = 1.5$

Spectral index and gamma-ray emissivity ($\alpha = 1.5$):

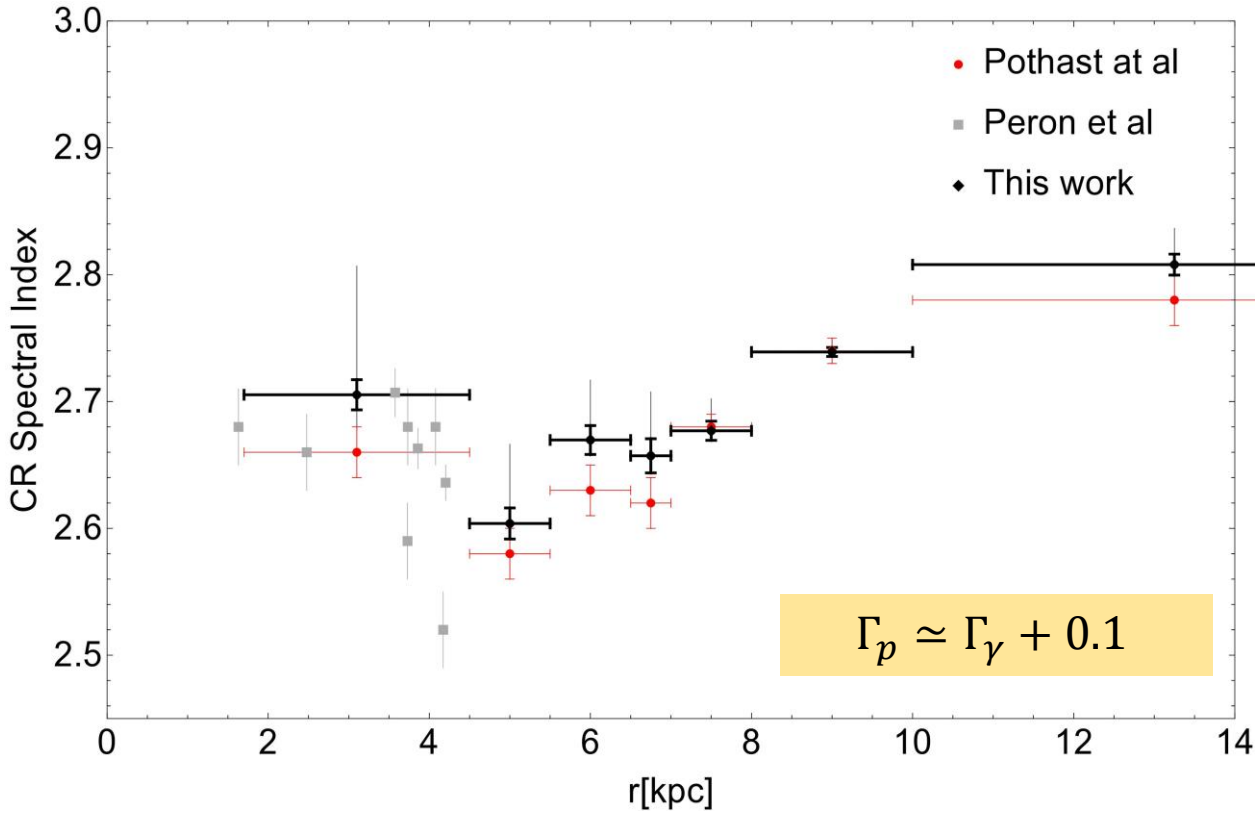

- In the case $\alpha = 1.5$ the contribution of TeV unresolved sources is smaller but still produces a non-negligible effect.

Results for $\alpha = 1.8$

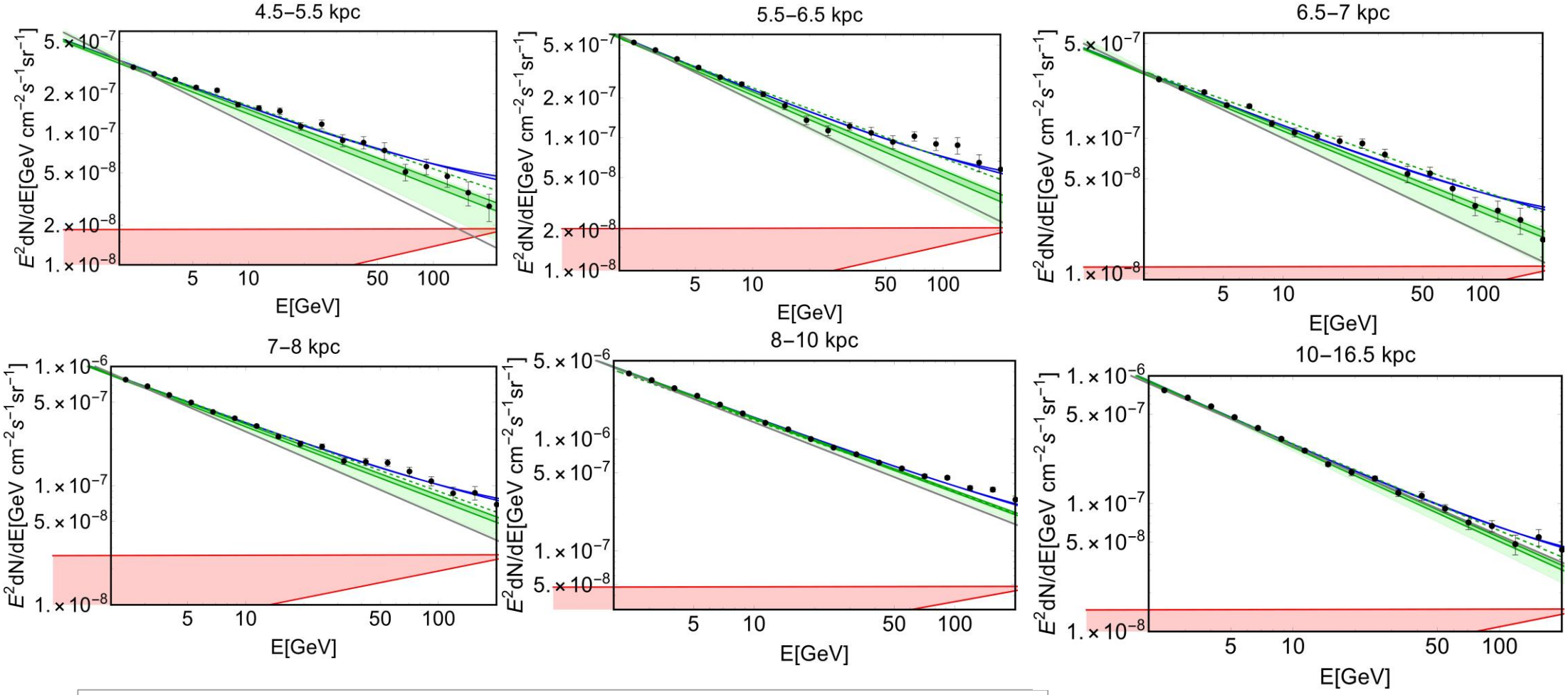

Gray line: speculative diffuse component with spectral index fixed to 2.7 normalized in order to interpolate the data at $\sim$ 2 GeV.

Absorption in the Sub PeV energy range:

Vernetto and Lipari, Phys. Rev. D 94, 063009 – Published 19 September 2016

The pair production cross section:

$$\sigma_{\gamma\gamma} = \sigma_T \left(\frac{3}{16}\right)(1-\beta^2)\left[2c(\beta^2-2) + (3-\beta^4)\ln\left(\frac{1+\beta}{1-\beta}\right)\right]$$

Where: $\beta = \sqrt{1-\frac{1}{x}}$ and $x = \frac{2E_\gamma \epsilon(1-\cos\theta)}{4\, m_e^2}$, $x > 1$

For a fixed values of ϵ the energy threshold is:

$$E_\gamma^{th} = \frac{2\, m_e}{\epsilon(1-cos\theta)} \simeq \frac{0.52}{\epsilon_{eV}(1-cos\theta)} TeV$$

The absorption probability per unit path length (for CMB) is:

$$K(E_\gamma) = \int \epsilon \int d\Omega (1-\cos(\theta)) n_{\gamma,CMB}(\epsilon)\sigma_{\gamma\gamma}(x(E_\gamma,\epsilon,\theta))$$

The optical depth is:

$$\tau(E_\gamma, r) = \int_0^r dr' \ \mathrm{K}(E_\gamma)$$

Absorption in the Sub PeV energy range:

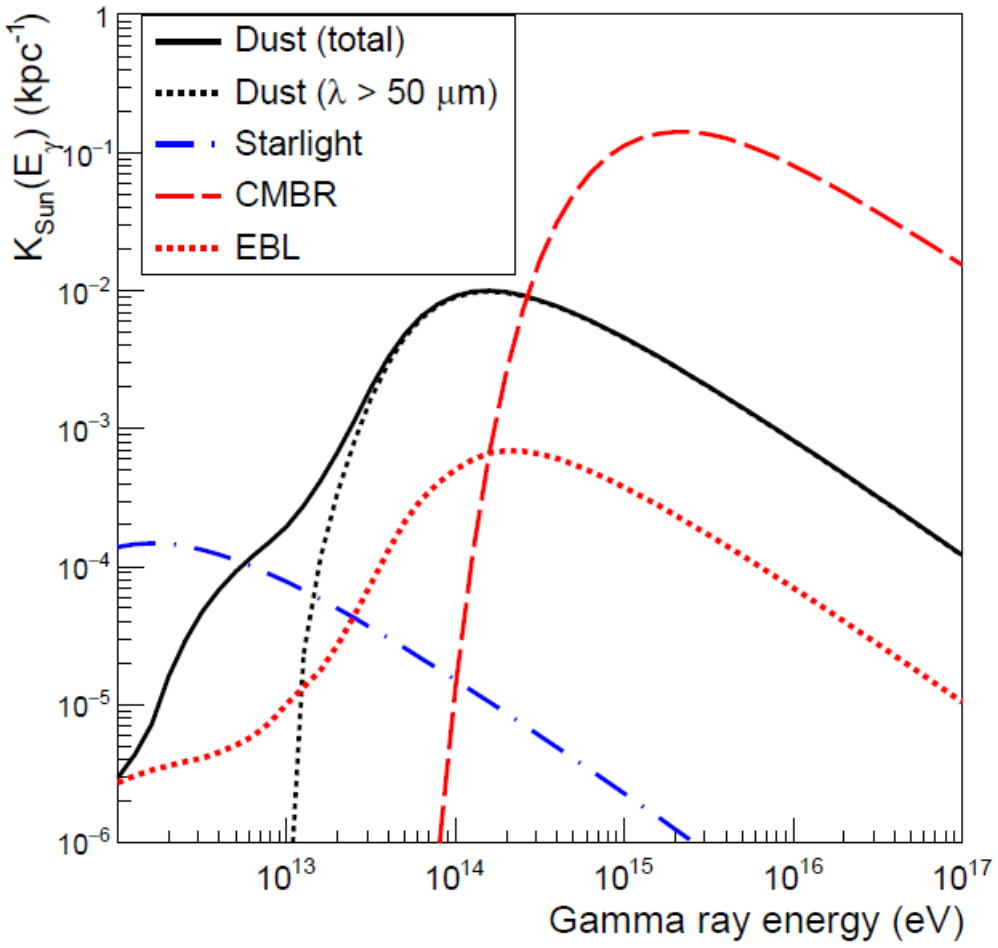

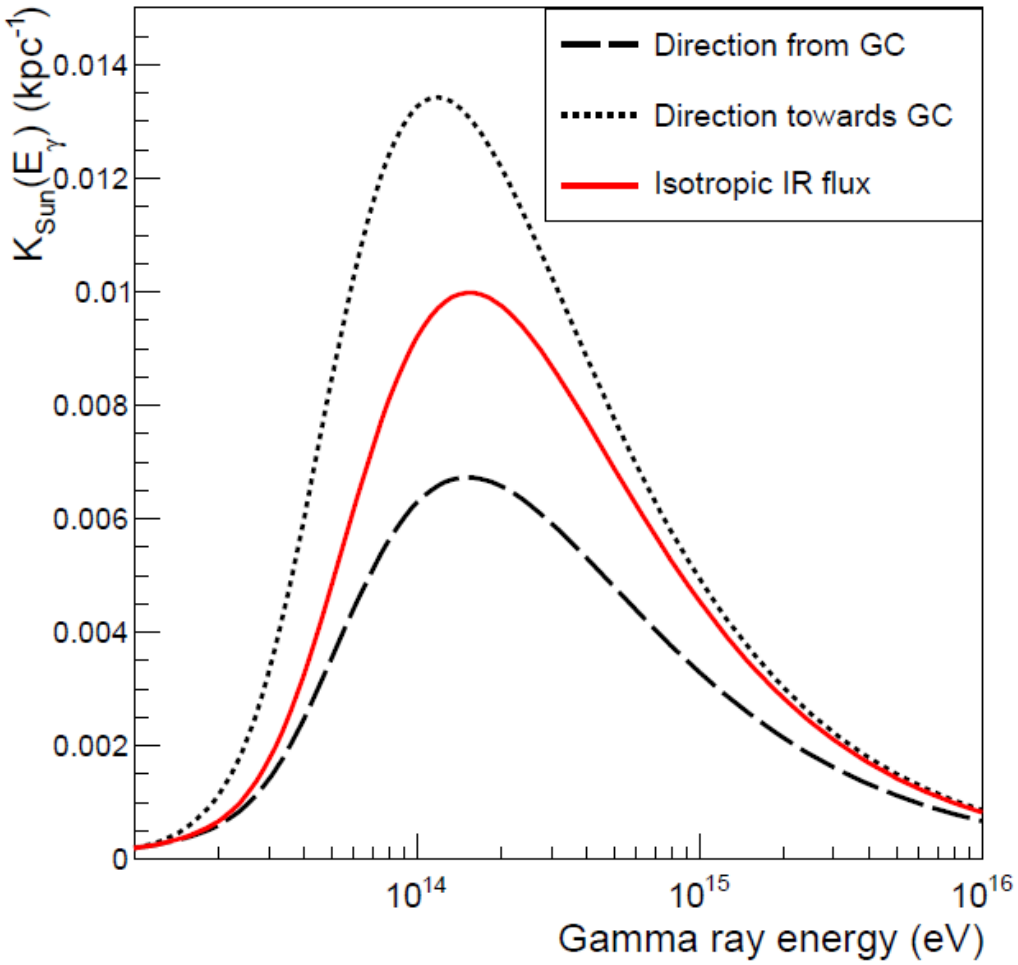

Vernetto and Lipari, Phys. Rev. D 94, 063009 – Published 19 September 2016

Comparison Diffuse models:

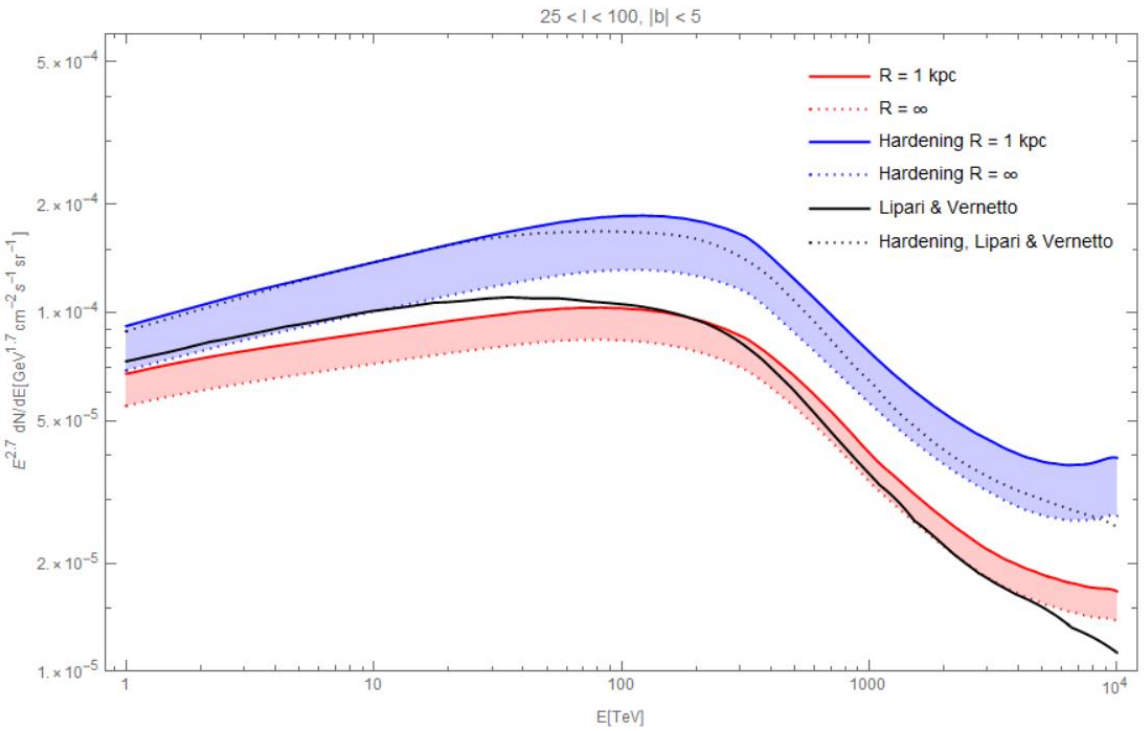

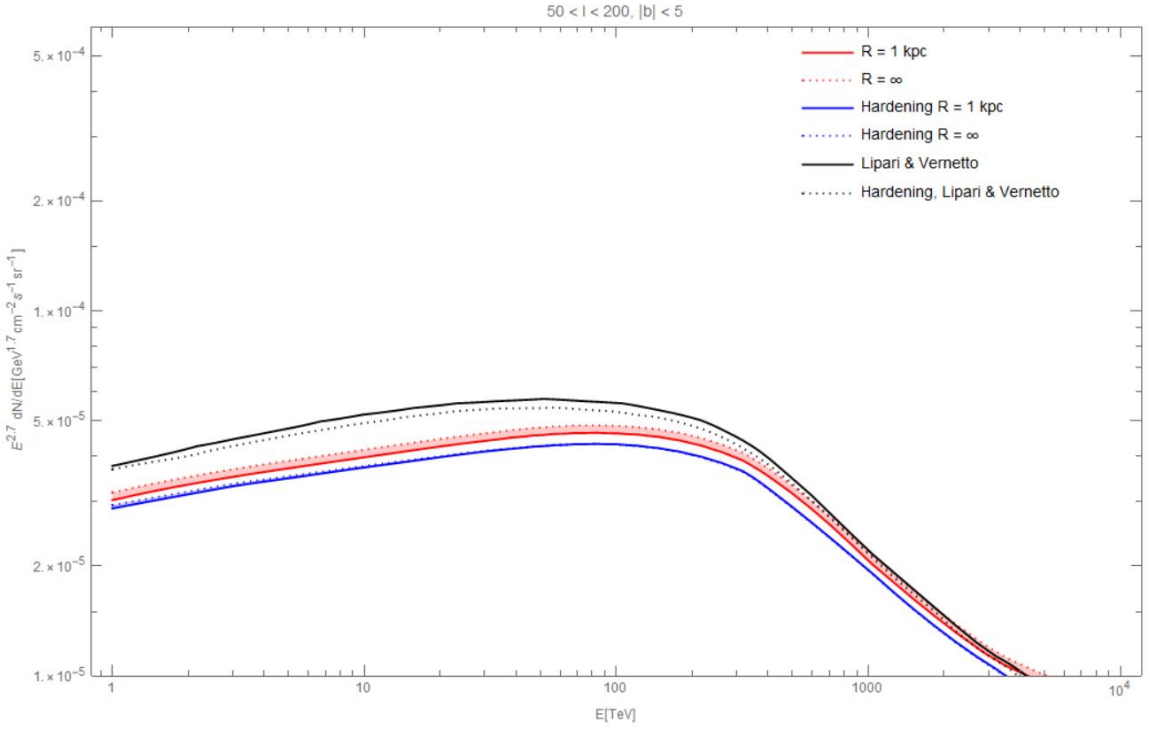

Cut-off effect:

Luminosity index: $\alpha = 1.5$

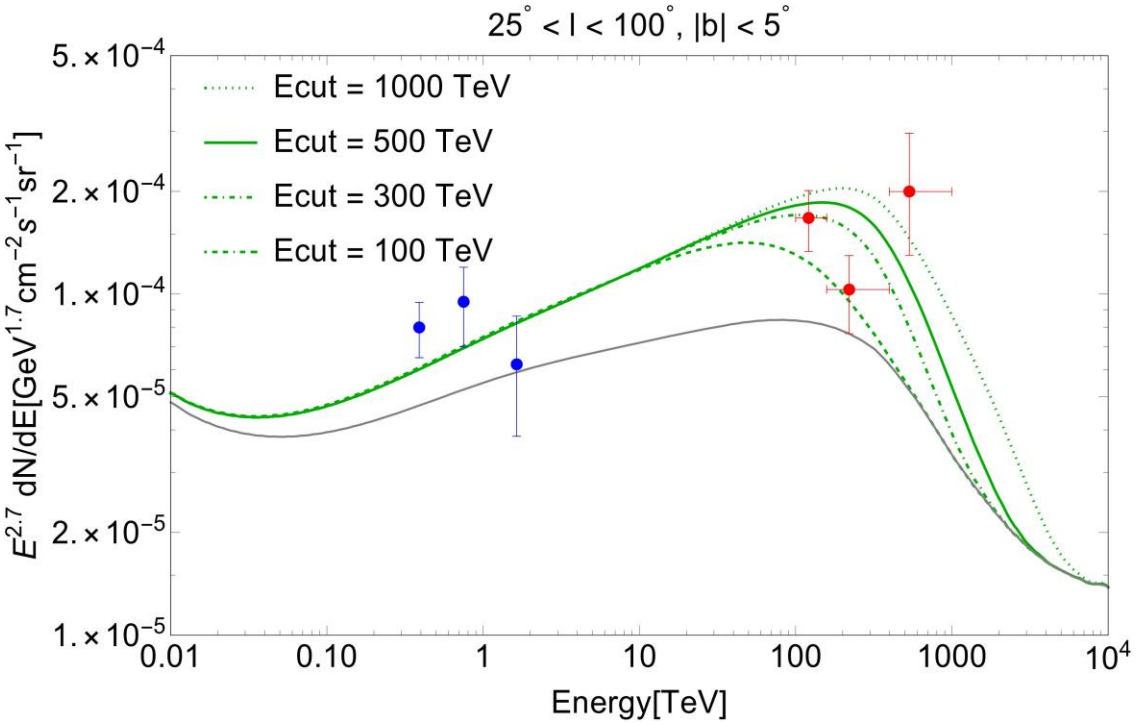

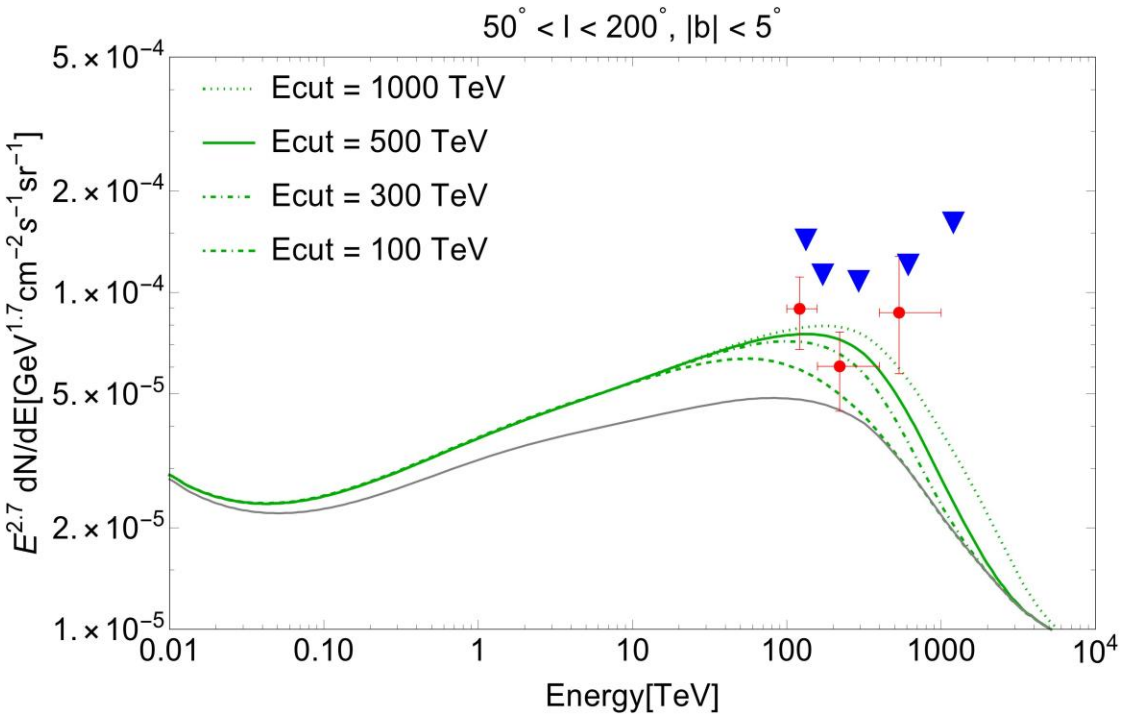

- The green lines are calculated assuming an intermediat threshold: $\phi_{th} = 0.5\phi_{crab}$
- The capability to explaine the first two data-points does not depend on the assumed cut-off;
- The third data point is out in case of Ecut<500 TeV

Cut-off effect:

Luminosity index: $\alpha = 1.8$

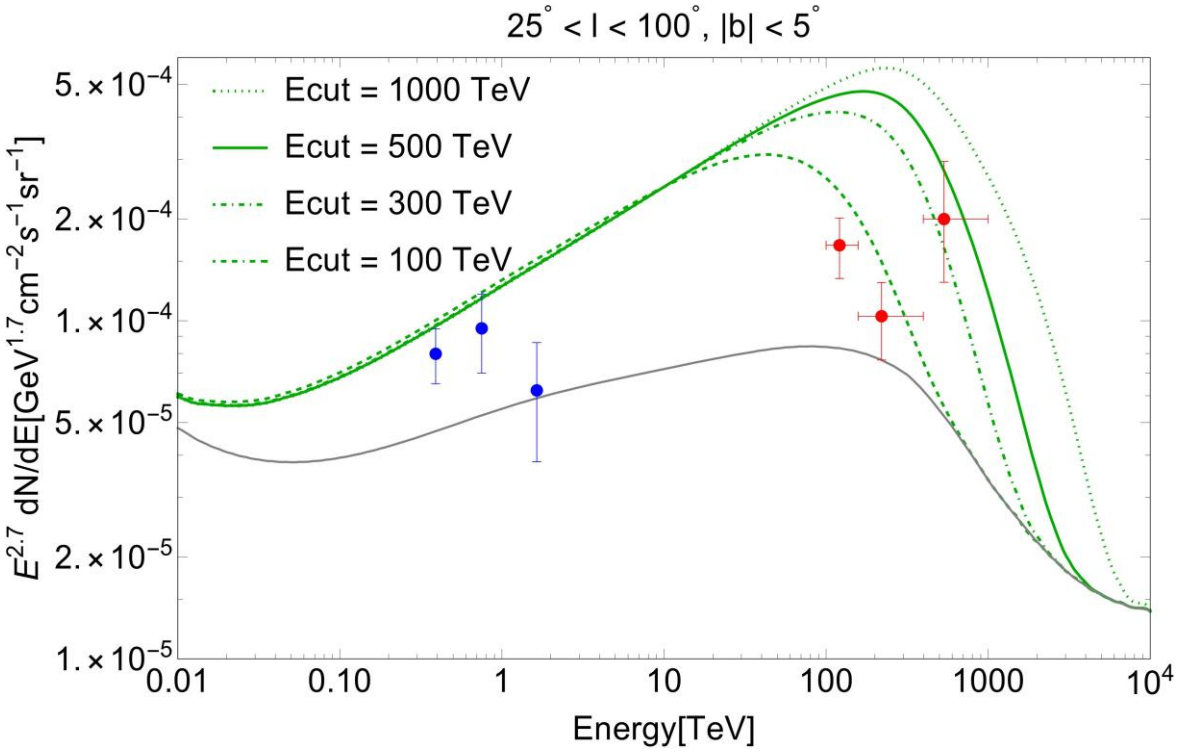

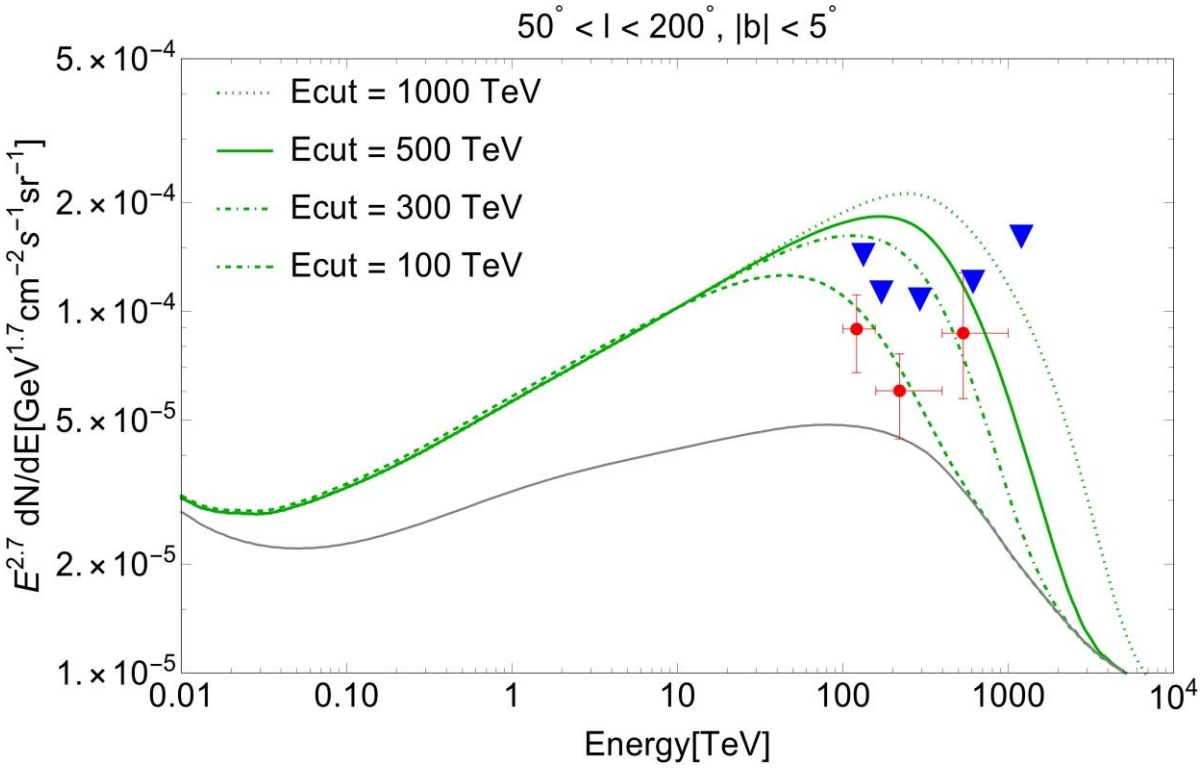

Tibet ASγ : Cut-off fixed to 100 TeV:

Luminosity index: $\alpha = 1.8$

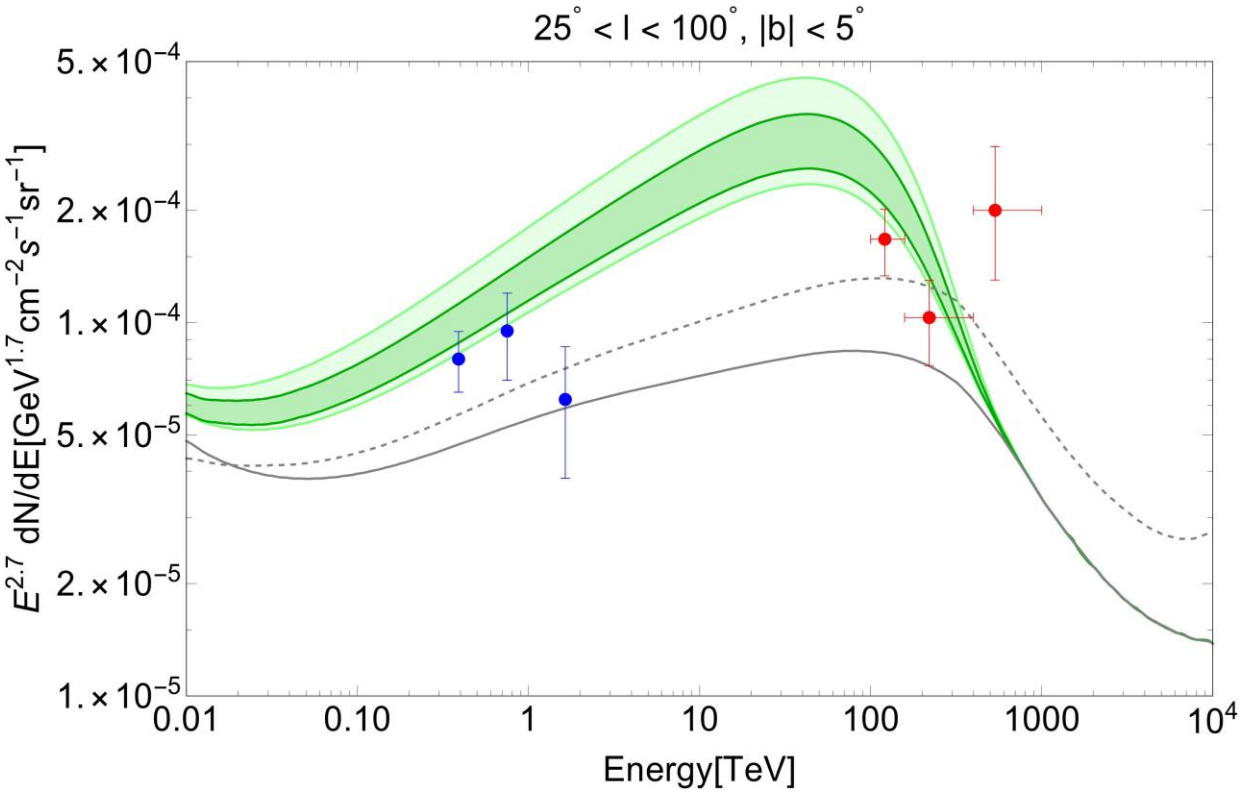

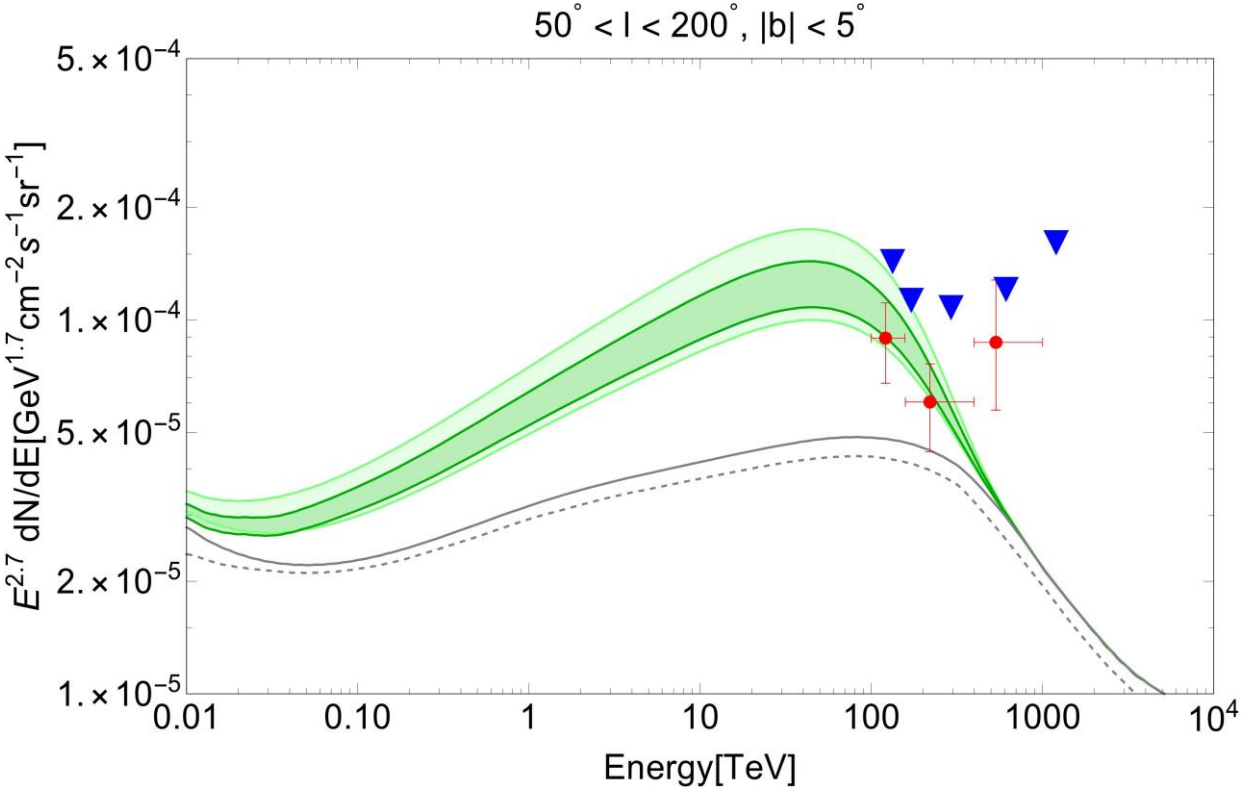

Ages of unresolved sources:

Luminosity index: $\alpha = 1.5$

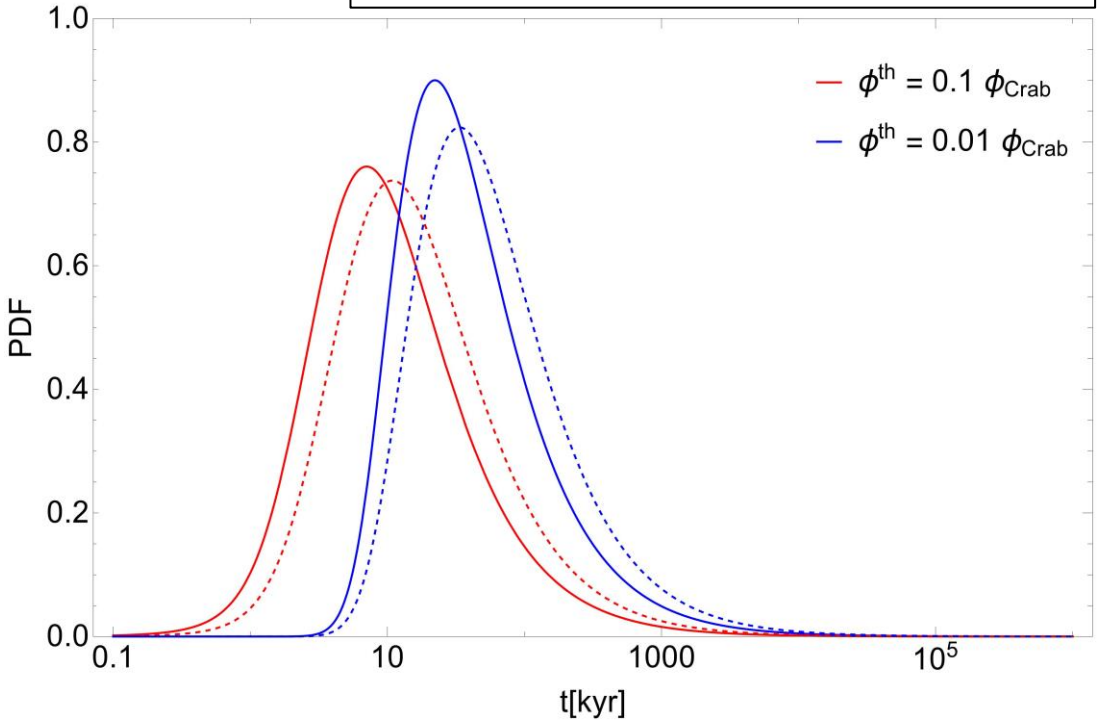

-- $t_{age} = (7 - 11)\ kyr$

-- $t_{age} = (22 - 33)\ kyr$

Sources older than 100 kyr contribute at most to 20 % to the unresolved signal .

Luminosity index: $\alpha = 1.8$

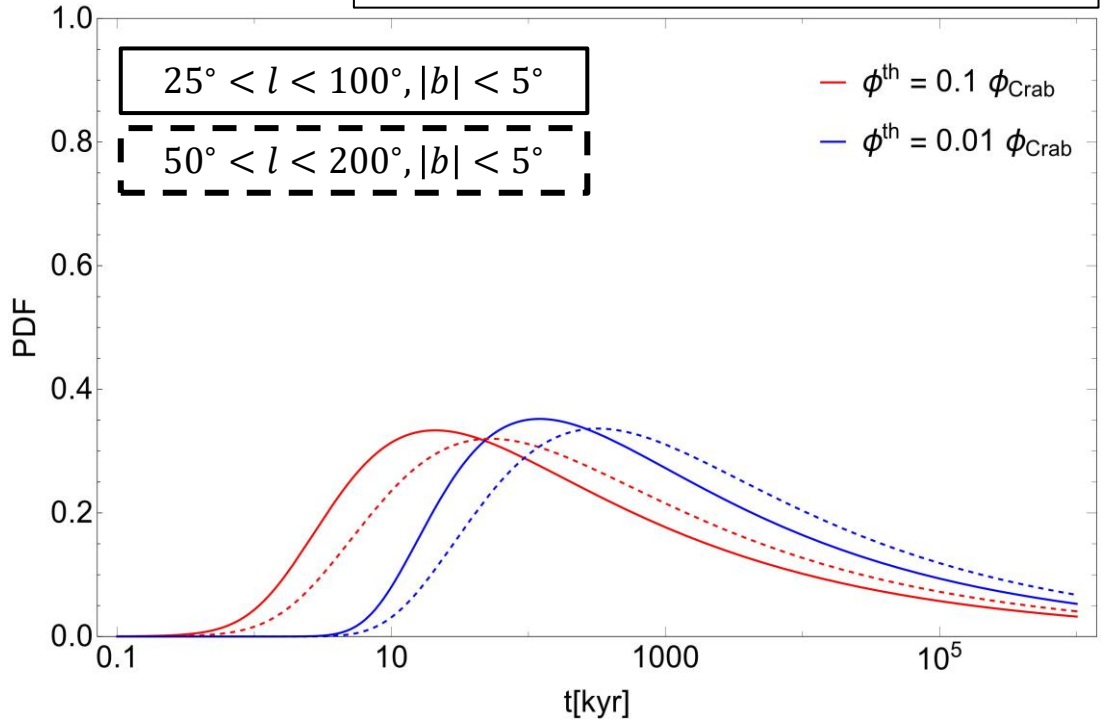

-- $t_{age} = (20 - 50)\ kyr$

-- $t_{age} = (120 - 130\ )kyr$

Sources older than 100 kyr provide 50 % - 80 % of the unresolved signal.

How many sources will CTA be able to resolve?

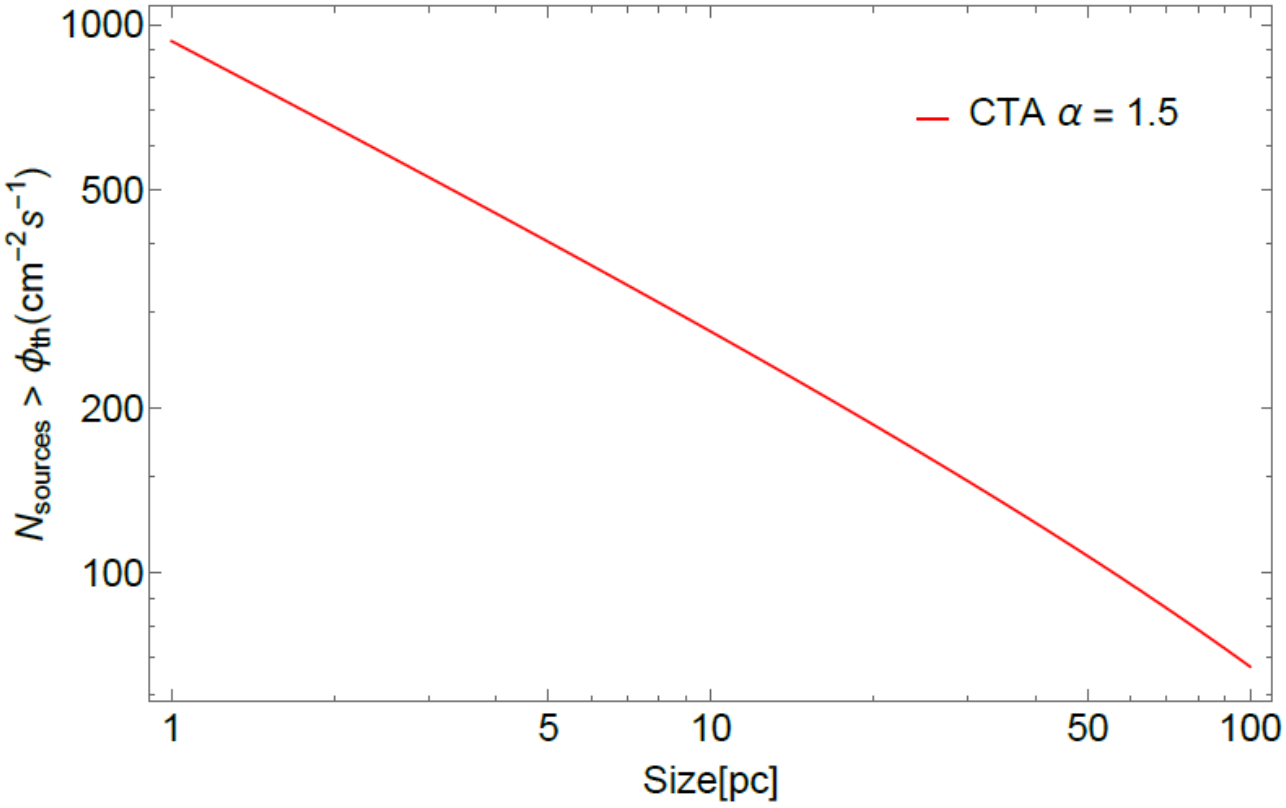

$$\phi_{th} \sim \phi_{th,ps} \frac{\theta_s}{\theta_{PSF}}$$

$$\phi_{th,ps} = 3 \times 10^{-3} \phi_{CRAB}$$

$$\theta_{PSF} = 0.05^o$$

$$280(10\,pc) - 140(40pc)$$

Why not LHAASO?

Extraction of Resolved Sources

Region:
Inner Galactic Plane
(25°<l<100°)

Masked radius $R < 2\sqrt{\text{p. s. f}^2 + \sigma_{ext}^2}$ ~ 1°

LHAASO Collaboration– ICRC 2021

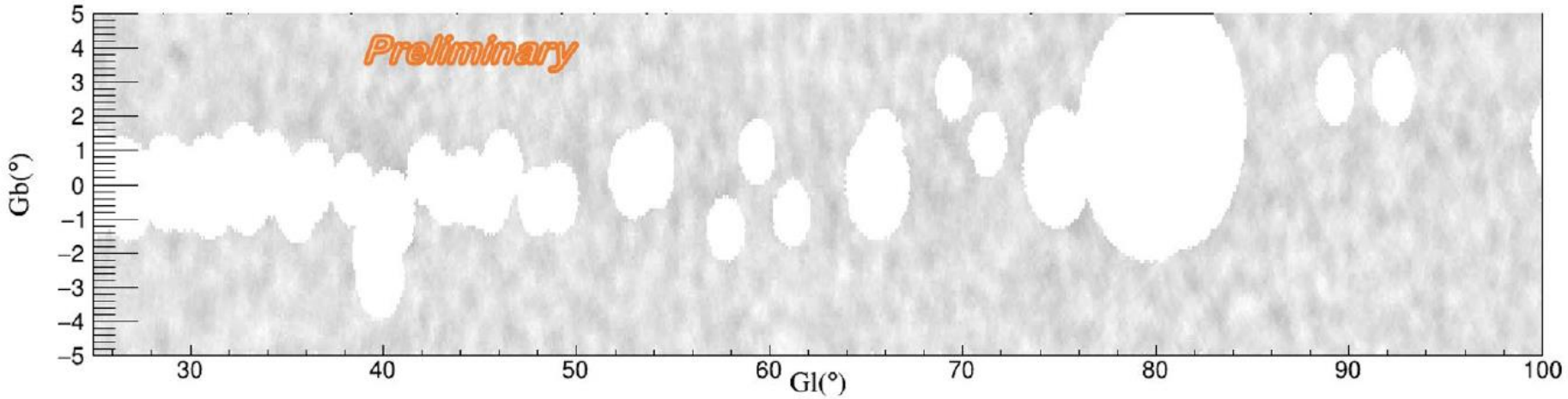

Monte Carlo: 1000 realizations:

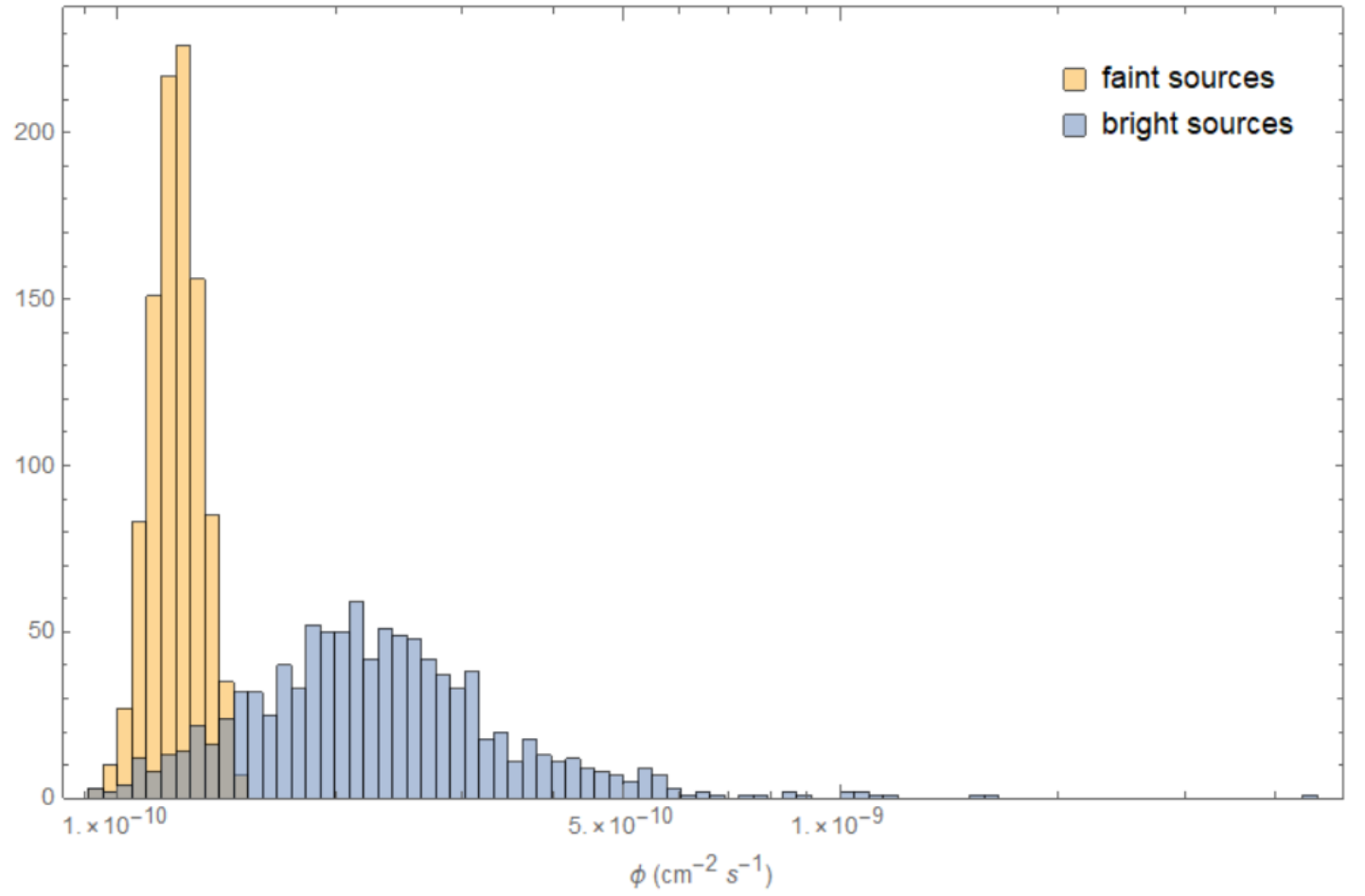

$\phi_{tot} = 16.6 \pm 8.9\ \phi_{Crab}$
$\phi_{bright}(\phi > 0.1\phi_{Crab}) = 11.3 \pm 8.4\ \phi_{Crab}$
$\phi_{faint}(\phi > 0.1\phi_{Crab}) = 5.3 \pm 0.4\ \phi_{Crab}$
$\phi_{Crab} = 2.26 \times 10^{-11} cm^{-2} s^{-1}$